universe

MDPI

Review

In the Quest for Cosmic Rotation

Vladimir A. Korotky [1], Eduard Masár [2] and Yuri N. Obukhov [3,*]

[1] Mathematics Department, Higher Military Institute of Air Defence, Moskovsky prospect 28, 150001 Yaroslavl, Russia; vkorotkii@yandex.ru
[2] Department of Theoretical Physics, Faculty of Mathematics, Physics and Informatics, Comenius University, Mlynská dolina 6280, 842 48 Bratislava, Slovakia; eduard.masar@fmph.uniba.sk
[3] Nuclear Safety Institute (IBRAE), Russian Academy of Sciences, B. Tulskaya 52, 115191 Moscow, Russia
* Correspondence: obukhov@ibrae.ac.ru

Received: 27 November 2019; Accepted: 8 January 2020; Published: 15 January 2020

Abstract: This paper analyzes the problem of global rotation in general relativity (GR) theory. Simple cosmological models with rotation and expansion are presented, which give a natural explanation of the modern values of the acceleration parameter at different red shifts without involving the concepts of "dark energy" and "dark matter". It is shown that due to the smallness of the cosmological rotation, for its detection one should use observations that do not depend on the magnitude of the angular velocity of the Universe. Such tests include the effects of the cosmic mirror and the cosmic lens. For the first time on the basis of modern electronic catalogs the search on the celestial sphere of images of our Galaxy and other galaxies is made. Viable candidates for both effects have been found.

Keywords: cosmology; cosmological effects; rotation of the Universe

1. Introduction

Rotational, vortex, and chiral phenomena are widely observed in physics on all scales including astrophysics, high-energy physics, and the heavy-ion collisions. Quoting E.T. Whittaker [1]: "Rotation is a universal phenomenon; the earth and all the other members of the solar system rotate on their axes, the satellites revolve round the planets, the planets revolve round the Sun, and the Sun himself is a member of the galaxy or Milky Way system which revolves in a very remarkable way. How did all these rotary motions come into being? What secures their permanence or brings about their modifications? And what part do they play in the system of the world?" Currently, the search for the similarities of vortex structures encountered in the heavy-ion physics and in astrophysical conditions attracts a lot of attention in the literature.

The hypothesis of a universe's rotation, in our opinion, belongs to the most intriguing issues of the modern cosmology. This idea is quite natural from the physical viewpoint and it does not contradict any of the astrophysical observations and still remains a challenging unsolved mystery.

In observational cosmology, the main difficulty for detecting a global rotation is its smallness—less than 10^{-13} yr^{-1} according to the generally accepted assessment. It is impossible in the Universe to distinguish the direction corresponding to the axis of rotation, with respect to which one could notice deviations (in the standard tests) from the Friedman standard cosmology.

In theoretical cosmology, the main difficulties are related, on the one hand, to the lack of simple models of an expanding and rotating Universe in general relativity (GR) similar to Friedman–Robertson–Walker models. On the other hand, there are no convincing predictive effects of cosmic rotation that are consistent with the capabilities of the equipment of modern astronomical observatories.

Observing rotating planets, stars, galaxies, and clusters of galaxies, we naturally come to two hypotheses. The first, the rotation was originally inherent in the content of "embryonic singularity"

("primeval atom" [2]). Following Einstein's assumption which linked properties of matter and properties of a space-time, it is natural to assume that *physical rotation of matter (orbital and intrinsic) generates geometrical rotation of space-time* (*universal and local*). Eventually, the rotation slows down and global orbital rotation becomes barely noticeable. Rotating cosmic objects are traces of that initial global rotation.

It is difficult to build a model of matter with orbital and inner angular momentum. The best candidate is the model of the perfect Weyssenhoff–Raabe fluid [3], whose elements have a "classical" spin. It remains to add the global rotation of the fluid as a whole (as a solid body for example) to the energy-momentum tensor of the Weyssenhoff fluid to obtain a realistic source for cosmology with rotation. One could attempt to do it directly, in the form of global rotation energy but this is hindered by a determination of the (local) orbital moment of inertia. Then one should look for an indirect introduction of orbital rotation.

This can be done in several ways. One of them is to consider a fluid with additional properties beyond a perfect fluid (for example, with viscosity, heat flow, or electric charge), taking into account the spin-spin and spin-electromagnetic interaction [4]. The next step is the consistent introduction of known physical fields into the energy-momentum tensor of the Universe matter. A promising generalization of the Weissenhoff fluid model from the point of view of adequacy to cosmological models with rotation, in our opinion, is the antisymmetric third rank tensor field, the sources of which are extended objects (cosmic strings, shells, or bags) in a perfect fluid (see [5] and the literature cited there) [4].

According to the second hypothesis, after the explosion of the "embryonic singularity", the matter particles run in different directions and gravitational interaction (within the framework of the Newtonian theory) inevitably leads to rotation relative to center of mass (and relative to each other (orbital rotation)) and to their own intrinsic rotation (in GR in harmonic coordinate system [6,7]). As a result, there are no non-rotating objects in the Universe. The latter is an instructive proof of the validity of GR and the Big Bang theory. The angular velocity of global and local rotation in this case increases from zero to modern values.

Let us start with *the requirement of spatial homogeneity*, since the fact of large-scale homogeneity of the Universe is considered to be proven in observational astronomy. We restrict ourselves to metrics of the form (t—cosmological time; x^i, i = 1,2,3—three spatial coordinates)

$$ds^2 = dt^2 - 2Rn_i dx^i dt - R^2\gamma_{ij}dx^i dx^j, \qquad i,j = 1,2,3. \tag{1}$$

We assume the same law of changing of scale factor $R = R(t)$ in all directions, therefore, all metrics (1) are *shear-free*. In all other aspects, (1) is space-time interval of the most general form. Here

$$n_i = \nu_a e_i^{(a)}, \gamma_{ij} = \beta_{ab} e_i^{(a)} e_j^{(b)}, \tag{2}$$

where ν_a, $\beta_{ab}(\det\beta_{ab} \neq 0)$, a, b = 1,2,3 are constant coefficients, $n_i = n_i\left(x^k\right), \gamma_{ij} = \gamma_{ij}\left(x^k\right)$ are functions of spatial coordinates x^i on the $t = const$ hypersurfaces, and

$$e^{(a)} = e_i^{(a)}(x)dx^i \tag{3}$$

are the invariant 1-forms with respect to the action of a three-parameter group of motion which is admitted by the space-time (1). One can prove that the isotropic expansion in (1) guarantees the isotropy of microwave background radiation (MBR) in such models [8]. Accordingly, the angular velocity of rotation should not be estimated on the basis of models with shear effects, contrary to the statements of [9].

The spatial homogeneity condition imposes a restriction on the group of motions which should act simplyransitively on the spatial ($t = const$) hypersurfaces. Such metrics are called Bianchi metrics, there are nine types of them. These manifolds are classified according to the Killing vectors $\xi_{(a)}$ and

their commutators $\left[\xi_{(a)}, \xi_{(b)}\right] = C^{c}_{ab}\xi_{(c)}$. The invariant forms (3) solve the Lie equations $L_{\xi_{(b)}} e^{(a)} = 0$ for each Bianchi type, so models n (1) are spatially homogeneous.

Besides the three Killing vector fields, space-times (1) admit a nontrivial conformal Killing vector $\xi_{conf} = R\partial_t$.The explicit form for all Bianchi metrics are given in [10]. Standard cosmologies (with $\nu_a = 0$ in (2)) are known to belong to types I, V, and IX.

The *rotation tensor* $\omega_{\mu\nu}$ and the *volume expansion scalar* θ for (1) are determined in the co-moving matter characterized by (average) 4-velocity vector $u^{\mu} = \delta^{\mu}_{0}$. They read as follows:

$$\omega_{\mu\nu} = \begin{cases} \omega_{0j} = 0, \\ \omega_{ij} = -\frac{R}{2}\overset{\frown}{C}{}^{k}_{ij} n_k, \end{cases} \quad \theta = \frac{3\dot{R}}{R}, \qquad \mu, \nu = 0, 1, 2, 3,$$

here, $\overset{\frown}{C}{}^{k}_{ij} = e^{k}_{(a)}\left(\partial_i e^{a}_{j} - \partial_j e^{a}_{i}\right)$. The explicit form of the structure constants C^{a}_{bc}, of the anholonomity objects $\overset{\frown}{C}{}^{k}_{ij}$ and also of $\xi_{(a)}$ and $e^{(a)}$ are given in [10]. It is easy to notice that $\omega_{\mu\nu} = 0$ for Bianchi-I models.

The *acceleration vector* a_{μ} for (1) is nontrivial

$$a_{\mu} = \begin{cases} a_0 = 0, \\ a_i = n_i \dot{R}, \end{cases}$$

for non-zero $\dot{R}$. It is easy to see that u^{μ} is not orthogonal to the hypersurface of homogeneity ("tilted" models).

Cosmological models (1) are parallax-free [10] (in terminology of [11]), and hence velocity of rotation cannot be estimated from parallax effects, contrary to the statements of [12,13].

It is worthwhile to mention an unusual physical property of metrics (1): there is no shear despite the non-zero rotation. In other words, despite the rotation, the expansion has the same magnitude in all directions. One usually thinks of a two-dimensional expanding and rotating elastic sphere and expects that at the poles the sphere should expand more slowly than at the equator. However imagine a two-dimensional expanding and rotating cylindrical surface: it is obvious that relative to any point on the axis of rotation, the expansion velocity is the same. The expansion along the axis of rotation can be arbitrary in magnitude; the observed MBR isotropy requires that the expansion along the axis of rotation is the same as in directions perpendicular to the axis of rotation. Note that this line of reasoning gives preference to models with non-zero initial spin in "embryonic singularity".

The correct causal structure of space-time, that is, the absence of closed time-like curves is considered as a serious restriction on the properties of a space-time manifold with rotation. K. G?del drew attention to the "non-physicality" of such models with rotation in his classical work [14]. S. Maitra found a simple and elegant way to describe such curves [15]. For (1) the absence of closed time-like geodesics is guaranteed when the matrix β_{ab} is positive-definite. Indeed, let a closed curve $x^{\mu}(s), 0 \le s \le 1, x^{\mu}(0) = x^{\mu}(1)$, be everywhere time-like, i.e., for arbitrary s,

$$g_{\mu\nu}\frac{dx^{\mu}}{ds}\frac{dx^{\nu}}{ds} > 0. \tag{4}$$

Choose s_0 as the value of the parameter s for which $\frac{dt}{ds} = 0$. Such a point necessarily exists by assumption that the curve is closed: with the growth of s, the coordinate t at first increases (decreases), and then decreases (increases). We compute the square of the modulus of the 4-velocity vector tangent to $x^{\mu}(s)$ at point s_0 for (1):

$$g_{\mu\nu}\frac{dx^{\mu}}{ds}\frac{dx^{\nu}}{ds}\bigg|_{s=s_0} = -R^2\beta_{ab}e^{(a)}_{i}e^{(b)}_{j}\frac{dx^{i}}{ds}\frac{dx^{j}}{ds}. \tag{5}$$

The right-hand side expression in (5) is always negative for a positive-definite β_{ab}, thus contradicting the initial condition (4) that $x^{\mu}(s)$ is time-like. It is important to emphasize that the presence or absence of causality is not connected in any way (except for the historic aspect [14]) with the presence or absence of cosmic rotation.

There are no other restrictions for (1).

2. Metric and Matter vs. Dark Energy and Oscillating Physics

Different cosmological scenarios can be described by the following special cases of metrics (1)

$$ds^2 = dt^2 - 2R(t)\sqrt{B}(dx - zdy)dt - R^2(t)\Big(A(dx - zdy)^2 + dy^2 + dx^2\Big), \tag{6}$$

$$ds^2 = dt^2 - 2R(t)\sqrt{C}e^{mx}dydt - R^2(t)\Big(dx^2 + De^{2mx}dy^2 + dz^2\Big), \tag{7}$$

$$ds^2 = dt^2 - 2R(t)\sqrt{K}e^{(1)}dt - R^2(t)\Big(L\Big(e^{(1)}\Big)^2 + \Big(e^{(2)}\Big)^2 + \Big(e^{(3)}\Big)^2\Big). \tag{8}$$

In (6)–(8) the following notation is introduced: A, B, C, D, m, K, L – *const*; $e^{(1)} = \cos y \cos zdx - \sin zdy$; ???$e^{(2)} = \cos y \sin zdx + \cos zdy$; ???$e^{(3)} = -\sin ydx + dz$. These metrics belong to Bianchi-II, Bianchi-III; Bianchi-IX classes respectively. In all metrics the rotation slows down with the growth of the scale factor $R(t)$. The modified spinning fluid [4] describes the material source in these cosmological models. This is a continuum whose elements are charged particles with spin: in the modern epoch these are galaxies or clusters of galaxies [16,17], whereas in the early cosmological stages these are fundamental particles with spin [18]. In general, the spin-electromagnetic and spin-spin coupling between fluid's elements is mediated by the scalar fields and antisymmetric tensor fields. As a result, the energy-momentum tensor $T_{\mu\nu}$ encompasses the usual contributions from the electromagnetic and scalar fields and different types of interactions between the matter elements are described by antisymmetric tensors: the electromagnetic field $F_{\mu\nu}$; the third-rank tensor field $F_{\mu\nu\alpha}$ whose sources are extended objects (strings, shells, and bags) [5]; and $F_{\mu\nu\alpha\beta}$ that is dynamically equivalent to the scalar field. The coupled system of the gravitational field equations and the equations of motion of physical fields and their sources [19–22] can be consistently solved for the class of cosmological metrics with expansion and rotation. These models take into account the cosmological constant (Λ-term) of either Einstein type ($\Lambda > 0$, which corresponds to negative pressure and repulsion) or G?del type ($\Lambda < 0$, which corresponds to positive pressure and attraction).

Let us consider *the nearest non-stationary cosmological generalization of G?del's solution* [19,21], when the gravitational field is described by the metrics (6) and (8).

In particular, for (6) we have [19]: for scale factor evolution ($0 < A << 1$, $A/B << 1$–constants)

$$\dot{R}^2 = cR^2 - \frac{B}{4}, \tag{9}$$

(where c is an integration constant) and for matter state equation

$$p = -??\varepsilon = \frac{1}{\kappa}\Lambda, \tag{10}$$

where $\kappa = 8\pi G$– Einstein's gravitational constant of GR and rotation is

$$\omega^2 = \omega_{\hat{2}\hat{3}}\omega^{\hat{2}\hat{3}} = \frac{B}{4R^2}. \tag{11}$$

Analyzing (9), we see that c cannot have a negative value since $B > 0$. Differentiating (9) over t, we obtain

$$\frac{\ddot{R}}{R} = c > 0, \tag{12}$$

consequently, this solution describes the accelerated expansion of Metagalaxy, which is apparently currently observed. The change of acceleration is of the Hubble type: the farther is the galaxy, the greater is its acceleration. It is assumed that scale factor is proportional to the distance between galaxies. The presence of acceleration and repulsion forces in a rotating Universe are absolutely natural physical factors to explain the accelerated scattering of galaxies. (Although it is more common to introduce dark matter and dark energy paradigm.) Rewrite (9) with (11) as

$$\dot{R}^2 + \omega^2 R^2 = cR^2. \tag{13}$$

Equation (13) is very similar to the equality of kinetic energy (the sum of translational expansion and rotation) and the potential energy of the Universe (as in a tensile and rotating spring). Relation (10) reproduces the equation of state of matter in the G?del model: $\Lambda < 0$; ε and p remain constant (as time goes on) despite the expansion and rotation. The relations (10) and (13) agree perfectly with each other in physical sense if we interpret the left-hand side of (13) as ε and the right-hand side as minus p. That is, at any time at small R and at large R the sum of kinetic and potential energy is zero. In this sense, this solution can be called stationary. It is also clear why the potential energy of gravity is proportional to R^2: this is because the potential energy is computed *inside* a homogeneous cylinder of a perfect fluid.

A completely similar solution exists for the metric (8) [21], in this sense, such a solution can be considered as *typical* one for models of the Universe with rotation and expansion.

Let us analyze the cosmological model (6) in which the source of the gravitational field is a neutral spinning Weyssenhoff-Raabe fluid and a scalar field $\phi = \phi(t)$ which determines the spin-spin coupling between elements of the fluid [4,19]. This model can be considered as the nearest generalization of the model (9) and (10). Indeed, in order to make the model (9) and (10) look more realistic, it is necessary to take into account that all the elements of the cosmological fluid (galaxies) are rotating. Therefore, Weyssenhoff-Raabe fluid provides an appropriate description for the cosmological matter. However, since one should also take into account the spin of galaxies, we cannot ignore their spin-spin interaction. It is known [6] that in GR rotating spherically symmetric gravitational bodies affect the rotation of each other. Such an interaction can be effectively modeled by means of a scalar field. Now instead of (9) and (10) we find ($0 < A << 1$, $A/B << 1$)

$$\dot{R}^2 = cR^2 - \frac{B}{4} + \frac{2\alpha}{R}, \tag{14}$$

$$p = \frac{1}{\kappa}\Lambda, ????\varepsilon = 2\chi_2 S\varphi^2 - \frac{1}{\kappa}\Lambda, \tag{15}$$

where $\dot{\varphi}^2 = 12\alpha/R^3$, $\alpha = const > 0$, $S = \frac{S_0}{R^3}$ – spin density of matter, S_0,–*const*, χ_2 – constant of spin-spin interaction (for more details see [4,23]); it is clear that (11) is the same; c and B are positive similarly to (9).

Differentiating (14) by time, we find instead of (12)

$$\frac{\ddot{R}}{R} = c - \frac{\alpha}{R^3} > 0, \tag{16}$$

that is, if $R < (\alpha/c)^{1/3}$ then the *acceleration is negative* (deceleration); if $R = (\alpha/c)^{1/3}$then the *acceleration is zero*, finally, if $R > (\alpha/c)^{1/3}$ the *acceleration is positive*; so (16) is in a full agreement with modern observations on the dependence of the acceleration parameter on the red shift (in 1998–1999 [24,25] the conclusion about the accelerated expansion of the universe was made; over the past decade, the results [24,25] have been repeatedly tested with ever-improving statistics but the main result remained unchanged: relatively recently at $z < 0.5$, the Universe had the transition from decelerated expansion to accelerated one).

Let us rewrite (14) with (11) as

$$\dot{R}^2 + \omega^2 R^2 = cR^2 + \frac{2\alpha}{R}. \tag{17}$$

We see that the equation again has the form of the law of conservation of energy. As compared to (13), a term corresponding to the potential energy of the gravitational field (there is no electromagnetic field) appeared in the ratio (17). However, this is exactly what was expected: to simulate ("*effectively*") the *gravitational* interaction of spins of galaxies. The structure of (17) fully confirms the validity of this approach.

A remark is in order about the equation of state of matter. (i) For G?del-type Λ-term we have: $p < 0$; $\varepsilon > 0$; $p + \varepsilon > 0$ which is to a large extent similar (10). (ii) For $\Lambda = 0$ we find: $p = 0$; $\varepsilon > 0$ – dust. (iii) For Einstein-type Λ-term: $p > 0$; $\varepsilon \geq 0$. As one can see, there are several variants of possible states of matter, and different signs of the Λ-term are allowed. However, following the logic of gradual complication of the model the first variant looks more preferable.

In 1990 [26] an apparently periodic structure of the number of sources was demonstrated as a function of red shift in the large-scale distribution of galaxies. A possible explanation of this fact was discussed in [27]. In particular, it was noticed that the periodic structure of the universe may arise from the "oscillating physics", e.g., oscillations of the gravitational or fine structure constants, or of a dark matter (scalar) fields. In [28] we pointed on global cosmological rotation as a possible reason of this observational effect.

Along with many known exotic and beautiful hypotheses in the history of cosmology, the cosmological rotation on the one hand does not contradict any of the *known observations*, on the other hand, it gives natural explanations to *new discoveries* in astrophysics and therefore it deserves closer attention from observational astronomy.

3. In the Theoretical Quest for Cosmic Rotation

The idea of cosmic rotation is revisited (perhaps less often than it deserves) when a certain anisotropy is detected in the Universe. The most famous attempt to explain such observations by a global rotation was due to P. Birch [29] in 1982. As it turned out later after a long discussion [30–32] the discovered effect, if it really exists, is not related to Universe rotation but this interpretation had nevertheless caused an explosion of interest in the theoretical development of this subject (particularly in the group of D. Ivanenko in Moscow).

Classical cosmological tests, such as apparent magnitude-red shift (m-z), number counts-red shift (N-z), angular size-red shift relations, and some other, reveal specific dependence of astrophysical observables on the angular coordinates (θ, φ) in a rotating world. Thus, a careful analysis of the angular variations of empirical data over the whole celestial sphere is necessary. The knowledge of null geodesics makes it possible to obtain the explicit form of the area distance r between an observer at a point P and a distant star S, which is a crucial step in deriving formulas for classical cosmological tests [33]. For metric (7) we derive an apparent magnitude-red shift relation (m-z).

$$\begin{aligned} m = M - 5\log_{10} H_0 + 5\log_{10} z + \tfrac{5}{2}\left(\log_{10} e\right)(1-q_0)z - ??5\log_{10}\left(1 + \sqrt{\tfrac{C}{C+D}}\sin\theta\sin\varphi\right) \\ ? - \tfrac{5}{2}\left(\log_{10} e\right)\frac{\omega_0}{H_0}\frac{\sin\theta\cos\varphi\left(\sqrt{\frac{C}{C+D}}+\sin\theta\sin\varphi\right)}{\left(1+\sqrt{\frac{C}{C+D}}\sin\theta\sin\varphi\right)^2}z + o\left(z^2\right), \end{aligned} \tag{18}$$

and number of sources-red shift relation (N-z)

$$\frac{dN}{d\Omega} = \frac{n_0 z^3}{3H_0^3\left(1+\sqrt{\frac{C}{C+D}}\sin\theta\sin\varphi\right)^3}\left(1-\frac{3}{2}(1+q_0)z\right.$$
$$\left.-3\,\frac{\omega_0}{H_0}\,\frac{\sin\theta\cos\varphi\left(\sqrt{\frac{C}{C+D}}+\sin\theta\sin\varphi\right)}{\left(1+\sqrt{\frac{C}{C+D}}\sin\theta\sin\varphi\right)^2}z+o\left(z^2\right)\right), \tag{19}$$

here $M = -\frac{5}{2}\log_{10} L_s$ is the absolute magnitude of a light source with an intrinsic luminosity L_s and n_0 is the modern value of number density of $n = n(t)$ (as usual, (19) is derived under the assumption of the absence of source evolution). The (N-z) relation describes the number of sources observed in a solid angle $d\Omega$ up to the value z of red shift. One can estimate the global difference of the number of sources visible in two hemispheres of the sky, N^+, N^- by integrating (19):

$$\frac{N^+ - N^-}{N^+ + N^-} = \frac{1}{2}\sqrt{\frac{C}{C+D}}\left(3-\frac{C}{C+D}\right)+o\left(z^2\right). \tag{20}$$

Note that (20) is independent of z and (18)–(20) obtained for nearby galaxies with $z < 1$. Similar formulas are not difficult to obtain for (6) and (8).

The main difficulty of using classical cosmological tests for the discovery of space rotation is that the angular velocity of the Universe is apparently very small and it is not easy to separate the effects of the evolution of the physical properties of the sources from the effects of rotation. The only possibility for observational astronomy is to detect some angular dependencies like in (18)–(20) or in similar metrics of Bianchi-type with rotation.

An experiment similar to Foucault's pendulum, which proves the rotation of the Earth, carried out in space rocket would be also inconclusive because of the very slow rotation.

Therefore, it is necessary to look for such effects of cosmic rotation, which would not depend on how great the velocity of rotation is, but would be possible only in the rotating Universe. Such effects were predicted in 1999 [34] for Bianchi-II (6) cosmological *model*.

In the geometric optics approximation light rays are *null* geodesics, i.e., curves $x^\mu(\lambda)$ with an affine parameter λ and tangent vector k^μ:

$$k^\mu = dx^\mu/d\lambda, \qquad k^\mu k_{\nu;\mu} = 0, \qquad k^\mu k_\mu = 0. \tag{21}$$

The metric (6) has three Killing and one conformal Killing vectors:

$$\xi^\mu_{(1)} = (0,1,0,0), \qquad \xi^\mu_{(2)} = (0,0,1,0), \qquad \xi^\mu_{(3)} = (0,y,0,1), \qquad \xi^\mu_{(conf)} \equiv \xi^\mu_{(4)} = (R,0,0,0). \tag{22}$$

Therefore, we easily get four first integrals of null geodesics (21):

$$k_\mu \xi^\mu_{(J)} = -q_J, \tag{23}$$

where q_J are constants along the null geodesics (J = 1, 2, 3, 4). From (22) and (23) we obtain

$$k^{\hat{0}} = -\frac{q_4}{R}, \qquad ?k^{\hat{1}} = \frac{q_1+\sqrt{B}q_4}{\sqrt{A+B}R}, \qquad ?k^{\hat{2}} = \frac{q_2+q_1 z}{R}, \qquad ?k^{\hat{3}} = \frac{q_3-q_1 y}{R}. \tag{24}$$

It is convenient to use the local orthonormal tetrad h^a_μ (Greek indices μ, ν, ... = 0, 1, 2, 3 refer to the local coordinates; a, b, ... = $\hat{0}, \hat{1}, \hat{2}, \hat{3}$ are tetrad indices):

$$h^{\hat{0}}_0 = 1, \quad h^{\hat{0}}_1 = -\sqrt{B}R, \quad h^{\hat{0}}_2 = \sqrt{B}Rz, \quad h^{\hat{1}}_1 = \sqrt{A+B}R, \quad h^{\hat{1}}_2 = -\sqrt{A+B}Rz, \quad h^{\hat{2}}_2 = R, \quad h^{\hat{3}}_3 = R. \tag{25}$$

We assume that an observer has coordinates $P(t = t_0, x = 0, y = 0, z = 0)$. The null geodesics through P are labeled with the help of spherical angles θ and φ which define direction of a light ray in the local Lorentz basis of the observer at P:

$$k_P^{\hat{0}} = 1, \qquad k_P^{\hat{1}} = \sin\theta\cos\varphi, \qquad k_P^{\hat{2}} = \sin\theta\sin\varphi, \qquad k_P^{\hat{3}} = \cos\theta. \tag{26}$$

From (25) and (26) we find the constants q_J:

$$q_4 = -R_0, \qquad q_1 = R_0\Big(\sqrt{B} + \sqrt{A+B}\sin\theta\cos\varphi\Big), \qquad q_2 = R_0\sin\theta\sin\varphi, \qquad q_3 = R_0\cos\theta, \tag{27}$$

where $R_0 \equiv R(t_0)$. Using (21), $k^0 = dt/d\lambda$, we can eliminate λ for t and convert (24) to the following system

$$k^0 = \frac{dt}{d\lambda} = \frac{R_0}{R}\left(1 + \sqrt{\frac{B}{A+B}}\sin\theta\cos\varphi\right) \equiv \frac{q_0}{R}, \tag{28}$$

$$\frac{dx}{d\tau} = \frac{q_1 - R_0\sqrt{B}}{q_0(A+B)} + \frac{z(q_2 + q_1 z)}{q_0}, \tag{29}$$

$$\frac{dy}{d\tau} = \frac{q_2 + q_1 z}{q_0}, \tag{30}$$

$$\frac{dz}{d\tau} = \frac{q_3 - q_1 y}{q_0}, \tag{31}$$

where $d\tau \equiv \frac{dt}{R}$. Solving (29)–(31), we get the exact form of null geodesics equations for $q_1 \neq 0$:

$$\begin{aligned} x = {} & -\tfrac{q_2 q_3}{2q_1^2} + \tau\Big(\tfrac{q_1 - R_0\sqrt{B}}{q_0(A+B)} + \tfrac{q_2^2+q_3^2}{2q_1 q_0}\Big) + \tfrac{q_2 q_3}{q_1^2}\cos\Big(\tfrac{q_1}{q_0}\tau\Big) - \\ & - \tfrac{q_2^2}{q_1^2}\sin\Big(\tfrac{q_1}{q_0}\tau\Big) - \tfrac{q_2 q_3}{2q_1^2}\cos\Big(\tfrac{2q_1\tau}{q_0}\Big) + \tfrac{q_2^2 - q_3^2}{4q_1^2}\sin\Big(\tfrac{2q_1\tau}{q_0}\Big), \end{aligned} \tag{32}$$

$$y = -\frac{q_3}{q_1}\cos\left(\frac{q_1}{q_0}\tau\right) + \frac{q_2}{q_1}\sin\left(\frac{q_1}{q_0}\tau\right) + \frac{q_3}{q_1}, \tag{33}$$

$$z = \frac{q_2}{q_1}\cos\left(\frac{q_1}{q_0}\tau\right) + \frac{q_3}{q_1}\sin\left(\frac{q_1}{q_0}\tau\right) - \frac{q_2}{q_1}. \tag{34}$$

From (33) and (34) we get

$$\left(y - \frac{q_3}{q_1}\right)^2 + \left(z + \frac{q_2}{q_1}\right)^2 = \frac{q_3^2 + q_2^2}{q_1^2}, \tag{35}$$

i.e., null geodesics in Bianchi-II metric (6) are circular helix and pitch of these helices that may be found from (32) (Figure 1). It is easy to see that all the loops of (35) touch the x-axis.

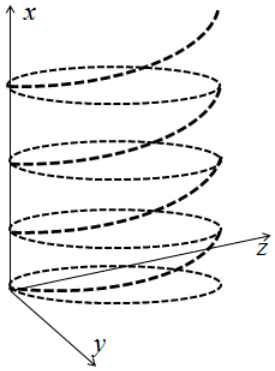

Figure 1. One of the helix-geodesics (32)–(35).

Time-like geodesics are circular helices too and all massive test particles in the Bianchi-II space-time (6) move along spirals [34].

Here we come to the particular case of the null-geodesics set in Bianchi-II rotating world: the existence of closed 3-curves. The necessary condition of their existence is

$$\frac{q_1 - R_0\sqrt{B}}{q_0(A+B)} + \frac{q_2^2 + q_3^2}{2q_1q_0} = 0. \tag{36}$$

Then (32)–(34) describe periodic functions of τ. The condition (36) gives the directions (θ, φ) on the celestial sphere, along which the light rays are closed (compare (36), (27)–(28)):

$$\sin\theta\cos\varphi = \frac{\sqrt{-A} - \sqrt{B}}{\sqrt{A+B}} < 0, \tag{37}$$

(negative values of A are acceptable for correct causality space-time structure [32]). From (32)–(34) it is clear that at the point of observation we have: $\tau = \tau_0 = 0$ and $t = t_0$, $x = 0$, $y = 0$, $z = 0$. Light returns to the same spatial point $x = 0$, $y = 0$, $z = 0$ at the moments of time

$$\tau_n = \frac{2\pi q_0}{q_1} n; \qquad ?n = 1, 2, ... \tag{38}$$

The existence of the closed null 3-curves gives rise to a number of new observational effects in rotating and expanding *models* of the Universe *independent on the magnitude of the angular velocity of the Universe.*

In what can be considered as a cosmological lens effect, let us assume that some galaxy is located at a point on the closed light ray (null geodesic). Then an observer can see the same galaxy in the two opposite directions (Figure 2b). In a generic case the observed galaxy is asymmetrically located relative to the opposite directions of observation. As a result, a detection of the two images of identical galaxies at different distances (with different redshifts) visible at the opposite semi-spheres of the sky would likely mean that this is the same galaxy, and we therefore observe the lens effect due to rotation of the Metagalaxy. Thus, the Universe as a whole becomes a lens.

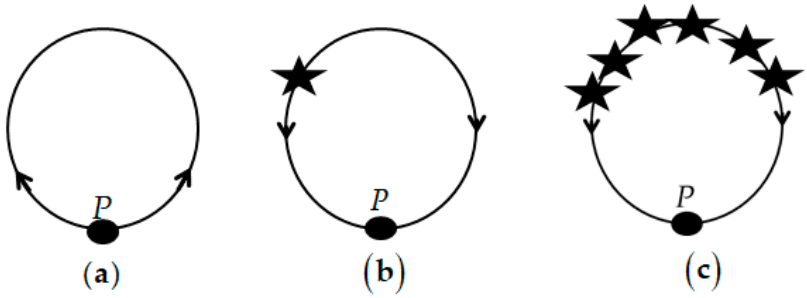

Figure 2. Possible observational effects in the rotating and expanding models independent of the magnitude of the angular velocity of the Universe: (**a**) cosmological mirror effect; (**b**) cosmological lens effect; (**c**) cosmological shadow effect.

In a different situation which could be described as a cosmological shadow effect, let us assume that two galaxies (or more) are located on the closed light ray (Figure 2c). Then the observer can see only the two closest galaxies, which screen one another and the other galaxies on this ray.

The lens (which was described above) is "broken" and the image of a galaxy is not duplicated.

This would also mean (though unlikely) that we may not be able to observe many galaxies that are in shadow of other galaxies. This effect can qualitatively (at least partially) contribute to the problem of the *hidden mass*.

Finally, one can think of cosmological mirror effect as follows. Suppose, that there are no galaxies on a closed light ray (Figure 2a). Then an observer would be able to see his own galaxy from the different sides. Thus, provided we are living in a rotating world, we would have a chance to look at ourselves from aside. The Universe as a whole becomes a mirror (similar local mirror effect can take place in the Kerr gravitational field of a rotating compact source). An astronomer on the Earth, by discovering absolutely identical images of galaxies in the pairwise opposite directions on the sky sphere, may in fact happen to observe just one and the same native Galaxy. Additionally, there could be many such mirror reflections! This would be an *observational evidence* of the existence of the universal rotation, even for a *small* value of the cosmic *vorticity*. In practice of course all the closed light paths may be blocked by other galaxies, which breaks the cosmic mirror.

These effects are due to the geometry and topology of our physical space and are inherent only to the rotating (no matter how fast) world. In contrast, the standard Friedman type universe with expansion does not have closed light rays, and the same is true for general expanding non-rotating models. It is worthwhile to clarify the understanding of "the galaxy is on the closed null-geodesic". Here we consider a null-geodesic, satisfying the condition (37) and labeled by angles θ and φ on the celestial sphere. The set of such curves forms a cone with a vertex at the observation point and intersecting with the celestial sphere along a circumference with the radius $\sqrt{2/\left(1-\sqrt{-B/A}\right)}$ and the center on x-axis: $x=\left(\sqrt{-A}-\sqrt{B}\right)/\sqrt{A+B}$ the points of which satisfy the condition n (37).

The real galaxy is an extended object, its image is a spot—not a point. The observer receives a bundle of light rays from the object of observation. In geometric optics approximation, rays of light are null-geodesics: the telescope receives a truncated light cone with one base at the galaxy and another base at the telescope lens (Figure 3).

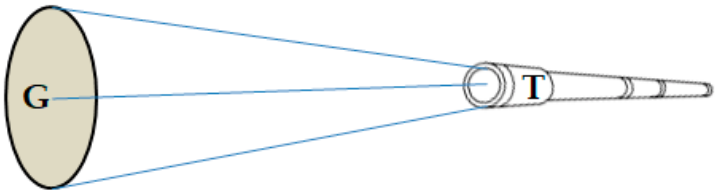

Figure 3. Formation of an image of the galaxy on a photographic plate of the telescope located in an arbitrary place on the celestial sphere. G—Galaxy; T—Telescope of an observer.

Let us call the middle ray GT in Figure 3 *central*, let it correspond to the *central null-geodesic*. The path of the rays in the formation of the image in the telescope lens with a closed central null-geodesic is shown on Figure 4a. It is clear that only a central geodesic "returns" exactly to the point from which it "started".

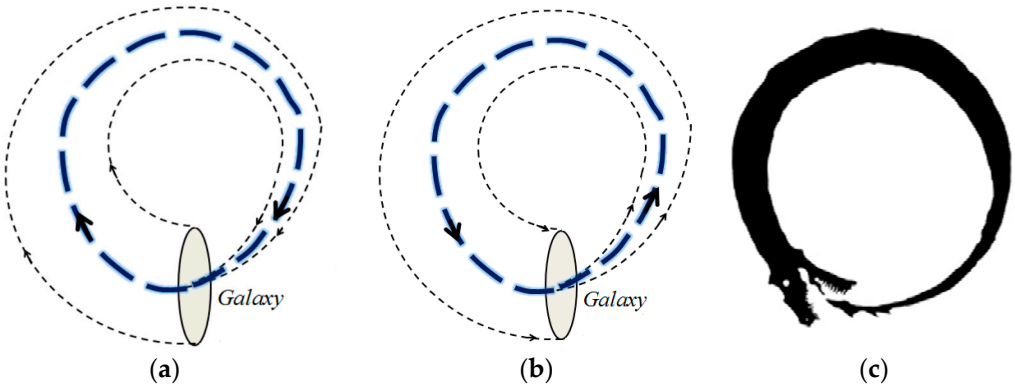

Figure 4. Loopback of the light cone: (**a**) the path of the rays which form the image of the Galaxy (cosmic mirror effect) in the telescope lens with a closed central null-geodesic; a thin dotted line shows the light cone between the Galaxy and the observer, the thick dotted line is the central null-geodesic; (**b**) an illustration of the fact that only the central ray is closed; (**c**) the Ouroboros (figure copied from the site "Ya-webdesign.com"—images for free download).

Other geodesics, taking part in the formation of the image in the telescope lens, have labels which do not satisfy (37), so they are not closed. Indeed, consider the "inverse" problem: imagine that an observer on Earth does not have a telescope, but a flashlight to detect the Galaxy in the darkness of the Universe (Figure 4b). Taking into account a continuity property, null-geodesics continuously fill the light cone around the central null-geodesic.

Some of them fall on the Galaxy and they form an image on the photo-plate of the telescope (light rays coming back); the rest is scattered in the Universe; and only a bunch of null-geodesics passing through the points (37) of the segment crossing the Galaxy will return exactly to the original places.

Figure 4a,b looks like the Ouroboros—a snake eating its own tail (Figure 4c).

It is thus reasonable to search for the effects of the cosmic lens and cosmic mirror on our sky. Clearly there are many galaxies and many other opaque objects in the Universe that can block the Milky Way image. However, the snapshots of the Galaxy are sent out along the (formally infinite) *set* of null-geodesics (37), so there is a non-zero possibility that at least one of them can return to us.

Analyzing the catalogs of galaxies and quasars in the quest for cosmic rotation, it is necessary to take into account that the equations of null-geodesics in the real world may differ from the equations of ideal homogeneous models. Local gravitational inhomogeneities can disrupt the smoothness of curves (the observer on the Earth is located at the edge (at the tail of spiral arm) of a spiral Galaxy, in the center of which there is the strongest center of gravity, possibly a black hole).

Important, though indirect, evidence of the rotation of the Universe could be the detection of *anisotropy in*: (i) the distribution of the directions of the *axes of galaxies*, i.e., the existence of some predominant direction of orientation of the axes; and (ii) the directions of *rotation* of galaxies: *clockwise or counterclockwise*. Theoretically, the existence of such anisotropy follows from the use of the Weyssenhoff–Raabe fluid model [3] as a cosmological material medium [17,35].

4. In the Experimental Quest for Cosmic Rotation

Let us now turn to the analysis of the experimental data accumulated in several online electronic catalogs of galaxies and quasars. We focus on looking for two effects, namely *the cosmic mirror effect* and *the cosmic lens effect*, described above. These effects will show up themselves if the Earth crosses a closed null geodesic and if we manage to find two similar object images, located on two opposite

sides of this null geodesic. Every pair of candidate objects must fulfill the condition of being mutually opposite on the celestial sphere.

For the cosmic lens effect, both objects in the pair must be of the same type (an elliptical galaxy or a spiral galaxy or a quasar). Their redshift may be different as those objects can actually be a double image of the same object located at an arbitrary point of the closed null geodesic.

However when looking for the cosmic mirror effect, we require both objects in the pair to have also the same redshift values (ideally, all other astrometric parameters should be the same as well). According to modern ideas, most of elliptical galaxies are created as a result of spiral galaxies collisions. On the celestial sphere we observe galaxies younger than their present state. For that reason, when searching for the effect of cosmic mirror, we limit ourselves to spiral galaxies and quasars.

For every catalog we obtain several series of pair sets characterized by their positional accuracy with which the locations of the two objects in the pair are opposite on the celestial sphere. The largest set in every series is always in the table for the cosmic lens effect. Tables for the cosmic mirror effect are subsets of tables for the lens effect.

4.1. RCSED (Reference Catalog of Spectral Energy Distributions of Galaxies) Catalog

We begin with the data of the electronic catalogue RCSED (Reference Catalog of Spectral Energy Distributions of galaxies) [36], which became public in 2016. This catalog contains spectroscopic and photometric data for 800,299 galaxies with low and intermediate redshift ($0.007 < z < 0.6$) selected from the Sloan Digital Sky Survey DR7 spectroscopic sample. A special program written to work with this catalog compares declination (*dec*), right ascension (*ra*), and redshift of galaxies (z). It turned out that the information about galaxies in the opposite parts of the sky with respect to celestial equator is extremely uneven. Only 65,610 galaxies (8.2%) out of 800,299 have a negative declination. That is, despite the impressive size of the catalog, we are able to use for our purpose only a small part of its volume which, of course, dramatically reduces the chances of detecting the effects of the cosmic mirror and lens. A second restriction comes from uneven angular distribution of observations done in northern and southern celestial hemispheres. Minimal value of the declination angle in this catalog is only $-11.25°$ what means that all possible candidates for pairs are distributed close to the celestial equator. The last restriction is that for the effect of the cosmic mirror, only spiral galaxies may be taken into account.

First we look for the cosmic mirror effect. With an accuracy of $0.01°$ for *ra* and *dec* and 0.01 for z, we have found 187 pairs of galaxies, composed of 371 galaxies, where three galaxies are found in more than one pair (Appendix A, Table A1). To reduce the number for pair candidates we can require a better accuracy. Within an accuracy of $0.001°$ for *ra* and *dec* and 0.01 for z, we have three pairs of galaxies (Table 1).

Table 1. Pairs of opposite galaxies for the effect of cosmic mirror [36]. Id SDSS DR7—objID identification number in the Sloan Digital Sky Survey. Accuracy is of $0.001°$ for *ra* and *dec* and 0.01 for z.

	Id SDSS DR7	***Ra***	***Dec***	***z***
(1)	587730818432041321	328.93761990	−7.06320875	0.0592138
	587732579378724931	148.93835864	7.06251179	0.0602015
(2)	587726879409635950	311.33617957	−5.13025247	0.100322
	587732703390204231	131.33587944	5.12942269	0.094418
(3)	588848899931963795	224.12922043	−0.10150706	0.376950
	588015509288648969	44.128540880	0.10090797	0.371090

All three pairs of galaxies in Table 1 may be interpreted not as real galaxies, but only as images of the Galaxy on the celestial sphere. All three pairs are not too far from us ($z < 0.4$), so they can be quite "fresh" pictures of the Galaxy (from the recent past), provided they are of spiral type.

Note that the accuracy in z in all three pairs in Table 1 is actually better than 0.006. The first pair has an even better match for z with accuracy value 0.001 (Table 2).

Table 2. The pair with the best positional and redshift accuracy for the effect of cosmic mirror in catalog [36]. Id SDSS DR7—objID identification number in the Sloan Digital Sky Survey. Accuracy is of 0.001° for *ra* and *dec* and 0.001 for z.

	Id SDSS DR7	*ra*	*dec*	*z*
(1)	587730818432041321	328.93761990	−7.06320875	0.0592138
	587732579378724931	148.93835864	7.06251179	0.0602015

RCSED catalog [36] contains also redshift error values *zerr*. For example, the first and second galaxy listed in Table 2 have *zerr* values of 0.000106854 and 0.000167721, respectively. Other objects in this catalog have similar *zerr* values so our search for galaxy pairs requiring they match in redshift z up to 0.001 is reasonable. These redshift values are from SDSS DR7 and in newer data releases they may change. For example, in SDSS DR15 the first galaxy in Table 2 has a listed redshift value z of 0.0591773 with *zerr* value of 0.0000133428. We see that these data are mutually consistent and that newer data are more precise.

However, the spectroscopic observations are not always available to determine an object's redshift with good precision. For faint objects it is very difficult to measure good spectra. In those cases the redshift may be estimated from colors, it is then called the photometric redshift. To illustrate possible differences in precision between outcomes of these two methods, let us take as an example the first galaxy from Table 2 (named SDSS J215545.02-070347.5). Its photometric redshift in DR7 is 0.074914 with error value *zerr* of 0.019358. In DR15 we find photomeric redshift of 0.076662 with *zerr* value of 0.017785. *zerr/z* ratio for photometric redshift is 0.26 in DR7 and 0.23 in DR15. This is 100–1000 times greater than the same ratio computed for spectroscopic redshift values. Our next example is the galaxy with maximum listed redshift value of $z = 0.599891$ (*zerr* = 0.0002402) in RCSED catalog. Its name is SDSS J125400.43+523835.4 and the listed photometric redshifts in DR7 and DR15 are $z = 0.554839$ with *zerr* = 0.018274 and $z = 0.559419$ with *zerr* = 0.026632, respectively. Although *zerr/z* ratio here is slightly better, the spectroscopic redshift value (0.6) is not even in the interval given by z and *zerr* values.

Next we will work also with objects having only photometric redshifts. To be safe, when filtering photometric redshifts, we should not consider the listed redshift values to be "good data" in the sense that at least several most significant digits in z values are valid. Instead, the listed photometric z values should be considered as only estimates of unknown true redshift values. We will work also with some other catalogs, which are collections of objects from various sources. In these catalogs, the situation is even worse, because the order of *zerr* estimations may vary considerably from one source to another and at the same time, we are not sure how good these estimates of z and *zerr* are.

This is why we use also an alternative approach for filtering objects when looking for the effect of cosmic mirror. In this approach for all objects with the listed redshift values we use the same estimate for *zerr* value equal to $z/2$. Redshift z then represents an interval of values from $0.5z$ to $1.5z$, and we consider two objects to be possible pair candidates if their redshift intervals overlap. There are cases when this more conservative approach may actually prove to be more realistic compared to our first approach in which z values are considered to be accurate numbers.

Filtering RCSED catalog [36] in this way with *ra* and *dec* accuracy of 0.001° gives 18 candidate pairs for the effect of cosmic mirror (Appendix A, Table A3). Among them, there are also all three galaxy pairs from Table 1 (pairs 7,9,18).

Requiring a relaxed z accuracy, one can then require better positional accuracy for the effect of cosmic mirror. In RCSED, one has three galaxy pairs with *ra* and *dec* accuracy of 0.0005° (Table 3).

Table 3. Pairs of opposite galaxies for the effect of cosmic mirror [36]—alternative approach. Id SDSS DR7 is objID identification number in the Sloan Digital Sky Survey. Accuracy is of 0.0005° for *ra* and *dec* and *z*/2 for *z*.

	Id SDSS DR7	*Ra*	*Dec*	*z*
(1)	587726879416648036	327.43326873	−7.24482558	0.120794
	587732770503458957	147.43340352	7.24510724	0.172101
(2)	587722981749620931	201.81109033	−1.15290891	0.0672574
	587731514217726115	21.810947880	1.15332655	0.0825304
(3)	588848899373138039	173.86518822	−0.55499635	0.105208
	588015509803565082	353.86519822	0.55470851	0.241575

Let us note that when filtering galaxies which are not too distant (like those in the RCSED catalog) in the search for opposite pairs there is no sense trying to get better positional (angular) accuracy than 0.0001° for *ra* and *dec* parameters. For example, the galaxy SDSS J215545.02-070347.5 (first galaxy in Table 2) has *ra*, *dec* coordinates of 328.93761990, −7.06320875 in DR7 and of 328.937618974, −7.063200482 in DR15. These are actually the same coordinates because their decimal parts have only five significant digits. Although in newer catalogs decimal parts of *ra*, *dec* may have more significant digits, for extended objects like galaxies it has no meaning. For example, when looking at the image of SDSS J215545.02-070347.5 we see its angular size is about 20 arcseconds = 0.0056°. Even the most distant galaxy in the RCSED catalog (SDSS J125400.43+523835.4 mentioned above) has the angular size of several arcseconds and 1 arcsecond = 0.00028°.

When searching for the effect of cosmic lens, it is natural to remove the restriction (filter) on the equality of galaxies redshifts *z*. With an accuracy of 0.01° for *ra* and *dec*, we get 2127 pairs of galaxies, composed of 4174 galaxies (76 galaxies are found in more than one pair). If we restrict ourselves to the accuracy of 0.001° for *ra* and *dec*, we have 22 pairs of galaxies (Appendix A, Table A2). These are all pairs from Table A3 plus four new pairs (1,14,19,22). Within accuracy of 0.0005° for *ra* and *dec*, we get four pairs of galaxies (Table 4).

Table 4. Pairs of opposite galaxies for the effect of cosmic lens [36]. Id SDSS DR7 is objID identification number in the Sloan Digital Sky Survey. Accuracy is of 0.0005° for *ra* and *dec*.

	Id SDSS DR7	*Ra*	*Dec*	*z*
(1)	587726879416648036	327.43326873	−7.24482558	0.120794
	587732770503458957	147.43340352	7.24510724	0.172101
(2)	587722981749620931	201.81109033	−1.15290891	0.0672574
	587731514217726115	21.810947880	1.15332655	0.0825304
(3)	588848899373138039	173.86518822	−0.55499635	0.105208
	588015509803565082	353.86519822	0.55470851	0.241575
(4)	587731511542349980	42.407177420	−0.84245813	0.023485
	587722984443019391	222.40757112	0.84279922	0.211561

Of course, Table 4 must list all pairs from Table 3 plus those pairs which do not fulfill the condition for the redshift values from Table 3. There is only one such pair—number 4.

Note that (1) all pairs in Table 4 are relatively close to us ($z < 0.3$), so each pair can be actually composed of doubled pictures of one nearby galaxy (different in each case); (2) any type of galaxies may be taken into account, the only limitation is that in every pair, both galaxies should be of the same type; so all the four pairs are still possible candidates because their type is still unknown, for now we only know that these eight objects are galaxies.

4.2. Kuminski and Shamir Catalogs

Next we turn to catalogs created by Kuminski and Shamir [37–40] in 2016. These catalogs contain about 3,000,000 galaxies. Catalogs [38,40] are almost of the same size (2,911,899 vs. 2,912,341 objects)

and contain mostly the same objects, differing only by morphological type parameters, calculated by computer algorithm. For our purpose, there is an angular restriction for pair candidates as the minimum declination angle is only −24.9° with only 22.03% of objects having negative declination angles. In the catalog of [39], the possible angular distribution of our pair candidates is even narrower as the minimum declination angle is only −19.7° with only 11.36% from 2,638,883 objects having negative declination angles. Moreover, a lot of objects in the catalog of [39] are classified as stars. The next complication is that many celestial objects (defined by their angular position *ra* and *dec* on the sky) are contained in these catalogs several times with different IDs. As for our purpose the position of an object is a key feature, we need to remove those redundant objects. For the catalogs of [38–40] we found 222,647, 18,739, and 222,655 redundant objects, respectively.

Our search in the catalogs of [38,40] gave the same resulting pair objects. Accordingly, we report only results of searching in the catalog of [40]. Without the redshift parameter in this catalog, we were looking for pair candidates with possible lens effect. With an accuracy of 0.001° for both *ra* and *dec* parameters, we find 1222 pairs of galaxies, composed of 725 galaxies (385 galaxies are found in more than one pair)[1]. If we restrict ourselves to the accuracy of 0.0005° for *ra* and *dec*, we have 605 pairs of galaxies, composed of 265 galaxies (176 galaxies are found in more than one pair). This is still too much uncertainty, so we require even better positional accuracy. Within an accuracy of 0.0002° for *ra* and *dec*, we get 32 pairs of galaxies, composed of 30 galaxies, where 12 galaxies are found in more than one pair (Appendix B, Table A4). For the lens effect both galaxies in a pair should be of the same type. Let us define, that a galaxy is elliptical when parameter "elliptical" > 0.5 and spiral when parameter "spiral" > 0.5. Then from 32 pairs in Table A4, only pairs 3, 6, and 8 are not composed from galaxies of the same type. We are then left with 29 valid candidates for the cosmic lens effect in Table A4.

Finally, searching in [40] for pairs with a positional accuracy of 0.00015° for *ra* and *dec*, we get five pairs of galaxies, composed of eight different galaxies and only two galaxies are found in more than one pair (Table 5).

Table 5. Pairs of galaxies for the effect of cosmic lens [40]. Id SDSS DR8—objID identification number in the Sloan Digital Sky Survey. Accuracy is of 0.00015° for *ra* and *dec*.

	Id SDSS DR8	*Ra*	*Dec*	*Elliptical*	*Spiral*
(1)	1237678888521237047	26.5696157538807	−3.036690882053760	0.009671	0.990329
	1237674469000413487	206.5697430121670	3.036761704248740	0.147295	0.852705
(2)	1237646748740026643	62.1747511145106	−1.016781419414090	0.097682	0.902318
	1237648705676575427	242.1748881053750	1.016716451442130	0.092952	0.907048
(3)	1237646748740026643	62.1747511145106	−1.016781419414090	0.097682	0.902318
	1237648705676575428	242.1748844511030	1.016720360108510	0.078252	0.921748
(4)	1237655177615638991	128.6682349968410	−0.926547264053684	0.883225	0.116775
	1237649942587703356	308.6681411440870	0.926418898103171	0.861631	0.138369
(5)	1237648720134537650	128.6682518312900	−0.926538367783351	0.902699	0.097301
	1237649942587703356	308.6681411440870	0.926418898103171	0.861631	0.138369

It is interesting that every pair in Table 5 has a high probability of both galaxies being of the same type. These five galaxy pairs are thus quite realistic candidates for discovering the cosmic lens effect.

The catalog of [41] adds a photometric redshift parameter *zphot* for objects in [40] and this is what we need to search for possible pair candidates for cosmic mirror effect. With an accuracy of 0.001° for *ra* and *dec* and 0.01 for *zphot* we get 115 pairs of galaxies with 52 galaxies in more than one pair. However, for cosmic mirror effect, both galaxies in pair should be spiral. Again, let us consider galaxy

[1] Let us note that without filtering original catalog to have only unique objects, one would have instead 1533 pairs of galaxies, composed of 802 galaxies where 448 galaxies are in more than one pair. However, only 725 from these 802 galaxies are unique objects so 77 galaxies are repeating objects with different IDs.

to be spiral if parameter "spiral" > 0.5. Then, keeping only spiral galaxies, we are left with 77 candidate pairs for cosmic mirror effect, with 36 objects in more than one pair (Appendix B, Table A5).

If we search the catalog [41] with a better accuracy for *zphot*, namely 0.001, we find seven pairs of galaxies with two galaxies in more than one pair (Table 6).

Table 6. Pairs of galaxies for the effect of cosmic mirror from catalog [41]. Id SDSS DR8—objID identification number in the Sloan Digital Sky Survey. Accuracy is of 0.001° for *ra* and *dec* and 0.001 for *zphot*.

	Id SDSS DR8	*Ra*	*Dec*	*Elliptical*	*Spiral*	*Zphot*
(1)	1237666409525739588	21.8109112443	1.15334613372	0.398	0.602	0.0798
	1237651709428367652	201.811088818	−1.15291424464	0.185	0.815	0.0789
(2)	1237678617427378399	21.8109254471	1.15335605428	0.343	0.657	0.0794
	1237651709428367652	201.811088818	−1.15291424464	0.185	0.815	0.0789
(3)	1237660237652623499	21.8109336601	1.15333316620	0.356	0.644	0.0710
	1237648702974525748	201.811090479	−1.15290686150	0.179	0.821	0.0713
(4)	1237666340801871988	21.8109380881	1.15333261091	0.413	0.587	0.0717
	1237648702974525748	201.811090479	−1.15290686150	0.179	0.821	0.0713
(5)	1237646588221128874	21.8109525056	1.15334337704	0.465	0.535	0.0707
	1237648702974525748	201.811090479	−1.15290686150	0.179	0.821	0.0713
(6)	1237646748740026643	62.1747511145	−1.01678141941	0.098	0.902	0.0756
	1237648705676575428	242.174884451	1.01672036011	0.078	0.922	0.0757
(7)	1237660776104657068	171.086130380	−0.99648723534	0.212	0.788	0.0294
	1237650011315241011	351.087087401	0.99670903212	0.738	0.262	0.0287

Here we searched [41] without filtering out elliptical galaxies. For the cosmic mirror effect we need both galaxies in the pair to be spiral. As we can see, only the seventh pair does not fulfil this condition. However the best probability for both galaxies be of spiral type has the sixth pair. Actually this is the third pair from Table 5 and at the same time it is the only pair from [41] with opposite position accuracy of 0.00015° for *ra* and *dec* and *zphot* accuracy of 0.001 (Table 7).

Table 7. The pair with the best positional accuracy for the effect of cosmic mirror in catalog [41]. At Table 6. this pair has the best probability for both galaxies to be of spiral type. Id SDSS DR8—objID identification number in the Sloan Digital Sky Survey. Accuracy is of 0.00015° for *ra* and *dec* and 0.001 for *zphot*.

	Id SDSS DR8	*Ra*	*Dec*	*Elliptical*	*Spiral*	*Zphot*
(1)	1237646748740026643	62.1747511145	−1.01678141941	0.098	0.902	0.0756
	1237648705676575428	242.174884451	1.01672036011	0.078	0.922	0.0757

An alternative approach (described in Section 4.1) for searching candidate pairs for the effect of cosmic mirror, using only spiral galaxies in the catalog of [41] with positional accuracy of 0.001° for both *ra* and *dec*, gives 171 pairs, with 58 galaxies in more than one pair (Appendix B, Table A6). Three pairs with the best positional accuracy of 0.00015° for both *ra* and *dec* within this approach are collected in Table 8.

Table 8. Pairs with the best positional accuracy for the effect of cosmic mirror in catalog [41]—alternative approach. Id SDSS DR8—objID identification number in the Sloan Digital Sky Survey. Accuracy is of 0.00015° for *ra* and *dec* and *zphot*/2 for *zphot*.

	Id SDSS DR8	*Ra*	*Dec*	*Elliptical*	*Spiral*	*Zphot*
(1)	1237678888521237046	26.5696157538807	−3.036690882053760	0.009671	0.99033	0.0757
	1237674469000413486	206.5697430121670	3.036761704248740	0.147295	0.85271	0.1149
(2)	1237646748740026643	62.1747511145106	−1.016781419414090	0.097682	0.90232	0.0756
	1237648705676575428	242.1748844511030	1.016720360108510	0.078252	0.92175	0.0757
(3)	1237646748740026643	62.1747511145106	−1.016781419414090	0.097682	0.90232	0.0756
	1237648705676575427	242.1748881053750	1.016716451442130	0.092952	0.90705	0.0839

This table should be the subset of Table 5 and indeed it is[2].

Finally we searched the catalog of [39]. In this catalog, parameters whose values are expressed by floating-point numbers have only six significant digits. Therefore, the best accuracy we can reasonably require in right ascension angle is 0.001°. Requiring accuracy 0.001° in *ra* and *dec* with *z* arbitrary we obtain 513 galaxy pairs (25 galaxies in more than one pair) as candidates for the cosmic lens effect, providing both galaxy types in the pair are the same. This is too many candidates to be useful, so we have to make some refinements in our search. We begin by selecting only elliptical galaxies first which we define as objects with parameter "elliptical" > 0.5. Searching for pairs of opposite galaxies in this selection with 1,185,705 objects requiring accuracy 0.001° for both *ra* and *dec* gives 106 pairs with two galaxies in more than one pair (Appendix B, Table A7). Then we select only spiral galaxies, defined as objects with parameter "spiral" > 0.5. Searching in this selection with 274,416 objects with accuracy 0.001° for *ra* and *dec* gives zero number of pairs. Searching with accuracy of 0.005° for *ra* and *dec* gives 58 pairs with two galaxies in more than one pair (Appendix B, Table A8). One can do the same also for stars (we define them as objects with parameter "star" > 0.5). There are 569,643 stars in the catalog. Although stars are too close to us and their angular velocities may be too large to be seriously considered as members of pair candidates, possibly lying on one null-geodesic, it is interesting to do such search just to compare the number of star pairs in catalog with the number of galaxy pairs. With an accuracy of 0.001° for *ra* and *dec* one finds 30 star pairs with two stars in more than one pair (Appendix B, Table A9). One can ask why searching among spiral galaxies with their half count compared to number of stars in this catalog returned no pairs. This is explained by the difference in distribution of stars and galaxies on the celestial sphere. While galaxies are distributed evenly across the whole celestial sphere, most of the stars are located near the celestial equator. With higher density near the celestial equator, stars have a better chance to participate in pairs of opposite objects.

When searching for the cosmic mirror effect, the two opposite galaxies in our pair should be spiral. We have already seen that positional accuracy of opposite spiral pairs in the catalog of [39] is within the limit of 0.005° in *ra* and *dec*. If we add requirement for equal redshift *z* with accuracy of 0.01, we get six pairs (Table 9).

[2] Here and in Table 5 we deliberately list all decimal digits in *ra* and *dec* coordinates to show that the six galaxies in Table 8 are indeed the same galaxies as are in the first three pairs in Table 5. This is true also for the first pair in spite of difference in the last digit of their ID's.

Table 9. Pairs of spiral galaxies for the effect of cosmic mirror [39]. Accuracy is of 0.005° for *ra* and *dec* and 0.01 for *z*. SpecObjID is ID of optical spectroscopic object in SDSS.

	SpecObjID	*Ra*	*Dec*	*z*	*Elliptical*	*Spiral*
(1)	774688716978415616	5.28659	−1.03586	0.1077	0.29	0.71
	324403517626279936	185.29	1.03245	0.0993	0.29	0.71
(2)	743129709168060416	19.6432	−10.9021	0.1409	0.17	0.83
	1911855335291774976	199.642	10.8989	0.1491	0.16	0.84
(3)	1399629972804495360	57.6003	0.0114088	0.0839	0.37	0.63
	385078137475590144	237.596	−0.00662002	0.0830	0.46	0.54
(4)	1393917732184942592	155.36	8.6444	0.0450	0.13	0.87
	809694968183547904	335.363	−8.64717	0.0373	0.24	0.75
(5)	306369326917642240	156.167	0.893717	0.0937	0.41	0.58
	422226519742507008	336.167	−0.897112	0.0990	0.42	0.51
(6)	309696723461105664	161.174	−0.503556	0.1161	0.13	0.87
	425721592429963264	341.171	0.498878	0.1068	0.22	0.78

Some pairs in Table 9 have quite a high probability ratio spiral/elliptical to be considered as serious candidates for the effect of cosmic mirror, even if positional accuracy is not very good. If one requires a better accuracy in *z*, eventually one obtains the best pair in parameters *ra*, *dec*, and *z* (Table 10).

Table 10. Spiral galaxy pair with the best accuracy in *ra*, *dec*, and *z* in catalog [39] for the effect of cosmic mirror. Accuracy is of 0.005° for *ra* and *dec* and 0.001 for *z*. SpecObjID is ID of optical spectroscopic object in SDSS.

	SpecObjID	*Ra*	*Dec*	*z*	*Elliptical*	*Spiral*
(1)	1399629972804495360	57.6003	0.0114088	0.0839	0.37	0.63
	385078137475590144	237.596	−0.00662002	0.0830	0.46	0.54

When using an alternative approach for filtering redshifts of spiral galaxies in catalog [39] for the effect of cosmic mirror, with the same accuracy of 0.005° for *ra* and *dec* one gets 36 candidate pairs (Appendix B, Table A10). This is of course a subset of pair candidates for the effect of cosmic lens in Table A8.

4.3. GAIA Data Release 2 Quasar Catalog

GAIA Data Release 2 [42–44] is based on 22 months of space observations (25 July 2014–23 May 2016). This catalog is known for its most precise astrometric parameters to date. Errors of right ascension, declination, and parallax are given in miliarcsecond units and typical error values are only fractions of mas. Specific to GAIA Data Release 2 celestial object database (compared to other catalogs we searched) is the use of the ICRS reference system, implemented by the International Celestial Reference Frame through the coordinates of a defining set of quasars. Resulting objects coordinates are given in reference epoch J2015.5 unlike old reference standard J2000.0. However, the difference between ICRS coordinates and mean J2000.0 equatorial coordinates is only ≈25 mas = 0.0000069°. This is sufficient for our purpose in the sense that it allows us to identify the same celestial objects across different catalogs, using their position coordinates. Then we can directly compare pairs found in GAIA to pairs from other catalogs.

Although the main objective of GAIA space observatory is to create detailed 3D map of objects in the Milky Way, its database contains many extragalactic objects as well. We are interested in GAIA DR2 quasar catalog database, to which we will refer as GAIADR2Q catalog. A list of 555,934 GAIA DR2 objects (their source_id parameters), matched to the AllWISE AGN catalog can be downloaded from http://cdn.gea.esac.esa.int/Gaia/gdr2/, together with the list of 2880 objects matched to the ICRF3-prototype. However, in the second list, only 935 records are unique, the rest are already contained in the first list. This gives together 556,869 unique GAIA DR2 sources, matched to quasars or

AGNs. The corresponding quasar database (GAIADR2Q) with astrometric and photometric parameters (97 parameters in total) can be downloaded from GAIA archive https://gea.esac.esa.int/archive/.

Being located in space, GAIA observatory produces almost symmetrical data with respect to declination sign. This is in big contrast to the asymmetry of data that is present in all catalogs of the ground-based observatories. Therefore, with a seemingly small volume of 556,869 quasars, we have almost the same number of quasars with negative (271,063 or 48.68%) and positive (285,806 or 51.32%) declinations. Angular distribution of quasars in declination angle is from −89.77° to 89.96°. All this significantly increases the chance of detecting the effects of the cosmic mirror and lens. Unfortunately, the database does not contain redshifts yet.

According to modern ideas, quasar is a pre-galaxy, i.e., a galaxy at an early stage of evolution. Therefore, when searching for opposite pairs of quasars assuming the cosmic mirror effect is real, then the young image of our Galaxy may well be found among these pairs. With the improvement of the quality of observation equipment in the future we would see our Earth and everything that happened on it in the distant past, recorded on null-geodesic as on a film.

Searching in GAIADR2Q catalog for pairs of opposite quasars with positional accuracy of 0.01° in *ra* and *dec* coordinate gives 1945 pairs, with 22 quasars in more than one pair. Searching with accuracy 0.005° in *ra* and *dec* gives 485 pairs, with two quasars in more than one pair. To reduce the count of candidate pairs to a reasonable number, we require a still better positional accuracy. In Table A11 (Appendix C), 17 pairs of opposite quasars with accuracy of opposite positions equal to 0.001° for *ra* and *dec* are given. Unfortunately, the data do not contain the information on the redshifts of quasars, so one cannot separate the quasars involved in the effect of the cosmic mirror from the quasars in the lens effect.

Finally, with an accuracy of 0.0005° in *ra* and *dec*, we get four pairs of quasars for mirror and lens effect (Table 11). The absence of redshift slightly reduces the effect of the result, but we can say that all of these four pairs can participate in the effect of the cosmic lens.

Table 11. Pairs of quasars from GAIADR2Q catalog for mirror and lens effects. Source_id—the unique identification number in GAIA DR2 database. Accuracy is of 0.0005° for *ra* and *dec*. Redshift *z* is unknown.

	Allwise_Name	*Source_Id*	*Ra*	*Dec*
(1)	J210304.14-762224.9	6368528062846000640	315.7673682	−76.37360527
	J090304.41+762224.0	1125452302531483520	135.7684166	76.37343393
(2)	J120429.60-215735.5	3493448195802870400	181.1233688	−21.95989953
	J000429.68+215736.0	2847161965440082176	1.123715043	21.9600063
(3)	J124510.71-180851.9	3522237773904469248	191.294554	−18.1478664
	J004510.62+180851.9	2782801120299995520	11.29451879	18.14802663
(4)	J035733.19-083041.3	3194958963846806144	59.38814002	−8.511587953
	J155733.13+083042.9	4454299557503538688	239.3880677	8.511930041

As quasars are point-like objects on the celestial sphere, it is important that their positions in the GAIADR2Q catalog are determined with an error (of order of 1 mas = 2.78×10^{-7} degrees), which is much smaller compared to the accuracy (0.0005°) with which objects in pairs are opposite.

4.4. Milliquas 6.3 Catalog

The Million Quasars (MILLIQUAS) catalog is maintained by Eric W. Flesch [45]. We have used the version 6.3 (16 June 2019) [46,47]. This version already uses GAIA-DR2 astrometry where available (approx. 63% of all objects in database). The number of used decimals in right ascension and declination coordinates is seven, which can then (for those 63% of all objects) be considered as a number of significant digits in the fraction part of coordinates.

Milliquas 6.3 database contains 1,986,800 objects, 525,349 (26.44%) with negative declination and 1,461,451 (73.56%) with positive declination. Positional distribution is over the whole sky, with declination values from −89.77° to 89.96°, the same as in GAIADR2Q.

We first search for pair candidates for the effect of cosmic lens. It means that we are interested only in positional accuracy with which two objects in pair are opposite and ignore their redshifts. Search with accuracy 0.01° for *ra* and *dec* gives 23,024 pairs with 1037 objects in more than one pair. This is nearly 12× more compared to the same search in GAIADR2Q catalog. Next we require the accuracy of 0.001° for *ra* and *dec*. This gives 219 pairs with every object in only one pair (Appendix D, Table A12). One can now compare Table A12 with Table A11 where corresponding 17 pairs from GAIA DR2 are given. We see that pairs 1, 2 in Table A11 are the same as pairs 2, 3 in Table A12. Pair 3 from Table A11 is missing in Table A12. Then pairs 4, 5 in Table A11 are the same as pairs 8, 9 in Table A12. Pairs 6, 7 in Table A11 looks almost like pairs 27, 29 in Table A12, but they are not the same. Thus, we see that not all quasars from GAIADR2Q catalog are contained in Milliquas 6.3 catalog as well.

Search with an accuracy 0.0005° for *ra* and *dec* gives 50 candidate pairs for the cosmic lens effect (Appendix D, Table A13). Comparing Table A13 with Table 11 we see that number of corresponding pairs in GAIADR2Q is only four. Pairs 1, 2, 4 in Table 11 are the same as pairs 1, 21, 29 in Table A13. Pair 3 from Table 11 is similar to pair 23 in Table A13, but they are not the same.

Eventually we searched Milliquas 6.3 with an accuracy 0.0001° for *ra* and *dec* which gives two pairs (Table 12).

Table 12. Pairs of quasars from Milliquas 6.3 catalog with the best positional accuracy for lens effect. Accuracy is of 0.0001° for *ra* and *dec*. Descrip column is the classification of object, see [47]. Redshift *z* is given, although not essential here.

	Ra	*Dec*	*Name*	*Descrip*	*z*
(1)	75.7744245	−40.7936211	WISEA J050305.91-404736.8	q	2.3
	255.7743683	40.7937126	SDSS J170305.84+404737.3	q	0.3
(2)	43.6995104	−17.1177057	WISEA J025447.88-170703.8	q	1.9
	223.699538	17.1176163	SDSS J145447.88+170703.4	q	1.1

These two pairs are not found in the GAIADR2Q catalog, because it contains only the first and the third quasar from Table 12. However, the number of significant digits in coordinates of second and fourth quasar in Table 12 may be questioned. Hopefully, the GAIA DR3 database will have also these two quasars so their coordinates will be known with better accuracy.

We now turn to the search for pair candidates for the effect of cosmic mirror. Objects in Milliquas 6.3 catalog are collected from various sources so redshift values are computed by various methods and with different relative errors. Thus, some redshifts in catalog are rounded to 0.1*z*, while others may have error up to 0.5*z*. Many redshift values in Milliquas 6.3 are estimated by Eric W. Flesch using the four-color based method described in his original HMQ article [45] Appendix 2. Therefore, although Milliquas 6.3 gives redshift values for 1,906,535 objects, it is hard to compare them using some kind of fixed filter value. We used 0.2 as the best redshift accuracy we can reasonably have and even this value may be too optimistic.

We begin with an accuracy of 0.001° for *ra* and *dec* and 0.2 for *z*. Search in Milliquas 6.3 then gives 27 pairs (Appendix D, Table A14). Search with an accuracy of 0.0005° for *ra* and *dec* and 0.2 for *z* gives four pairs (Table 13).

Table 13. Pairs of opposite quasars with the best accuracy in position and redshift found in Milliquas 6.3 catalog as candidate pairs for cosmic mirror effect. Accuracy is of 0.0005° for *ra* and *dec* and 0.2 for *z*. Descrip column is the classification of object, see [47].

	Ra	*Dec*	*Name*	*Descrip*	*z*	*Rmag*	*Bmag*
(1)	5.8514071	−7.0936418	SDSS J002324.33-070537.1	q	0.6	21.75	21.73
	185.8513794	7.093749	SDSS J122324.33+070537.4	qX	0.6	21.82	21.61
(2)	356.0054037	−4.4881222	SDSS J234401.30-042917.1	q	2.1	19.79	20.52
	176.0057901	4.4880115	SDSS J114401.38+042916.8	q	2.2	21.32	21.32
(3)	215.9122427	−3.1485981	SDSS J142338.93-030854.9	q	2	21.54	21.34
	35.911743	3.1485686	SDSS J022338.81+030854.7	q	2.173	20.03	20.59
(4)	148.4235067	−0.1395639	2QZ J095341.5-000822	q	0.284	19.06	19.96
	328.4236129	0.1398213	SDSS J215341.66+000823.3	q	0.1	22.55	23.38

Here we added two columns ***Rmag***, ***Bmag*** to show also red and blue colors magnitudes to see striking similarity in these parameters in the first pair, which has also the best match in redshift.

We now repeat our search in Milliquas 6.3 database for the effect of cosmic mirror with an alternative filtering of redshift, described in Section 4.1. With an accuracy of 0.001° for *ra* and *dec* we found 135 pairs (Appendix D, Table A15). Requiring the accuracy of 0.0005° for *ra* and *dec* we found 30 pairs (Appendix D, Table A16). The pair with the best positional accuracy of 0.0001° for *ra* and *dec* is listed in Table 14. As always, every table created by alternative filtering of redshift is a subset of corresponding set of pairs for the lens effect with the same positional accuracy.

Table 14. Pair of quasars from Milliquas 6.3 catalog with the best positional accuracy for mirror effect—alternative approach. Accuracy is of 0.0001° for *ra* and *dec* and *z*/2 for *z*. Descrip column is the classification of object, see [47]. Redshift *z* is given, although not essential here.

	Ra	*Dec*	*Name*	*Descrip*	*z*
(1)	43.6995104	−17.1177057	WISEA J025447.88-170703.8	q	1.9
	223.699538	17.1176163	SDSS J145447.88+170703.4	q	1.1

4.5. KQCG (Known Quasars Catalog for GAIA Mission)

Authors of catalog [48] compiled QSOs and AGNs from several sources, resulting in 1,842,076 objects in total. According to the authors, the purpose of this compilation is to provide positions of known QSOs, which can be used for cross matching with the GAIA observations.

After removing two objects with duplicate positions, the KQCG catalog has actually 1,842,074 unique objects, 595,535 of them with redshift value. There are 721,960 objects (39.19%) with negative declination and 1,120,114 objects (60.81%) with positive declinaton. The catalog has good declination angle distribution (from −89.82° to 89.97°).

When searching for pair candidates for the effect of cosmic lens, we first search KQCG catalog with the accuracy of 0.01° for *ra* and *dec* which gives 19,250 pairs with 849 objects in more than one pair. Search with an accuracy of 0.001° for *ra* and *dec* gives 167 pairs with three objects in more than one pair (Appendix E, Table A17). When searching with accuracy of 0.0005° for *ra* and *dec* one gets 36 pairs (Appendix E, Table A18). The best positional accuracy we can achieve here is 0.0001° for *ra* and *dec* which gives two pairs (Table 15).

Table 15. Pairs of opposite quasars from the KQCG catalog [48] with the best positional accuracy for the lens effect. Accuracy is of 0.0001° for *ra* and *dec*. Redshift *z* is given when available, although not essential here.

	Name	*Ra*	*Dec*	*z*
(1)	J013702.04-513252.3	24.2585004	−51.5478865	
	133702.07+513252.1	204.2586596	51.54780646	3.123
(2)	J035233.36-211221.7	58.1390267	−21.2060385	
	J155233.38+211221.7	238.1391178	21.2060426	

Next we are looking for opposite quasar pair candidates for the effect of cosmic mirror. With only one-third of objects in KQCG database having nonempty redshift value, we can not expect big numbers of pairs. Search with an accuracy of 0.01° for *ra* and *dec* and 0.1 for *z* gives 109 pairs (Appendix E, Table A19). Search with an accuracy of 0.001° for *ra* and *dec* and 0.1 for *z* gives only three pairs (Table 16).

Table 16. Pairs of opposite quasars from the KQCG catalog [48] with the best accuracy in position and redshift for the cosmic mirror effect. Accuracy is of 0.001° for *ra* and *dec* and 0.1 for *z*.

	Name	*Ra*	*Dec*	*z*
(1)	LQAC_179-001_037	179.9377083	−1.372166667	1.2752
	235945.22+012216.3	359.9384346	1.371206026	1.2224771
(2)	004034.86-003821.0	10.14525273	−0.63918039	1.8359182
	LQAC_190+000_011	190.1443333	0.638194444	1.8557
(3)	LQAC_352-000_049	352.8172404	−0.117229211	1.69638
	LQAC_172+000_041	172.8182083	0.118	1.7844

The last quasar in Table 16 may not have a required precision in the *dec* coordinate so the third pair in that table should be taken with care.

An alternative filtering of redshift for quasar pairs with a positional accuracy of 0.001° for *ra* and *dec* gives 16 pairs (Appendix E, Table A20). Three pairs with the best possible positional accuracy of 0.0005° in *ra* and *dec* are listed in Table 17.

Table 17. Pairs of opposite quasars from the KQCG catalog [48] as candidates for the cosmic mirror effect with the best positional accuracy—alternative approach. Accuracy is of 0.0005° for *ra* and *dec* and *z*/2 for *z*.

	Name	*Ra*	*Dec*	*z*
(1)	LQAC_038-009_025	38.5649606	−9.392240877	3.15853
	LQAC_218+009_031	218.5647428	9.392719278	1.79609
(2)	022538.91-012519.8	36.41214596	−1.422178345	0.7273704
	LQAC_216+001_018	216.4125417	1.4225	1.1363
(3)	LQAC_322-001_003	322.04071	−1.110389	2.0165
	LQAC_142+001_019	142.0406947	1.109906236	0.69137

5. Numerical Experiments

We searched several databases of galaxies and quasars for the presence of pairs of objects, with opposite location on the sky sphere and with certain angular accuracy. This is main feature of the null geodesics which reveals their existence in our part of the Universe. However, in a large sample of celestial objects, pairs of opposite objects may exist by pure chance also in a non-rotating Universe. With rotation, their number just should be greater and the difference should be due to the presence of closed null geodesics.

Therefore it would be useful if we could estimate number of pair objects in our part of the Universe considering the standard three-dimensional space without rotation using randomly generated objects

positions on the celestial sphere. For each real global catalog, we can create a set of randomized counterparts with the same number of objects. Then, their filtering with a certain angular precision in *dec* and *ra* coordinates, will give us a set of counts of opposite pairs, from which we can estimate the corresponding values for the real world catalogs in the case of a non-rotating Universe.

Let us begin with the RCSED catalog. Although it contains 800,299 galaxies, they are located mostly on the northern part of the celestial sphere and only 221,502 of them, located within the interval from −11.25° to 11.25° in *dec* angle have a chance to participate in opposite pairs. Therefore it makes sense to create random catalogs of only 221,502 objects, located randomly in *dec* interval from −11.25° to 11.25°. Results of this simulation with four random catalogs are collected in Table 18.

Table 18. Number of opposite pairs for selected angular accuracy values *eps* in the Reference Catalog of Spectral Energy Distributions of galaxies (RCSED) catalog and in four random catalogs with objects evenly distributed on the celestial sphere within interval of *dec* values from −11.25° to 11.25°.

Eps	*0.1*	*0.01*	*0.005*	*0.001*	*0.0005*	*0.0001*	*№ of Objects*	*Dec Interval*
RCSED	214,050	2127	542	22	4	0	800,299	−11.25 . . . 70.29
Random 1	121,672	1204	288	14	2	0	221,502	−11.25 ... 11.25
Random 2	121,918	1261	332	14	4	0	221,502	−11.25 ... 11.25
Random 3	121,391	1269	323	14	4	0	221,502	−11.25 ... 11.25
Random 4	121,263	1250	284	11	0	0	221,502	−11.25 ... 11.25
Random 5	121,192	1163	288	6	0	0	221,502	−11.25 ... 11.26

Apparently the RCSED catalog contains a suspiciously large number of opposite pairs. However this has nothing to do with closed null geodesics. It only means that objects in the RCSED catalog within *dec* interval from −11.25° to 11.25° are not evenly randomly distributed in the *dec* coordinate. Of course this is due to the fact that data in the RCSED catalog were obtained in observatories located mostly on the northern hemisphere. The value of *eps* = 0.1 is not suitable for the search of closed null geodesics, because it corresponds to cone with too wide solid angle. However, it is useful for testing if our random catalogs correspond to the real world catalog[3]. Objects located on the null geodesic should be opposite with good angular accuracy so for our purpose values of *eps* from 0.001 to 0.0001 are more useful. For such *eps* values, our random catalogs and RCSED catalog give similar numbers of pairs. However, we should consider this with caution, because we know from results for *eps* = 0.1 that our random catalogs do not emulate real world data in the RCSED catalog.

Our simple experiment with evenly distributed random catalogs does not help to decide if the data in the RCSED catalog could indicate the possible presence of null geodesics. The situation is similar for other catalogs with the data from the Earth-based observatories. Fortunately, the GAIA observatory is located in space so we can expect better angular distribution of quasars in the GAIA DR2 catalog.

Let us then repeat our numerical experiment with evenly distributed random catalogs for the GAIA DR2 quasar catalog. Objects in this catalog have *dec* positions from −89.77° to 89.96° so our random catalogs can use the full range of *dec* coordinates and they should have the same number of objects as the GAIA DR2 catalog (Table 19).

[3] It also tests our filtering which, for evenly distributed objects, should give approximately 100-times less pairs when *eps* decreases 10 times.

Table 19. Number of opposite pairs for selected angular accuracy values *eps* in GAIA DR2 quasar catalog and five random catalogs with the same number of objects, evenly randomly distributed on the celestial sphere.

Eps	*0.1*	*0.01*	*0.005*	*0.001*	*0.0005*	*0.0001*
GAIADR2Q	198,621	1945	485	17	4	0
Random 1	150,489	1506	401	15	5	0
Random 2	150,358	1512	381	15	3	0
Random 3	150,550	1495	382	13	5	0
Random 4	151,013	1520	372	14	4	1
Random 5	150,306	1503	357	16	6	0

Again we see that, although for small *eps* values, opposite pairs counts in the GAIA DR2 catalog are similar to those from random catalogs, results for higher *eps* values are different. This is due to the fact that objects positions in the GAIA DR2 catalog are not quite evenly distributed across the celestial sphere. Indeed, the histogram of GAIA DR2 *dec* angular position values shows the difference from an ideal angular distribution in *dec* angle, represented by the cosine function (Figure 5). We should expect also some deviation from an ideal (linear) distribution of the *ra* coordinate since GAIA cannot see quasars hidden behind the Milky way.

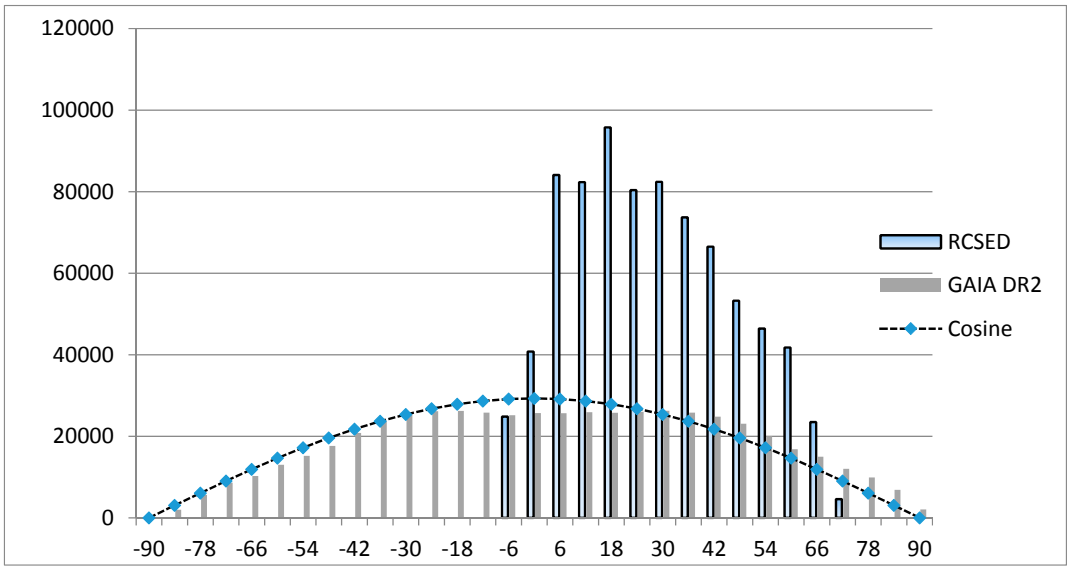

Figure 5. Histograms of *dec* coordinate distribution in RCSED and GAIA DR2 quasar catalogs. While Table 2. catalog shows some difference from an ideal *dec* angular distribution represented by the cosine function, the histogram of RCSED catalog clearly demonstrates its big angular nonuniformity.

This means that our test catalogs with evenly distributed random positions on the celestial sphere are not good emulations of GAIA DR2 positions data.

Since in all real world catalogs which we processed in Section 4, the number of opposite pairs for small *eps* values is very small, to find some hints for the presence of closed null geodesics, we should use as good random catalogs as possible. On a large angular scale, positions in a reasonably good test catalog should copy deviations of the real world catalog from ideal angular distribution. On a small scale, its angular positions should be distributed randomly.

The following two tables summarize the results of such a simulation for two different angular distributions. The first (Table 20) is simulating an uneven angular distribution in the RCSED catalog. The second (Table 21) is a simulation of an almost evenly distributed quasars in the GAIA DR2 catalog. Every random catalog named RandomN_x where x = 1, . . . , 5 contains the same number of positions as its real world counterpart, distributed to an Nx2N angular mesh in *dec* and *ra* coordinates with

number of objects in every cell which copies the corresponding real world catalog. In order to provide a sufficient space for local randomness, we limited the range of N to a maximum of 180 mesh cells in *dec* coordinate (and 360 cells in *ra* coordinate).

Table 20. Number of opposite pairs for selected angular accuracy values *eps* in the RCSED catalog and in several random catalogs with the same number of objects and the same angular distribution on the celestial sphere.

Eps	*0.1*	*0.01*	*0.005*	*0.001*	*0.0005*	*0.0001*
RCSED	214,050	2127	542	22	4	0
Random18_1	176,055	1676	417	21	4	2
Random18_2	176,584	1723	440	20	6	1
Random18_3	175,916	1728	428	22	9	0
Random18_4	176,006	1826	429	15	6	0
Random18_5	175,810	1789	425	13	4	0
Random30_1	185,460	1794	423	14	5	1
Random30_2	185,681	1881	467	26	7	0
Random30_3	187,713	1827	428	20	8	1
Random30_4	185,976	1862	466	18	5	0
Random30_5	184,818	1883	462	17	4	0
Random90_1	208,266	2062	496	27	11	0
Random90_2	208,645	2092	562	23	6	0
Random90_3	207,692	2051	491	22	4	0
Random90_4	208,046	2029	513	15	6	0
Random90_5	208,289	2077	517	25	10	1
Random180_1	212,404	2107	591	32	11	1
Random180_2	213,252	2201	559	22	4	0
Random180_3	212,848	2080	529	29	7	1
Random180_4	212,768	2077	482	16	5	0
Random180_5	213,511	2077	529	19	8	1
Average of 20 runs with N = 180				**21.95**	**5.3**	**0.15**
Standard deviation				**3.43**	**1.95**	**0.36**

Table 21. Number of opposite pairs for selected angular accuracy values *eps* in the GAIA DR2 quasar catalog and in several random catalogs with the same number of objects and the same angular distribution on the celestial sphere.

Eps	*0.1*	*0.01*	*0.005*	*0.001*	*0.0005*	*0.0001*
GAIADR2	198,621	1945	485	17	4	0
Random18_1	196,114	1893	483	17	3	0
Random18_2	197,388	1972	479	16	5	0
Random18_3	196,415	1972	502	18	4	1
Random18_4	197,010	1984	475	22	3	0
Random18_5	198,107	1961	511	12	2	0
Random30_1	196,396	1979	470	16	2	0
Random30_2	198,441	2039	491	17	4	0
Random30_3	198,034	1926	476	19	5	0
Random30_4	198,060	2009	490	21	5	0
Random30_5	198,763	1984	510	23	3	0
Random90_1	198,481	2020	491	11	2	0
Random90_2	198,438	2044	500	21	7	0
Random90_3	197,632	2020	517	21	2	0
Random90_4	198,300	1958	472	20	2	0
Random90_5	199,184	1967	501	23	4	0
Random180_1	197,900	1888	489	14	4	1
Random180_2	198,556	2002	511	21	2	0
Random180_3	198,563	2007	487	18	5	0

Table 21. *Cont.*

Eps	*0.1*	*0.01*	*0.005*	*0.001*	*0.0005*	*0.0001*
Random180_4	199,210	1980	492	21	7	0
Random180_5	199,532	1962	499	19	4	0
Average of 20 runs with N = 180				**19.2**	**4.65**	**0.5**
Standard deviation				**3.72**	**1.49**	**0.81**

As expected, with higher number of mesh cells, the number of opposite pairs for larger *eps* values in random catalogs is closer to the corresponding values of the real world catalog. Thus random catalog with a more detailed angular mesh is indeed a better simulation of the real world catalog. Next, we see that the better the uniform angular distribution of the real world catalog, the less detailed mesh is needed for a good reproduction of its opposite pairs number for given *eps* value.

Tables with filtering results for real world catalogs together with data from of our random catalogs have a twofold purpose. Firstly, they show that our simulation catalogs can be useful as imitations of real world catalogs. Secondly, for large N values they show how the numbers of opposite pairs for the given real world catalog should look like in the case of a non-rotating Universe. To give a better prediction for the case of a non-rotating Universe, we attached two lines with results of 20 simulations using random catalogs with N = 180 for small *eps* values, together with corresponding standard deviation values.

In Tables 17 and 18 we see that, in RCSED and GAIA DR2 catalogs, the observed number of pairs for small *eps* value does not exceed predicted values for a non-rotating Universe. However, it is not clear, if those *eps* values are small enough for our task, because observing null geodesics may require a very narrow observation cone. To register the presence of closed null geodesics, we need to estimate number of pairs in a non-rotating Universe for as small *eps* values as possible. From our random catalogs we see the feature shared with the real world catalogs, namely that number of opposite pairs for small *eps* values can be predicted from the number of pairs for greater *eps* values. If, for example, number of pairs for *eps* = 0.1 is 200,000, then we can expect about 20 pairs for *eps* = 0.001. This feature is expected for evenly distributed objects and from our simulations we see it remains valid for non-even angular distributions as well.

To observe several pairs for *eps* = 0.0001, we need hundreds of pairs for *eps* = 0.001 and millions for *eps* = 0.1. Therefore, let us proceed to emulate larger databases.

The biggest database we are dealing here with is Kuminski and Shamir [38–40]. We chose the catalog of [40], cleaned from repeated objects, containing only galaxies (and not stars like in [39]). The number of objects is 26,899,686 and *dec* values start at −24.93. Here we are filtering it without distinguishing galaxy type (Table 22).

Table 22. Number of opposite pairs for selected angular accuracy values *eps* in Kuminski and Shamir catalog [40] and in several random catalogs with the same number of objects and the same angular distribution on the celestial sphere.

Eps	*0.1*	*0.01*	*0.005*	*0.001*	*0.0005*	*0.0001*
K&S [40]	7,612,266	76,867	18,024	1222	605	0
Random18_1	4,475,466	45,104	11,333	441	126	7
Random18_2	4,468,199	44,838	11,320	456	114	6
Random18_3	4,526,555	44,884	11,162	448	118	2
Random18_4	4,475,244	44,714	11,163	462	113	4
Random18_5	4,478,613	44,762	11,166	473	137	6

Table 22. *Cont.*

Eps	*0.1*	*0.01*	*0.005*	*0.001*	*0.0005*	*0.0001*
Random90_1	6,533,538	65,955	16,568	720	185	6
Random90_2	6,534,673	65,300	16,417	616	161	6
Random90_3	6,538,237	65,311	16,266	674	187	5
Random90_4	6,538,688	65,529	16,250	663	155	5
Random90_5	6,536,033	65,938	16,531	643	152	8
Random180_1	7,005,872	70,357	17,657	702	178	3
Random180_2	7,010,050	70,260	17,538	663	172	6
Random180_3	7,006,156	70,465	17,578	729	174	6
Random180_4	7,008,239	70,197	17,455	678	182	3
Random180_5	7,006,665	70,257	17,669	708	178	11
Average of 20 runs with N = 180				**697.3**	**174.5**	**7.35**
Standard deviation				**26.7**	**13.8**	**2.52**

From Table 22 we see that according to our random catalogs, number of pairs for *eps* = 0.0001 should be about seven. However, we found zero pairs in [40], although for close *eps* value of 0.0002 (not in the table) we found 32 pairs. On the other hand, the number of pairs for *eps* = 0.0005, 0.001 is too large compared to our random catalogs. Finally, while data in the first row for *eps* = 0.1–0.005 follow the approximate square rule dependence of pairs numbers on *eps* (like 7,612,266/76,867 $\approx (0.1/0.01)^2$), data for *eps* = 0.001–0.0001 do not follow this rule.

We have no explanation for these strange results of catalog [40] filtering. Our random catalogs have the same number of objects and the same angular distribution. Nevertheless, the number of opposite objects for *eps* values 0.001, 0.0005, 0.0001 is quite different even for detailed angular mesh. While it may be just large statistical deviations, we did not see such behavior in other catalogs.

Next we will emulate the quasar catalog Milliquas 6.3. Its angular distribution is not far from uniform so it should be easy to reproduce outcomes of its filtration with our random catalogs. The results are in Table 23.

Table 23. Number of opposite pairs for selected angular accuracy values *eps* in the Milliquas 6.3 catalog and in several random catalogs with the same number of objects and the same angular distribution on the celestial sphere.

Eps	*0.1*	*0.01*	*0.005*	*0.001*	*0.0005*	*0.0001*
Milliquas 6.3	2,272,887	23,024	5795	219	50	2
Random90_1	2,261,589	22,473	5564	214	60	1
Random90_2	2,259,751	22,559	5581	215	66	3
Random90_3	2,261,151	22,391	5496	245	70	2
Random90_4	2,262,077	22,672	5702	264	55	2
Random90_5	2,262,742	22,643	5683	239	59	2
Random180_1	2,270,577	22,426	5527	219	59	2
Random180_2	2,270,319	22,829	5722	219	59	2
Random180_3	2,269,632	22,637	5630	224	53	3
Random180_4	2,270,186	23,136	5814	233	48	1
Random180_5	2,270,844	22,680	5738	237	59	1
Average of 20 runs with N = 180				**225.7**	**57.25**	**2.3**
Standard deviation				**13.28**	**8.12**	**1.7**

According to our simulations, the number of opposite pairs in Milliquas 6.3 catalog for small *eps* values is standard for a non-rotating Universe so there is no evidence for the presence of closed null geodesics.

Our last studied database is the the KQCG quasar catalog (Table 24).

Table 24. Number of opposite pairs for selected angular accuracy values *eps* in the KQCG catalog and in several random catalogs with the same number of objects and the same angular distribution on the celestial sphere.

Eps	***0.1***	***0.01***	***0.005***	***0.001***	***0.0005***	***0.0001***
KQCG	1,933,692	19,250	4735	167	36	2
Random90_1	1,930,091	19,298	4838	217	49	3
Random90_2	1,928,432	19,588	4806	201	50	5
Random90_3	1,930,965	19,463	4774	191	46	1
Random90_4	1,927,537	19,340	4821	196	48	0
Random90_5	1,930,231	19,183	4787	189	50	2
Random180_1	1,929,688	19,326	4745	182	53	2
Random180_2	1,933,921	19,436	4810	175	49	4
Random180_3	1,931,871	19,442	4892	213	43	3
Random180_4	1,930,751	19,212	4800	206	53	1
Random180_5	1,934,750	19,483	4785	161	36	4
Average of 20 runs with N = 180				**190.9**	**47.8**	**1.5**
Standard deviation				**16.14**	**6**	**1.2**

Again numbers of observed opposite pairs in KQCG catalog for small *eps* values are not greater than corresponding estimations from the analysis of similar random databases. We should therefore conclude that observations cannot be definitely interpreted as a consequence of the presence of closed null geodesics in our part of Universe.

We conclude this section with two remarks.

Firstly, in order to get better statistics for small *eps* values, we need bigger catalogs than are available today. Only then there is a hope to see them on the background of random coincidence where two objects are opposite just by chance.

Secondly, perhaps one does not need statistical methods at all. When the number of closed null geodesics is very small, say one or two, what we actually need is to observe the opposite pair in which both objects are astrophysically identified as being the images of the same cosmic object, possibly from different time of its evolution. Astrophysical analysis is even more important than the angular accuracy with which the two objects are opposite, as a light path across the Universe may be diverted by gravitational lensing of other cosmic objects. For example, let us consider the first quasar pair in Table 13. These two quasars are not only opposite with a good accuracy, but also have close values of *Rmag*, *Bmag* and redshift z parameters as well. This may well be a pure coincidence and a further astrophysical analysis may eventually prove that they are different objects. However, if one finds a similar pair and the two images are indeed from the same object, then one should seriously consider the existence of a closed null geodesic even for a single pair. If a small number of closed null geodesics is a reality, then we need to catalogize a very large number of distant cosmic objects and be lucky to find two of them located precisely on such geodesic.

6. Conclusions

The study of the rotational and chiral phenomena is of fundamental importance in astrophysics, high-energy physics, and the heavy-ion collisions [49–51]. In particular, it is worthwhile to mention the recent discovery of observational evidence for the coherence between galaxy rotation and neighbor rotational motions on the scale of several megaparsecs [16,17]. Moreover, the search for the similarities of vortex structures in the heavy-ion physics and in astrophysical conditions attracts considerable attention in the current research [52–55].

Here we considered possible observational manifestations of the global cosmic rotation. The goal of our analysis of modern electronic catalogues of galaxies and quasars was to find, among the observed galaxies and quasars, pairs of images that might not be real different objects, but instead that could be several images of a single object. This might have been a demonstration that the Universe is

not only expanding, but also rotating. Our analysis of the number of opposite pairs did not find a clear statistical evidence of the global rotation. However, currently available catalogs are far from being perfect. They collect only a small number of very distant celestial objects with an uneven angular distribution (except for the GAIA DR2 quasar catalog). Therefore further work is needed in order to verify and improve our current results for bigger catalogs with better distribution of objects. One cannot exclude a possibility that an appearance of closed null geodesics, as a manifestation of the cosmic rotation, is rare and is not statistically significant. In that case, one needs more thorough astrophysical observations which could reveal that two opposite objects are actually images of the same object, possibly in different epoch of its evolution.

Author Contributions: Conceptualization, methodology: Y.N.O. and V.A.K.; validation, formal analysis, investigation: V.A.K. (analytical part) and E.M. (numerical part); software and data processing: E.M.; writing—original draft preparation: V.A.K. (analytical part), Y.N.O. (analytical part), E.M. (numerical part); writing—review and editing: V.A.K., E.M., and Y.N.O.; supervision, project administration: Y.N.O. All authors have read and agreed to the published version of the manuscript.

Funding: For Y.N.O. this work was partially supported by the Russian Foundation for Basic Research (Grant No. 18-02-40056-mega).

Acknowledgments: Y.N.O. and V.A.K. are grateful to Inna Sandina for the fruitful discussions and Danil Kuznetsov for the stimulating interest in the work and helpful advice. The authors thank the anonymous referees for the valuable comments and suggestions.

Conflicts of Interest: The authors declare no conflict of interest.

Appendix A

Table A1. Pairs of galaxies for the effect of cosmic mirror [36]. *Id SDSS DR7* is objID identification number in the Sloan Digital Sky Survey. Accuracy is of 0.01° for *ra* and *dec* and 0.01 for *z*. Pair is a valid candidate for the effect only if both galaxies in the pair are spiral.

	Id SDSS DR7	*Ra*	*Dec*	*z*
(1)	587727177915301989	6.31801788	−11.12899674	0.164466
	587734894366425177	186.3215957	11.12945461	0.167687
(2)	587727177911304300	356.9463884	−11.1131664	0.11336
	587734894362427519	176.9362082	11.12183186	0.10569
(3)	587727177915367567	6.473508	−11.08978967	0.109483
	587734894366490714	186.4752183	11.09098806	0.103002
(4)	587727225157451822	9.78490157	−10.97586123	0.0656358
	587732772669292660	189.7803892	10.98178272	0.0667346
(5)	587727177921069125	19.65932903	−10.93368609	0.141083
	588017569241432335	199.6689547	10.93044205	0.145941
(6)	587727177921069119	19.64324854	−10.90207866	0.140991
	588017569241432309	199.6421776	10.89885453	0.149119
(7)	587727225157779575	10.47400922	−10.89314855	0.115176
	587732772669554736	190.4693767	10.88349483	0.113392
(8)	587727873696006248	354.4140938	−10.76728771	0.0980759
	587732772662673520	174.4078391	10.76580767	0.0941737
(9)	587727178450665633	2.84320186	−10.72060849	0.0626986
	587734893828112436	182.834768	10.72901371	0.0684232
(10)	587727178453483585	9.28275768	−10.70100563	0.130024
	587734893830864981	189.2821245	10.70562335	0.128155
(11)	587727178451452024	4.57186615	−10.67135056	0.061156
	587734893828833380	184.568407	10.66631434	0.0513871
(12)	587727225693536361	7.83605949	−10.59958384	0.0905357
	587732772131569821	187.8259964	10.59469904	0.0927822
(13)	587727229447962769	23.72675428	−10.51170548	0.0992561
	587736543623839915	203.7347943	10.50510464	0.103054

Table A1. *Cont.*

	Id SDSS DR7	*Ra*	*Dec*	*z*
(14)	587727178458333267	20.61377325	−10.47315078	0.109546
	587736543622529169	200.6164952	10.48116533	0.10888
(15)	587727229448028286	23.8634114	−10.4420383	0.0872344
	587736543623905435	203.8644965	10.44923329	0.083543
(16)	587727874233335894	355.4913684	−10.41356256	0.0980471
	587732772126261484	175.4967819	10.419777	0.106774
(17)	587727178459644099	23.56363216	−10.30676641	0.087484
	588017992299970676	203.560364	10.29826366	0.0842322
(18)	587727874232942672	354.5407195	−10.2905162	0.115404
	587732772125802696	174.5311941	10.29906788	0.112148
(19)	587727178989240463	6.75089715	−10.28452672	0.141096
	587734893292879988	186.7541572	10.2905859	0.138833
(20)	587727178459775095	23.99049618	−10.24662329	0.16844
	588017992300167307	203.9854969	10.23670831	0.159882
(21)	587727178992320618	13.92268478	−10.23798263	0.0545347
	588017991758970941	193.9286925	10.23919618	0.0576316
(22)	587726877275324641	341.4198226	−10.22775339	0.0854893
	587732772657037548	161.4250258	10.2288603	0.0864014
(23)	587727178459775058	23.95379218	−10.20892227	0.170874
	588017992300167290	203.9605329	10.21263285	0.16155
(24)	587727178459775059	23.9542841	−10.20863418	0.167602
	588017992300167290	203.9605329	10.21263285	0.16155
(25)	587727178992386152	14.00945119	−10.16938834	0.0582089
	588017991758971000	194.0154632	10.17011785	0.0547655
(26)	587727178983473249	353.3035011	−10.11314013	0.175384
	587734893287112784	173.3054337	10.10802598	0.171464
(27)	587730815751291175	336.940361	−9.95373677	0.0563963
	587734864295166164	156.9394599	9.94507402	0.046747
(28)	587727179526701090	8.03597019	−9.91194747	0.0790208
	587734892756598903	188.0361662	9.91573124	0.0763644
(29)	587727178995335253	20.82821245	−9.86158021	0.128453
	588017991761920153	200.8255428	9.86031309	0.125208
(30)	587730815750045949	334.0325931	−9.85353658	0.349603
	588017702382403743	154.0277586	9.85157764	0.356585
(31)	587727178996449304	23.51060112	−9.77414538	0.0408057
	588017991763099797	203.5206978	9.78398572	0.0398321
(32)	587730815749980360	334.0089931	−9.76351938	0.0919012
	588017702382403698	154.016896	9.76374758	0.0834979
(33)	587727179531354122	18.84193042	−9.69197199	0.0623454
	588017991224197282	198.8506924	9.7002904	0.0665447
(34)	587727230521311310	22.64387404	−9.63632312	0.121776
	587736542549704781	202.645084	9.64360108	0.123518
(35)	587730815749128409	331.9847156	−9.62353845	0.105015
	587735342655471787	151.9840169	9.63233216	0.114253
(36)	587730815748866357	331.395196	−9.60640427	0.0800119
	587735342655209578	151.3870255	9.60693788	0.0783352
(37)	587726877811934142	340.8324856	−9.59191986	0.439336
	587732772119904870	160.8394092	9.59742067	0.433453
(38)	587730816827326649	342.3741793	−9.56574501	0.0821777
	587746210520367211	162.3699937	9.56609192	0.0862479
(39)	587727230522163362	24.74103715	−9.56325433	0.0862579
	587736542550556886	204.7496386	9.55691982	0.0868169
(40)	587727177929457776	39.13882791	−9.51991056	0.081008
	588017702410453175	219.1457622	9.51836998	0.088222

Table A1. *Cont.*

	Id SDSS DR7	*Ra*	*Dec*	*z*
(41)	587727180061868049	4.08337588	−9.46368127	0.0872652
	587734892218023997	184.0819229	9.45884063	0.094822
(42)	587727230522425495	25.33108177	−9.42130098	0.104163
	587736542550818989	205.3372284	9.41874675	0.0996079
(43)	587727177929785591	39.92521168	−9.33831191	0.0532149
	588017702410846353	219.9175712	9.34391573	0.0516048
(44)	587727177930113154	40.58369451	−9.32630004	0.155765
	588017702411108409	220.5908395	9.3201034	0.1517
(45)	587730816826212465	339.7809475	−9.28473191	0.0631319
	587734863222669402	159.7726217	9.27776767	0.0686803
(46)	587727230524260481	29.54831241	−9.28065885	0.0912357
	587736542552653969	209.5405473	9.27495593	0.0982227
(47)	587730816287113330	334.562248	−9.27926377	0.097067
	587732772117217405	154.5603312	9.27525384	0.1006
(48)	587726877808787613	333.5596377	−9.10873	0.125766
	587732772116758696	153.5547995	9.10677581	0.117325
(49)	587727227308802155	18.62293278	−9.09116739	0.0828624
	587736541474193627	198.6259619	9.08656038	0.0928012
(50)	587727231058837640	24.24960403	−9.07220804	0.116431
	587736542013489445	204.258942	9.07093891	0.122971
(51)	587727231059034221	24.70990827	−9.050773	0.0766974
	587736542013685982	204.707667	9.05688215	0.0775408
(52)	587724240688382034	38.55751214	−8.98833628	0.111355
	588017992306458874	218.563633	8.99273253	0.116682
(53)	587727180595134577	355.7997977	−8.987712	0.0753556
	587734891677548628	175.8078012	8.98622382	0.0829316
(54)	587727180594479192	354.2791585	−8.98725868	0.0806326
	587732770515124373	174.277534	8.99625689	0.0760123
(55)	587726878886723739	343.2696496	−8.98547579	0.170464
	587732771047211211	163.2757834	8.99239073	0.166468
(56)	587726879426150556	349.2821756	−8.9139055	0.0837956
	587732770512961595	169.2765643	8.90951915	0.0850834
(57)	587726877269229794	327.3372251	−8.88489879	0.0911886
	587732772650942640	147.3341982	8.8846179	0.0977782
(58)	587727227843510349	13.58226852	−8.82669194	0.0775205
	587732769986576485	193.5776433	8.82324646	0.0802786
(59)	587727227841544334	9.17385956	−8.81343367	0.161788
	587732769984675893	189.1800829	8.81570619	0.165148
(60)	587727227840823364	7.41474543	−8.78739786	0.134174
	587732769983889559	187.4173796	8.79260319	0.141713
(61)	587726879424774256	346.0556579	−8.74818209	0.097193
	587732770511519918	166.0566685	8.740358	0.0875037
(62)	587727180071501902	26.40085465	−8.73107212	0.121164
	588017990690603214	206.3924788	8.73386769	0.120342
(63)	587726877268902222	326.6199672	−8.72026028	0.135262
	587734863753838722	146.6245995	8.71266702	0.134986
(64)	587727227842986122	12.49783122	−8.70198555	0.0739487
	587732769986117760	192.5043783	8.69610353	0.0837418
(65)	587726878345265364	332.6514376	−8.66253229	0.103393
	587732771579494537	152.6458706	8.66485751	0.0973786
(66)	587730817361182802	335.363148	−8.64716609	0.0373209
	587734862683832453	155.3597555	8.64438959	0.0450276
(67)	587724240689102969	40.22878711	−8.64369517	0.0380482
	587736543094177958	220.2206679	8.64675197	0.0308106

Table A1. *Cont.*

	Id SDSS DR7	*Ra*	*Dec*	*z*
(68)	587726877268312182	325.2592388	−8.63777296	0.0863781
	587732772650025128	145.2509033	8.63971077	0.0846345
(69)	587727227843510316	13.66287605	−8.63255357	0.0778701
	588017730839642176	193.6626503	8.63958689	0.0827405
(70)	587730818439512260	346.092724	−8.50560084	0.172473
	587734891673354322	166.094645	8.51369065	0.175036
(71)	587727231597478004	28.3056497	−8.42097287	0.0471675
	587736541478387896	208.3127137	8.41497984	0.0450439
(72)	587730818439053410	344.9876466	−8.39745108	0.0779055
	587734891672895587	164.9894861	8.39564562	0.073904
(73)	587727212272943399	320.8338911	−8.39485218	0.117779
	587734948049912071	140.8422313	8.39661384	0.11207
(74)	587727212273271140	321.5992953	−8.37544229	0.158414
	587734948050239774	141.6072698	8.3832973	0.152886
(75)	587724240155705507	48.22814118	−8.33581316	0.0735155
	587736477058990249	228.2378153	8.33940235	0.0804487
(76)	587727177934307453	50.24970865	−8.29951375	0.0330458
	588017702952173868	230.2488442	8.308433	0.0393475
(77)	587726878343823623	329.4183427	−8.27673436	0.148898
	587732771578052774	149.4134499	8.27527956	0.15852
(78)	587726877804855542	324.4594709	−8.21209911	0.0871732
	587732772112826583	144.4574674	8.20228244	0.0867666
(79)	587727178469802145	46.9844432	−8.18224969	0.0744629
	588017992310128884	226.9932375	8.19029998	0.0765801
(80)	587726878882332761	333.2058322	−8.14083953	0.0837303
	587732771042820325	153.2151481	8.1369431	0.0842566
(81)	587727232134873177	29.37707349	−7.94639568	0.10361
	587736526444560520	209.3793586	7.94487803	0.103126
(82)	587727232134742064	29.16828094	−7.91303927	0.0989567
	587736526444429478	209.1635351	7.91749915	0.103407
(83)	587730817895629069	329.9017868	−7.78737555	0.0856975
	587732771041378462	149.8929509	7.78668911	0.0914809
(84)	587726878341726580	324.6422074	−7.75110002	0.0880603
	587732771576021174	144.6379017	7.74239199	0.0931418
(85)	587730818435317875	336.3522559	−7.7508616	0.109669
	587732769970454629	156.3434173	7.74177121	0.103487
(86)	587726877264839112	317.3101898	−7.73854853	0.0732018
	587734948048404618	137.3147516	7.72945807	0.0821823
(87)	587730818433155251	331.3679425	−7.45623643	0.0592957
	587734861608321127	151.3713518	7.46400606	0.0621482
(88)	587724240694542491	52.76892686	−7.35645715	0.138503
	587736543099617547	232.7601059	7.34722426	0.129012
(89)	587724241765007480	45.13170845	−7.34640725	0.161412
	587736542022598934	225.1285679	7.34491587	0.154524
(90)	587727179008311337	50.7121024	−7.32739104	0.0845821
	588017991774896410	230.7190341	7.3349747	0.0783759
(91)	587724240694673500	52.96494777	−7.25533989	0.133988
	587736543099683339	232.959273	7.24727706	0.128557
(92)	587730818432041321	328.9376199	−7.06320875	0.0592138
	587732579378724931	148.9383586	7.06251179	0.0602015
(93)	587726879954370763	329.3517007	−7.04637715	0.0859399
	587732579378921673	149.3440319	7.03988761	0.0784532
(94)	587724242302533699	46.63534829	−6.83786511	0.028473
	587736541486383232	226.6284051	6.83905419	0.0376736
(95)	587726879953322317	327.0174505	−6.78848336	0.0898924
	587732579377873009	147.0128383	6.79790707	0.0932444

Table A1. *Cont.*

	Id SDSS DR7	*Ra*	*Dec*	*z*
(96)	587727180081660026	49.76721128	−6.65462997	0.171731
	588017990700826690	229.7751332	6.65265276	0.17779
(97)	587726879952732589	325.6644648	−6.53424217	0.0882166
	587732703396430084	145.6718053	6.52802864	0.0933982
(98)	587727179011195092	57.28409909	−6.5146857	0.0656059
	588017991777780111	237.2916735	6.51711338	0.0727241
(99)	587726879413371300	319.8134098	−6.4153901	0.0633028
	587732770500116746	139.8142344	6.40937891	0.0725347
(100)	587726879950045526	319.5050187	−5.89992385	0.0887226
	587732578837725451	139.5035274	5.89314752	0.090063
(101)	587724241234690202	60.1469532	−5.82246607	0.128101
	587736542566023562	240.1442599	5.81544137	0.120623
(102)	587724241771102391	59.12398332	−5.6749918	0.0597927
	587736542028693952	239.1163388	5.66555938	0.0621059
(103)	587724241770709041	58.1813494	−5.66402869	0.124912
	587736542028300451	238.1814968	5.66896383	0.132543
(104)	587724242307448950	57.81327563	−5.44193649	0.12508
	587736541491298661	237.8139452	5.4320315	0.117586
(105)	587727180085919882	59.45274909	−5.37776939	0.112835
	588017990705086634	239.459686	5.3730717	0.114617
(106)	587726879409635950	311.3361796	−5.13025247	0.100322
	587732703390204231	131.3358794	5.12942269	0.0944183
(107)	587727214952710451	310.6951216	−5.00957318	0.0533286
	587732578833859013	130.7039891	5.01590373	0.0516006
(108)	587726879408915112	309.7014626	−5.00378611	0.0822278
	587732703389483300	129.7102373	5.0038262	0.0759225
(109)	587727180622528725	58.85069515	−4.88213314	0.0739501
	587730023336902902	238.8427352	4.88395362	0.0681825
(110)	587724650869686415	184.6727131	−1.25620133	0.0803352
	587731187816595528	4.66679487	1.26085556	0.0876818
(111)	587724650869424248	184.0892593	−1.25371914	0.108284
	587731187816333417	4.09325126	1.25789316	0.105123
(112)	588015507671089581	28.14765501	−1.22061106	0.174438
	587726031187148932	208.1479272	1.22578036	0.174331
(113)	587729971792052457	228.9119379	−1.22029557	0.120609
	587731514229588106	48.91797559	1.21584566	0.112363
(114)	587748927626608776	172.1310313	−1.21504223	0.113913
	587731187811090545	352.1225299	1.21974134	0.119537
(115)	587734303270764663	341.5351663	−1.20503473	0.0583548
	587726031166701712	161.5251899	1.20328815	0.0671257
(116)	587722981747458159	196.8323221	−1.10495117	0.0858605
	587731514215563418	16.84068508	1.10383695	0.0941228
(117)	588015507676987550	41.62918519	−1.09799691	0.0740636
	587726014013440008	221.6264322	1.10413737	0.0735006
(118)	587722981750931657	204.8306575	−1.06369837	0.0707877
	587731514219036795	24.83154818	1.06710408	0.078975
(119)	587731511532454043	19.75110345	−0.99674932	0.044761
	587722984433057983	199.7536973	0.99668931	0.0541101
(120)	587731185125359869	349.0427567	−0.98745757	0.091398
	587748930309587102	169.0524929	0.9931595	0.0962012
(121)	587731185116315784	328.3852669	−0.92491413	0.0954053
	587728950120612023	148.3899618	0.92361081	0.0948823
(122)	588848898860056883	228.2742186	−0.90832571	0.129659
	588015510364225797	48.27957041	0.91491284	0.131263
(123)	587731185119723924	336.1672691	−0.89711779	0.0991819
	587728950124019803	156.1666319	0.89373435	0.0938088

Table A1. *Cont.*

	Id SDSS DR7	*Ra*	*Dec*	*z*
(124)	588848898847539378	199.7024399	−0.8926827	0.0818081
	588015510351708322	19.70776073	0.89908792	0.0800928
(125)	588848898830172339	159.9730114	−0.85567902	0.0908891
	587734305954463933	339.9668426	0.86319413	0.0873762
(126)	588848898843279472	189.8915184	−0.85366277	0.0242445
	588015510347448339	9.89514685	0.85996826	0.0146933
(127)	587728947975291011	153.3264231	−0.8327221	0.0490744
	587731187265962312	333.3213035	0.83853245	0.0571919
(128)	587729778526781840	234.5183544	−0.8262151	0.144058
	587731513695142080	54.52663634	0.82450886	0.139076
(129)	587722982293176752	217.0007899	−0.82291535	0.399234
	587731513687474437	36.99722415	0.81755209	0.397598
(130)	587734303804031262	333.3022362	−0.80519986	0.129767
	588848900974706861	153.3035057	0.80991503	0.120938
(131)	587722982300123441	232.9101284	−0.79167934	0.0766653
	587731513694421196	52.90549275	0.79102086	0.0856506
(132)	587722982285508856	199.6286217	−0.78745739	0.0882834
	587731513679872138	19.62375817	0.78798276	0.0898079
(133)	587734303805866210	337.4814454	−0.7517174	0.0903008
	588848900976541910	157.4856125	0.75898364	0.099725
(134)	588015508192624827	353.1832021	−0.74826734	0.0574768
	588848900983423150	173.1767412	0.75630883	0.0674753
(135)	588015508203241620	17.35657948	−0.73451621	0.103116
	588848900994039948	197.3614164	0.72866873	0.0944896
(136)	588015508216873237	48.61535843	−0.71640599	0.0873679
	588848901007671746	228.6074205	0.70948451	0.0915592
(137)	588015508218904634	53.23858074	−0.70414471	0.0331694
	588848901009703095	233.2419617	0.71068808	0.0378785
(138)	587722982280593611	188.3839313	−0.69206406	0.0716765
	587731187281297523	8.38761185	0.69265965	0.0666569
(139)	587748928166887621	179.9836371	−0.68306759	0.0800753
	587731187277627630	359.9849222	0.67510242	0.0848031
140)	588015508212285576	38.07654238	−0.66091986	0.152935
	588848901003084008	218.0833898	0.65782354	0.148348
(141)	587722982275154175	175.8949958	−0.63154972	0.0777659
	587731187275858096	355.9025156	0.63455671	0.0830219
(142)	588848899399090470	233.1265588	−0.60318561	0.0834699
	588015509829517446	53.12424142	0.60899384	0.0888991
(143)	588848899394830608	223.4164629	−0.59793901	0.0757585
	588015509825257582	43.4242485	0.59779667	0.0674929
(144)	587731172768809842	312.9796387	−0.5957954	0.0542642
	587725075526189422	132.9735106	0.58860398	0.0512173
(145)	588848899367698514	161.4291165	−0.59321324	0.0850623
	587734305418182948	341.4353393	0.59869345	0.0853401
(146)	588848899377791164	184.5422801	−0.54941729	0.0806642
	588015509808218204	4.53334222	0.54320436	0.0883403
(147)	588848899381395678	192.8322052	−0.54359022	0.0823546
	588015509811822661	12.82661496	0.54938195	0.0838967
(148)	587731512070570074	22.52506877	−0.53886851	0.0752843
	587722983897432095	202.5292389	0.53144561	0.0753058
(149)	588848899365142729	155.7201062	−0.52903144	0.161499
	587734305415692542	335.7266832	0.52749615	0.161789
(150)	587731185656922427	336.925539	−0.52188082	0.142554
	587728949587476580	156.9318551	0.51420834	0.147027
(151)	587731512085708963	57.24298571	−0.52109991	0.0398141
	587722983912636747	237.2401798	0.51948336	0.0326624

Table A1. *Cont.*

	Id SDSS DR7	*Ra*	*Dec*	*z*
(152)	588848899365208074	155.7345006	−0.52048483	0.152984
	587734305415692542	335.7266832	0.52749615	0.161789
(153)	587731512075026623	32.7941736	−0.51697122	0.104186
	587722983901888776	212.7874643	0.51757655	0.10494
(154)	587731512070570080	22.53092957	−0.51301286	0.0754378
	587722983897432249	202.5290072	0.50960505	0.0842453
(155)	588848899367567503	161.1736846	−0.50354558	0.116059
	587734305418117322	341.1713409	0.49887529	0.10686
(156)	587731185663738041	352.414892	−0.49559734	0.0610491
	587748929774223562	172.4212536	0.49196292	0.0617746
(157)	587731185657315605	337.8171047	−0.46714883	0.089706
	587728949587869853	157.8165583	0.46875388	0.0972739
(158)	588848899365011498	155.3428317	−0.46621861	0.0616145
	587734305415561419	335.3404111	0.46782104	0.0585452
(159)	587731185654825160	332.0329757	−0.45305431	0.0966575
	587728949585314077	152.0316255	0.44515599	0.096859
(160)	588848899369599194	165.777933	−0.43232161	0.408335
	588015509800026315	345.7681431	0.42889055	0.406645
(161)	588848899392012585	217.0954067	−0.42921954	0.13692
	588015509822505078	37.10056005	0.42263247	0.13819
(162)	587748928964460711	162.3131562	−0.4126741	0.0631013
	587731186733023422	342.3072456	0.40960475	0.0687452
(163)	588015508738474102	13.66692127	−0.40711197	0.0431046
	588848900455530621	193.6587778	0.40977996	0.048432
(164)	588015508744241268	26.76827379	−0.39658262	0.0921257
	588848900461232473	206.7714106	0.39999281	0.0904585
(165)	587730846891377212	322.2164035	−0.36530606	0.0524633
	588848900432986349	142.2201617	0.3629534	0.0564073
(166)	587722982818971844	191.8125016	−0.35898776	0.126037
	587731186745933956	11.82036541	0.35818073	0.117239
(167)	588015508741030001	19.45674285	−0.34082464	0.0468492
	588848900458086553	199.4599698	0.34994819	0.048473
(168)	588015508727529597	348.5866992	−0.33249466	0.0806627
	588848900444520624	168.5870372	0.32365469	0.0784033
(169)	588015508727136416	347.7652686	−0.32576489	0.0983488
	588848900444192846	167.7733221	0.32533721	0.0968191
(170)	587730846890132061	319.3488484	−0.31274778	0.0580555
	588848900431741191	139.3414636	0.32191469	0.0540347
(171)	587734304341426385	334.4289933	−0.29072537	0.0946837
	588848900438360204	154.434898	0.2951535	0.0948182
(172)	587734304340640020	332.7387428	−0.26301595	0.180004
	588848900437573950	152.7359484	0.25633147	0.186205
(173)	587722982822772953	200.5231175	−0.25712776	0.0755962
	587731513143394377	20.52539083	0.26106339	0.0739661
(174)	587730846892097872	323.7534775	−0.25580372	0.23578
	588848900433641580	143.7508871	0.25087206	0.230907
(175)	587722982818578564	190.8538024	−0.25574711	0.108047
	587731186745540781	10.85230943	0.25272055	0.108846
(176)	587728948512882891	155.0284918	−0.24893939	0.0946879
	587731186729877696	335.0272875	0.25118887	0.0976836
(177)	587722982829588620	215.9538986	−0.24834938	0.0845643
	587731513150144670	35.96309274	0.24429916	0.0878976
(178)	587728948515438760	160.8665986	−0.24408333	0.0612075
	587731186732433592	340.8655553	0.23643433	0.0602342
(179)	587728948515438760	160.8665986	−0.24408333	0.0612075
	587731186732433605	340.8750138	0.24261057	0.0586656

Table A1. *Cont.*

	Id SDSS DR7	*Ra*	*Dec*	*z*
(180)	587722982817202308	187.6635646	−0.21513005	0.112303
	587731186744164449	7.6553343	0.21555044	0.114242
(181)	587731512609996966	28.42414238	−0.20766632	0.116707
	587722983363117368	208.4229163	0.20947298	0.116208
(182)	587731512620351626	52.0486704	−0.18938222	0.0851471
	587722983373472062	232.0581374	0.18368629	0.0798633
(183)	588848899901030743	153.4421478	−0.13358412	0.096212
	587734304877838573	333.4461883	0.14101877	0.0959779
(184)	588848899931963795	224.1292204	−0.10150706	0.37695
	588015509288648969	44.12854088	0.10090797	0.37109
(185)	587731512620613919	52.66581732	−0.08391774	0.0747399
	587722983373733982	232.6567434	0.09144794	0.0712474
(186)	587731512616550555	43.4068315	−0.02922721	0.0437379
	587722983369670840	223.4084883	0.02099328	0.0447694
(187)	587731186188353997	324.4826276	−0.02063334	0.0912575
	587725074994364633	144.4802056	0.02165878	0.0908592

Table A2. Pairs of galaxies for the effect of cosmic lens [36]. Id SDSS DR7 is objID identification number in the Sloan Digital Sky Survey. Accuracy is of 0.001° for *ra* and *dec*. The redshift *z* is indicated to make it easier to imagine the degree of asymmetry of the galaxy's location on the circumference (null-geodesic) with respect to the observer on Earth. The candidate pair is valid if both galaxies in a pair are of the same type.

	Id SDSS DR7	*Ra*	*Dec*	*z*
(1)	587727227839578254	4.62339359	−8.82776469	0.104797
	587732769982709974	184.6230609	8.826889	0.481948
(2)	587726877268312182	325.2592388	−8.63777296	0.0863781
	587732772650025129	145.2584188	8.63747987	0.182619
(3)	587727227845804151	19.00360312	−8.53841652	0.125065
	587736540937519274	199.003274	8.53767648	0.0523744
(4)	587726879422152915	340.0250784	−8.32576871	0.211179
	587732770508898457	160.0243395	8.32579967	0.46663
(5)	587727212272943498	320.9004948	−8.31734032	0.118795
	587734948049977496	140.900737	8.31661374	0.132243
(6)	587724240691855395	46.59481629	−8.02287019	0.119974
	587736543096930620	226.5946368	8.0234898	0.141641
(7)	587726879416648036	327.4332687	−7.24482558	0.120794
	587732770503458957	147.4334035	7.24510724	0.172101
(8)	587730818432041321	328.9376199	−7.06320875	0.0592138
	587732579378724931	148.9383586	7.06251179	0.0602015
(9)	587726879951618320	323.0326676	−6.24542716	0.0835999
	587732703395315898	143.0324689	6.2463979	0.152482
(10)	587726879409635950	311.3361796	−5.13025247	0.100322
	587732703390204231	131.3358794	5.12942269	0.0944183
(11)	587724242308432093	60.09682211	−5.0670592	0.139483
	587736541492281504	240.0961397	5.06798605	0.161674
(12)	587722981749620931	201.8110903	−1.15290891	0.0672574
	587731514217726115	21.81094788	1.15332655	0.0825304
(13)	588848898840002840	182.4290969	−0.99010277	0.101162
	588015510344171606	2.42945951	0.99083329	0.0595599

Table A2. *Cont.*

	Id SDSS DR7	*Ra*	*Dec*	*z*
(14)	587731511542349980	42.40717742	−0.84245813	0.023485
	587722984443019391	222.4075711	0.84279922	0.211561
(15)	588848899373138039	173.8651882	−0.55499635	0.105208
	588015509803565082	353.8651982	0.55470851	0.241575
(16)	588015508736114824	8.29352396	−0.35022869	0.0803753
	588848900453171355	188.2937459	0.35119113	0.091289
(17)	587722982819365056	192.6996089	−0.24023107	0.082066
	587731186746327197	12.69923244	0.23965712	0.243192
(18)	588848899913482481	181.8731715	−0.20286898	0.086595
	588015509270167718	1.87315452	0.20227552	0.139049
(19)	587731186189599168	327.3151749	−0.17472973	0.475598
	587725074995609777	147.314463	0.17484814	0.0847248
(20)	587731512608817253	25.67986817	−0.10862577	0.114301
	587722983361937622	205.6799242	0.10944099	0.0763704
(21)	588848899931963795	224.1292204	−0.10150706	0.37695
	588015509288648969	44.12854088	0.10090797	0.37109
(22)	588848899903258801	158.5313323	−0.04817315	0.0649146
	587734304880066822	338.5305229	0.04819563	0.212747

Table A3. Pairs of opposite galaxies for the effect of cosmic mirror [36]—alternative approach. Id SDSS DR7 is objID identification number in the Sloan Digital Sky Survey. Accuracy is of 0.001° for *ra* and *dec* and *z*/2 for *z*.

	Id SDSS DR7	*Ra*	*Dec*	*z*
(1)	587726877268312182	325.2592388	−8.63777296	0.0863781
	587732772650025129	145.2584188	8.63747987	0.182619
(2)	587727227845804151	19.00360312	−8.53841652	0.125065
	587736540937519274	199.003274	8.53767648	0.0523744
(3)	587726879422152915	340.0250784	−8.32576871	0.211179
	587732770508898457	160.0243395	8.32579967	0.46663
(4)	587727212272943498	320.9004948	−8.31734032	0.118795
	587734948049977496	140.900737	8.31661374	0.132243
(5)	587724240691855395	46.59481629	−8.02287019	0.119974
	587736543096930620	226.5946368	8.0234898	0.141641
(6)	587726879416648036	327.4332687	−7.24482558	0.120794
	587732770503458957	147.4334035	7.24510724	0.172101
(7)	587730818432041321	328.9376199	−7.06320875	0.0592138
	587732579378724931	148.9383586	7.06251179	0.0602015
(8)	587726879951618320	323.0326676	−6.24542716	0.0835999
	587732703395315898	143.0324689	6.2463979	0.152482
(9)	587726879409635950	311.3361796	−5.13025247	0.100322
	587732703390204231	131.3358794	5.12942269	0.0944183
(10)	587724242308432093	60.09682211	−5.0670592	0.139483
	587736541492281504	240.0961397	5.06798605	0.161674
(11)	587722981749620931	201.8110903	−1.15290891	0.0672574
	587731514217726115	21.81094788	1.15332655	0.0825304
(12)	588848899840002840	182.4290969	−0.99010277	0.101162
	588015510344171606	2.42945951	0.99083329	0.0595599
(13)	588848899373138039	173.8651882	−0.55499635	0.105208
	588015509803565082	353.8651982	0.55470851	0.241575
(14)	588015508736114824	8.29352396	−0.35022869	0.0803753
	588848900453171355	188.2937459	0.35119113	0.091289

Table A3. *Cont.*

	Id SDSS DR7	*Ra*	*Dec*	*z*
(15)	587722982819365056	192.6996089	−0.24023107	0.082066
	587731186746327197	12.69923244	0.23965712	0.243192
(16)	588848899913482481	181.8731715	−0.20286898	0.086595
	588015509270167718	1.87315452	0.20227552	0.139049
(17)	587731512608817253	25.67986817	−0.10862577	0.114301
	587722983361937622	205.6799242	0.10944099	0.0763704
(18)	588848899931963795	224.1292204	−0.10150706	0.37695
	588015509288648969	44.12854088	0.10090797	0.37109

Appendix B

Table A4. Pairs of galaxies for the effect of cosmic lens [40]. Id SDSS DR8—objID identification number in the Sloan Digital Sky Survey. Accuracy is of 0.0002° for *ra* and *dec*. Candidate pair is valid if both galaxies in pair are of the same type (elliptical or spiral).

	Id SDSS DR8	*Ra*	*Dec*	*Ell*	*Sp*
(1)	1237678888521237047	26.56961575	−3.036690882	0.009671	0.990329
	1237674469000413487	206.569743	3.036761704	0.147295	0.852705
(2)	1237655693017940456	231.1268834	−1.237362786	0.153929	0.846071
	1237646588233974200	51.12707011	1.237392067	0.471205	0.528795
(3)	1237655693017940456	231.1268834	−1.237362786	0.153929	0.846071
	1237657815275471153	51.12706887	1.237400496	0.52382	0.47618
(4)	1237655693017940456	231.1268834	−1.237362786	0.153929	0.846071
	1237653000613921219	51.12707746	1.237402214	0.486234	0.513766
(5)	1237655693017940456	231.1268834	−1.237362786	0.153929	0.846071
	1237659915511726413	51.12707585	1.237404045	0.484072	0.515928
(6)	1237655693017940456	231.1268834	−1.237362786	0.153929	0.846071
	1237666516881834000	51.12704369	1.237412566	0.545912	0.454088
(7)	1237655693017940456	231.1268834	−1.237362786	0.153929	0.846071
	1237666662937788799	51.12706696	1.23741968	0.492949	0.507051
(8)	1237655693017940456	231.1268834	−1.237362786	0.153929	0.846071
	1237663330011251042	51.127083	1.237427134	0.502022	0.497978
(9)	1237655693017940456	231.1268834	−1.237362786	0.153929	0.846071
	1237666409538519489	51.12708146	1.237445228	0.461594	0.538406
(10)	1237655693017940456	231.1268834	−1.237362786	0.153929	0.846071
	1237666340814716950	51.12708141	1.237451208	0.435734	0.564266
(11)	1237655693017940456	231.1268834	−1.237362786	0.153929	0.846071
	1237657587639386438	51.12708243	1.237457695	0.432267	0.567733
(12)	1237655693017940456	231.1268834	−1.237362786	0.153929	0.846071
	1237657587639321096	51.12707884	1.237457919	0.457914	0.542086
(13)	1237646748740026642	62.17470211	−1.016792147	0.095611	0.904389
	1237648705676575427	242.1748881	1.016716451	0.092952	0.907048
(14)	1237646748740026642	62.17470211	−1.016792147	0.095611	0.904389
	1237648705676575428	242.1748845	1.01672036	0.078252	0.921748
(15)	1237652997934416225	62.1747088	−1.016787397	0.108173	0.891827
	1237648705676575427	242.1748881	1.016716451	0.092952	0.907048
(16)	1237652997934416225	62.1747088	−1.016787397	0.108173	0.891827
	1237648705676575428	242.1748845	1.01672036	0.078252	0.921748
(17)	1237657761048166683	62.17471976	−1.016786518	0.114383	0.885617
	1237648705676575427	242.1748881	1.016716451	0.092952	0.907048
(18)	1237657761048166683	62.17471976	−1.016786518	0.114383	0.885617
	1237648705676575428	242.1748845	1.01672036	0.078252	0.921748

Table A4. *Cont.*

	Id SDSS DR8	*Ra*	*Dec*	*Ell*	*Sp*
(19)	1237646748740026643	62.17475111	−1.016781419	0.097682	0.902318
	1237655551815123559	242.1749457	1.01671526	0.083047	0.916953
(20)	1237646748740026643	62.17475111	−1.016781419	0.097682	0.902318
	1237648705676575427	242.1748881	1.016716451	0.092952	0.907048
(21)	1237646748740026643	62.17475111	−1.016781419	0.097682	0.902318
	1237648705676575428	242.1748845	1.01672036	0.078252	0.921748
(22)	1237649823937986797	62.17470476	−1.016778157	0.109712	0.890288
	1237648705676575427	242.1748881	1.016716451	0.092952	0.907048
(23)	1237649823937986797	62.17470476	−1.016778157	0.109712	0.890288
	1237648705676575428	242.1748845	1.01672036	0.078252	0.921748
(24)	1237646585554469394	62.17471262	−1.016759557	0.087926	0.912074
	1237648705676575427	242.1748881	1.016716451	0.092952	0.907048
(25)	1237646585554469394	62.17471262	−1.016759557	0.087926	0.912074
	1237648705676575428	242.1748845	1.01672036	0.078252	0.921748
(26)	1237666497028096411	62.17470133	−1.016724343	0.06974	0.93026
	1237648705676575427	242.1748881	1.016716451	0.092952	0.907048
(27)	1237666497028096411	62.17470133	−1.016724343	0.06974	0.93026
	1237648705676575428	242.1748845	1.01672036	0.078252	0.921748
(28)	1237666497028096412	62.17471675	−1.016711222	0.07633	0.92367
	1237648705676575427	242.1748881	1.016716451	0.092952	0.907048
(29)	1237666497028096412	62.17471675	−1.016711222	0.07633	0.92367
	1237648705676575428	242.1748845	1.01672036	0.078252	0.921748
(30)	1237655177615638991	128.668235	−0.926547264	0.883225	0.116775
	1237649942587703356	308.6681411	0.926418898	0.861631	0.138369
(31)	1237648720134537650	128.6682518	−0.926538368	0.902699	0.097301
	1237649942587703356	308.6681411	0.926418898	0.861631	0.138369
(32)	1237648720166060380	200.6434022	−0.866110951	0.989174	0.010826
	1237663480353259732	20.64339386	0.86631035	0.958359	0.041641

Table A5. Pairs of galaxies for the effect of cosmic mirror from catalog [41]. Id SDSS DR8—objID identification number in the Sloan Digital Sky Survey. Accuracy is of 0.001° for *ra* and *dec* and 0.01 for *zphot*. All galaxies are spiral (defined as those with parameter spiral (sp) > 0.5).

	Id SDSS DR8	*Ra*	*Dec*	*Sp*	*Zphot*
(1)	1237650372102127690	201.8110906	−1.1529332	0.80	0.061
	1237666662924943502	21.81093325	1.15332143	0.56	0.070
(2)	1237650372102127690	201.8110906	−1.1529332	0.80	0.061
	1237660237652623499	21.81093366	1.15333317	0.64	0.071
(3)	1237650372102127690	201.8110906	−1.1529332	0.80	0.061
	1237663205460607081	21.81092528	1.15333562	0.61	0.070
(4)	1237650372102127690	201.8110906	−1.1529332	0.80	0.061
	1237660010021060695	21.8109353	1.15333828	0.58	0.069
(5)	1237650372102127690	201.8110906	−1.1529332	0.80	0.061
	1237660010021060693	21.8109426	1.1533383	0.58	0.069
(6)	1237650372102127690	201.8110906	−1.1529332	0.80	0.061
	1237646588221128874	21.81095251	1.15334338	0.54	0.071
(7)	1237651709428367652	201.8110888	−1.1529142	0.82	0.079
	1237656909048971424	21.81094041	1.1533158	0.59	0.072
(8)	1237651709428367652	201.8110888	−1.1529142	0.82	0.079
	1237666662924943502	21.81093325	1.15332143	0.56	0.070
(9)	1237651709428367652	201.8110888	−1.1529142	0.82	0.079
	1237657235442630860	21.8109474	1.15332466	0.57	0.078
(10)	1237651709428367652	201.8110888	−1.1529142	0.82	0.079
	1237657815262625899	21.81092583	1.15333002	0.57	0.075

Table A5. *Cont.*

	Id SDSS DR8	*Ra*	*Dec*	*Sp*	*Zphot*
(11)	1237651709428367652	201.8110888	−1.1529142	0.82	0.079
	1237646588221128876	21.81094599	1.15333221	0.67	0.074
(12)	1237651709428367652	201.8110888	−1.1529142	0.82	0.079
	1237666340801871988	21.81093809	1.15333261	0.59	0.072
(13)	1237651709428367652	201.8110888	−1.1529142	0.82	0.079
	1237660237652623499	21.81093366	1.15333317	0.64	0.071
(14)	1237651709428367652	201.8110888	−1.1529142	0.82	0.079
	1237662969220497579	21.81093606	1.15333365	0.67	0.073
(15)	1237651709428367652	201.8110888	−1.1529142	0.82	0.079
	1237663205460607081	21.81092528	1.15333562	0.61	0.070
(16)	1237651709428367652	201.8110888	−1.1529142	0.82	0.079
	1237657106606063792	21.81092612	1.15333705	0.65	0.077
(17)	1237651709428367652	201.8110888	−1.1529142	0.82	0.079
	1237659915498881211	21.81093881	1.15333749	0.64	0.076
(18)	1237651709428367652	201.8110888	−1.1529142	0.82	0.079
	1237660010021060693	21.8109426	1.1533383	0.58	0.069
(19)	1237651709428367652	201.8110888	−1.1529142	0.82	0.079
	1237663544779276481	21.8109381	1.15334331	0.59	0.074
(20)	1237651709428367652	201.8110888	−1.1529142	0.82	0.079
	1237646588221128874	21.81095251	1.15334338	0.54	0.071
(21)	1237651709428367652	201.8110888	−1.1529142	0.82	0.079
	1237657737950789725	21.81092483	1.15334534	0.64	0.073
(22)	1237651709428367652	201.8110888	−1.1529142	0.82	0.079
	1237666409525739588	21.81091124	1.15334613	0.60	0.080
(23)	1237651709428367652	201.8110888	−1.1529142	0.82	0.079
	1237656513889894587	21.81092948	1.15334793	0.59	0.072
(24)	1237651709428367652	201.8110888	−1.1529142	0.82	0.079
	1237656513889894586	21.81093578	1.15334862	0.64	0.073
(25)	1237651709428367652	201.8110888	−1.1529142	0.82	0.079
	1237657072230400220	21.81093259	1.15334873	0.61	0.076
(26)	1237651709428367652	201.8110888	−1.1529142	0.82	0.079
	1237678617427378399	21.81092545	1.15335605	0.66	0.079
(27)	1237651709428367652	201.8110888	−1.1529142	0.82	0.079
	1237678617427378397	21.81093158	1.15336241	0.59	0.076
(28)	1237651279931506991	201.8110746	−1.1529118	0.76	0.085
	1237657235442630860	21.8109474	1.15332466	0.57	0.078
(29)	1237651279931506991	201.8110746	−1.1529118	0.76	0.085
	1237657815262625899	21.81092583	1.15333002	0.57	0.075
(30)	1237651279931506991	201.8110746	−1.1529118	0.76	0.085
	1237657106606063792	21.81092612	1.15333705	0.65	0.077
(31)	1237651279931506991	201.8110746	−1.1529118	0.76	0.085
	1237659915498881211	21.81093881	1.15333749	0.64	0.076
(32)	1237651279931506991	201.8110746	−1.1529118	0.76	0.085
	1237666409525739588	21.81091124	1.15334613	0.60	0.080
(33)	1237651279931506991	201.8110746	−1.1529118	0.76	0.085
	1237657072230400220	21.81093259	1.15334873	0.61	0.076
(34)	1237651279931506991	201.8110746	−1.1529118	0.76	0.085
	1237678617427378399	21.81092545	1.15335605	0.66	0.079
(35)	1237651279931506991	201.8110746	−1.1529118	0.76	0.085
	1237678617427378397	21.81093158	1.15336241	0.59	0.076
(36)	1237648702974525748	201.8110905	−1.1529069	0.82	0.071
	1237656909048971424	21.81094041	1.1533158	0.59	0.072
(37)	1237648702974525748	201.8110905	−1.1529069	0.82	0.071
	1237666662924943502	21.81093325	1.15332143	0.56	0.070

Table A5. *Cont.*

	Id SDSS DR8	*Ra*	*Dec*	*Sp*	*Zphot*
(38)	1237648702974525748	201.8110905	−1.1529069	0.82	0.071
	1237657235442630860	21.8109474	1.15332466	0.57	0.078
(39)	1237648702974525748	201.8110905	−1.1529069	0.82	0.071
	1237657815262625899	21.81092583	1.15333002	0.57	0.075
(40)	1237648702974525748	201.8110905	−1.1529069	0.82	0.071
	1237646588221128876	21.81094599	1.15333221	0.67	0.074
(41)	1237648702974525748	201.8110905	−1.1529069	0.82	0.071
	1237666340801871988	21.81093809	1.15333261	0.59	0.072
(42)	1237648702974525748	201.8110905	−1.1529069	0.82	0.071
	1237660237652623499	21.81093366	1.15333317	0.64	0.071
(43)	1237648702974525748	201.8110905	−1.1529069	0.82	0.071
	1237662969220497579	21.81093606	1.15333365	0.67	0.073
(44)	1237648702974525748	201.8110905	−1.1529069	0.82	0.071
	1237663205460607081	21.81092528	1.15333562	0.61	0.070
(45)	1237648702974525748	201.8110905	−1.1529069	0.82	0.071
	1237657106606063792	21.81092612	1.15333705	0.65	0.077
(46)	1237648702974525748	201.8110905	−1.1529069	0.82	0.071
	1237659915498881211	21.81093881	1.15333749	0.64	0.076
(47)	1237648702974525748	201.8110905	−1.1529069	0.82	0.071
	1237660010021060695	21.8109353	1.15333828	0.58	0.069
(48)	1237648702974525748	201.8110905	−1.1529069	0.82	0.071
	1237660010021060693	21.8109426	1.1533383	0.58	0.069
(49)	1237648702974525748	201.8110905	−1.1529069	0.82	0.071
	1237663544779276481	21.8109381	1.15334331	0.59	0.074
(50)	1237648702974525748	201.8110905	−1.1529069	0.82	0.071
	1237646588221128874	21.81095251	1.15334338	0.54	0.071
(51)	1237648702974525748	201.8110905	−1.1529069	0.82	0.071
	1237657737950789725	21.81092483	1.15334534	0.64	0.073
(52)	1237648702974525748	201.8110905	−1.1529069	0.82	0.071
	1237666409525739588	21.81091124	1.15334613	0.60	0.080
(53)	1237648702974525748	201.8110905	−1.1529069	0.82	0.071
	1237656513889894587	21.81092948	1.15334793	0.59	0.072
(54)	1237648702974525748	201.8110905	−1.1529069	0.82	0.071
	1237656513889894586	21.81093578	1.15334862	0.64	0.073
(55)	1237648702974525748	201.8110905	−1.1529069	0.82	0.071
	1237657072230400220	21.81093259	1.15334873	0.61	0.076
(56)	1237648702974525748	201.8110905	−1.1529069	0.82	0.071
	1237678617427378399	21.81092545	1.15335605	0.66	0.079
(57)	1237648702974525748	201.8110905	−1.1529069	0.82	0.071
	1237678617427378397	21.81093158	1.15336241	0.59	0.076
(58)	1237666406859014666	62.17467447	−1.016796	0.90	0.081
	1237655551815123559	242.1749457	1.01671526	0.92	0.088
(59)	1237666406859014666	62.17467447	−1.016796	0.90	0.081
	1237648705676575427	242.1748881	1.01671645	0.91	0.084
(60)	1237666406859014666	62.17467447	−1.016796	0.90	0.081
	1237648705676575428	242.1748845	1.01672036	0.92	0.076
(61)	1237652997934416225	62.1747088	−1.0167874	0.89	0.074
	1237648705676575427	242.1748881	1.01671645	0.91	0.084
(62)	1237652997934416225	62.1747088	−1.0167874	0.89	0.074
	1237648705676575428	242.1748845	1.01672036	0.92	0.076
(63)	1237646748740026643	62.17475111	−1.0167814	0.90	0.076
	1237648705676575427	242.1748881	1.01671645	0.91	0.084
(64)	1237646748740026643	62.17475111	−1.0167814	0.90	0.076
	1237648705676575428	242.1748845	1.01672036	0.92	0.076
(65)	1237649823937986797	62.17470476	−1.0167782	0.89	0.071
	1237648705676575428	242.1748845	1.01672036	0.92	0.076
(66)	1237646585554469394	62.17471262	−1.0167596	0.91	0.083
	1237655551815123559	242.1749457	1.01671526	0.92	0.088

Table A5. *Cont.*

	Id SDSS DR8	*Ra*	*Dec*	*Sp*	*Zphot*
(67)	1237646585554469394	62.17471262	−1.0167596	0.91	0.083
	1237648705676575427	242.1748881	1.01671645	0.91	0.084
(68)	1237646585554469394	62.17471262	−1.0167596	0.91	0.083
	1237648705676575428	242.1748845	1.01672036	0.92	0.076
(69)	1237666497028096411	62.17470133	−1.0167243	0.93	0.085
	1237655551815123559	242.1749457	1.01671526	0.92	0.088
(70)	1237666497028096411	62.17470133	−1.0167243	0.93	0.085
	1237648705676575427	242.1748881	1.01671645	0.91	0.084
(71)	1237666497028096411	62.17470133	−1.0167243	0.93	0.085
	1237648705676575428	242.1748845	1.01672036	0.92	0.076
(72)	1237660007354335814	62.17467871	−1.016717	0.89	0.068
	1237648705676575428	242.1748845	1.01672036	0.92	0.076
(73)	1237666497028096412	62.17471675	−1.0167112	0.92	0.089
	1237655551815123559	242.1749457	1.01671526	0.92	0.088
(74)	1237666497028096412	62.17471675	−1.0167112	0.92	0.089
	1237648705676575427	242.1748881	1.01671645	0.91	0.084
(75)	1237648721222828169	161.910801	−0.1931421	0.69	0.123
	1237653012428554879	341.9117668	0.19238554	0.59	0.131
(76)	1237648721222828169	161.910801	−0.1931421	0.69	0.123
	1237663479262544284	341.9117693	0.19240627	0.63	0.119
(77)	1237648721222828169	161.910801	−0.1931421	0.69	0.123
	1237663479262544283	341.9117693	0.19240627	0.62	0.116

Table A6. Pairs of galaxies for the effect of cosmic mirror from catalog [41]—alternative approach. Id SDSS DR8—objID identification number in the Sloan Digital Sky Survey. Accuracy is of 0.001° for *ra* and *dec* and *zphot*/2 for *zphot*. All galaxies are spiral (defined as those with parameter spiral (sp) > 0.5).

	Id SDSS DR8	*Ra*	*Dec*	*Sp*	*Zphot*
(1)	1237671139859628503	164.797490	−21.936403	0.99	0.103
	1237680273114923318	344.796820	21.936782	0.88	0.142
(2)	1237671139859628503	164.797490	−21.936403	0.99	0.103
	1237679478537912674	344.796831	21.936789	0.85	0.123
(3)	1237671239182254464	165.440684	−20.397881	0.56	0.079
	1237679476390560006	345.439848	20.398063	0.96	0.059
(4)	1237671239182254464	165.440684	−20.397881	0.56	0.079
	1237680270967636262	345.439859	20.398065	0.95	0.058
(5)	1237671239182254464	165.440684	−20.397881	0.56	0.079
	1237680270967636263	345.439855	20.398073	0.93	0.064
(6)	1237671239182254464	165.440684	−20.397881	0.56	0.079
	1237679476390560005	345.439850	20.398083	0.96	0.058
(7)	1237668756705771673	313.351245	−17.157470	0.99	0.092
	1237667539074023810	133.351503	17.157239	0.62	0.210
(8)	1237668756705771673	313.351245	−17.157470	0.99	0.092
	1237667292113011156	133.351519	17.157253	0.56	0.154
(9)	1237667247022604530	55.572846	−11.962790	0.96	0.099
	1237668350292328878	235.572915	11.963025	0.76	0.072
(10)	1237667247022604530	55.572846	−11.962790	0.96	0.099
	1237668270839038355	235.572925	11.963054	0.78	0.058
(11)	1237667726440530093	83.727284	−6.167019	0.63	0.274
	1237671693914146439	263.726548	6.167152	0.99	0.092
(12)	1237680066953806059	334.767374	−3.511891	0.99	0.067
	1237654600491729036	154.766800	3.511264	0.97	0.117

Table A6. *Cont.*

	Id SDSS DR8	*Ra*	*Dec*	*Sp*	*Zphot*
(13)	1237679079114932401	334.767352	−3.511879	0.99	0.076
	1237654600491729036	154.766800	3.511264	0.97	0.117
(14)	1237679433981362251	359.485290	−3.315196	0.65	0.063
	1237651737367347360	179.485647	3.314965	0.84	0.086
(15)	1237679433981362251	359.485290	−3.315196	0.65	0.063
	1237651737367347361	179.485641	3.314973	0.80	0.079
(16)	1237679433981362253	359.485278	−3.315192	0.74	0.066
	1237651737367347360	179.485647	3.314965	0.84	0.086
(17)	1237679433981362253	359.485278	−3.315192	0.74	0.066
	1237651737367347361	179.485641	3.314973	0.80	0.079
(18)	1237672836917362790	359.485272	−3.315190	0.71	0.061
	1237651737367347360	179.485647	3.314965	0.84	0.086
(19)	1237672836917362790	359.485272	−3.315190	0.71	0.061
	1237651737367347361	179.485641	3.314973	0.80	0.079
(20)	1237678888521237046	26.569616	−3.036691	0.99	0.076
	1237674469000413486	206.569743	3.036762	0.85	0.115
(21)	1237650372102127690	201.811091	−1.152933	0.80	0.061
	1237656909048971424	21.810940	1.153316	0.59	0.072
(22)	1237650372102127690	201.811091	−1.152933	0.80	0.061
	1237666662924943502	21.810933	1.153321	0.56	0.070
(23)	1237650372102127690	201.811091	−1.152933	0.80	0.061
	1237657235442630860	21.810947	1.153325	0.57	0.078
(24)	1237650372102127690	201.811091	−1.152933	0.80	0.061
	1237657815262625899	21.810926	1.153330	0.57	0.075
(25)	1237650372102127690	201.811091	−1.152933	0.80	0.061
	1237646588221128876	21.810946	1.153332	0.67	0.074
(26)	1237650372102127690	201.811091	−1.152933	0.80	0.061
	1237666340801871988	21.810938	1.153333	0.59	0.072
(27)	1237650372102127690	201.811091	−1.152933	0.80	0.061
	1237660237652623499	21.810934	1.153333	0.64	0.071
(28)	1237650372102127690	201.811091	−1.152933	0.80	0.061
	1237662969220497579	21.810936	1.153334	0.67	0.073
(29)	1237650372102127690	201.811091	−1.152933	0.80	0.061
	1237663205460607081	21.810925	1.153336	0.61	0.070
(30)	1237650372102127690	201.811091	−1.152933	0.80	0.061
	1237657106606063792	21.810926	1.153337	0.65	0.077
(31)	1237650372102127690	201.811091	−1.152933	0.80	0.061
	1237659915498881211	21.810939	1.153337	0.64	0.076
(32)	1237650372102127690	201.811091	−1.152933	0.80	0.061
	1237660010021060695	21.810935	1.153338	0.58	0.069
(33)	1237650372102127690	201.811091	−1.152933	0.80	0.061
	1237660010021060693	21.810943	1.153338	0.58	0.069
(34)	1237650372102127690	201.811091	−1.152933	0.80	0.061
	1237663544779276481	21.810938	1.153343	0.59	0.074
(35)	1237650372102127690	201.811091	−1.152933	0.80	0.061
	1237646588221128874	21.810953	1.153343	0.54	0.071
(36)	1237650372102127690	201.811091	−1.152933	0.80	0.061
	1237657737950789725	21.810925	1.153345	0.64	0.073
(37)	1237650372102127690	201.811091	−1.152933	0.80	0.061
	1237666409525739588	21.810911	1.153346	0.60	0.080
(38)	1237650372102127690	201.811091	−1.152933	0.80	0.061
	1237656513889894587	21.810929	1.153348	0.59	0.072
(39)	1237650372102127690	201.811091	−1.152933	0.80	0.061
	1237656513889894586	21.810936	1.153349	0.64	0.073
(40)	1237650372102127690	201.811091	−1.152933	0.80	0.061
	1237657072230400220	21.810933	1.153349	0.61	0.076

Table A6. *Cont.*

	Id SDSS DR8	*Ra*	*Dec*	*Sp*	*Zphot*
(41)	1237650372102127690	201.811091	−1.152933	0.80	0.061
	1237678617427378399	21.810925	1.153356	0.66	0.079
(42)	1237650372102127690	201.811091	−1.152933	0.80	0.061
	1237678617427378397	21.810932	1.153362	0.59	0.076
(43)	1237655500274270455	201.811109	−1.152926	0.76	0.116
	1237656909048971424	21.810940	1.153316	0.59	0.072
(44)	1237655500274270455	201.811109	−1.152926	0.76	0.116
	1237666662924943502	21.810933	1.153321	0.56	0.070
(45)	1237655500274270455	201.811109	−1.152926	0.76	0.116
	1237657235442630860	21.810947	1.153325	0.57	0.078
(46)	1237655500274270455	201.811109	−1.152926	0.76	0.116
	1237657815262625899	21.810926	1.153330	0.57	0.075
(47)	1237655500274270455	201.811109	−1.152926	0.76	0.116
	1237646588221128876	21.810946	1.153332	0.67	0.074
(48)	1237655500274270455	201.811109	−1.152926	0.76	0.116
	1237666340801871988	21.810938	1.153333	0.59	0.072
(49)	1237655500274270455	201.811109	−1.152926	0.76	0.116
	1237660237652623499	21.810934	1.153333	0.64	0.071
(50)	1237655500274270455	201.811109	−1.152926	0.76	0.116
	1237662969220497579	21.810936	1.153334	0.67	0.073
(51)	1237655500274270455	201.811109	−1.152926	0.76	0.116
	1237663205460607081	21.810925	1.153336	0.61	0.070
(52)	1237655500274270455	201.811109	−1.152926	0.76	0.116
	1237657106606063792	21.810926	1.153337	0.65	0.077
(53)	1237655500274270455	201.811109	−1.152926	0.76	0.116
	1237659915498881211	21.810939	1.153337	0.64	0.076
(54)	1237655500274270455	201.811109	−1.152926	0.76	0.116
	1237660010021060695	21.810935	1.153338	0.58	0.069
(55)	1237655500274270455	201.811109	−1.152926	0.76	0.116
	1237660010021060693	21.810943	1.153338	0.58	0.069
(56)	1237655500274270455	201.811109	−1.152926	0.76	0.116
	1237663544779276481	21.810938	1.153343	0.59	0.074
(57)	1237655500274270455	201.811109	−1.152926	0.76	0.116
	1237646588221128874	21.810953	1.153343	0.54	0.071
(58)	1237655500274270455	201.811109	−1.152926	0.76	0.116
	1237657737950789725	21.810925	1.153345	0.64	0.073
(59)	1237655500274270455	201.811109	−1.152926	0.76	0.116
	1237666409525739588	21.810911	1.153346	0.60	0.080
(60)	1237655500274270455	201.811109	−1.152926	0.76	0.116
	1237656513889894587	21.810929	1.153348	0.59	0.072
(61)	1237655500274270455	201.811109	−1.152926	0.76	0.116
	1237656513889894586	21.810936	1.153349	0.64	0.073
(62)	1237655500274270455	201.811109	−1.152926	0.76	0.116
	1237657072230400220	21.810933	1.153349	0.61	0.076
(63)	1237655500274270455	201.811109	−1.152926	0.76	0.116
	1237678617427378399	21.810925	1.153356	0.66	0.079
(64)	1237655500274270455	201.811109	−1.152926	0.76	0.116
	1237678617427378397	21.810932	1.153362	0.59	0.076
(65)	1237651709428367652	201.811089	−1.152914	0.82	0.079
	1237656909048971424	21.810940	1.153316	0.59	0.072
(66)	1237651709428367652	201.811089	−1.152914	0.82	0.079
	1237666662924943502	21.810933	1.153321	0.56	0.070
(67)	1237651709428367652	201.811089	−1.152914	0.82	0.079
	1237657235442630860	21.810947	1.153325	0.57	0.078
(68)	1237651709428367652	201.811089	−1.152914	0.82	0.079
	1237657815262625899	21.810926	1.153330	0.57	0.075
(69)	1237651709428367652	201.811089	−1.152914	0.82	0.079
	1237646588221128876	21.810946	1.153332	0.67	0.074

Table A6. *Cont.*

	Id SDSS DR8	*Ra*	*Dec*	*Sp*	*Zphot*
(70)	1237651709428367652	201.811089	−1.152914	0.82	0.079
	1237666340801871988	21.810938	1.153333	0.59	0.072
(71)	1237651709428367652	201.811089	−1.152914	0.82	0.079
	1237660237652623499	21.810934	1.153333	0.64	0.071
(72)	1237651709428367652	201.811089	−1.152914	0.82	0.079
	1237662969220497579	21.810936	1.153334	0.67	0.073
(73)	1237651709428367652	201.811089	−1.152914	0.82	0.079
	1237663205460607081	21.810925	1.153336	0.61	0.070
(74)	1237651709428367652	201.811089	−1.152914	0.82	0.079
	1237657106606063792	21.810926	1.153337	0.65	0.077
(75)	1237651709428367652	201.811089	−1.152914	0.82	0.079
	1237659915498881211	21.810939	1.153337	0.64	0.076
(76)	1237651709428367652	201.811089	−1.152914	0.82	0.079
	1237660010021060695	21.810935	1.153338	0.58	0.069
(77)	1237651709428367652	201.811089	−1.152914	0.82	0.079
	1237660010021060693	21.810943	1.153338	0.58	0.069
(78)	1237651709428367652	201.811089	−1.152914	0.82	0.079
	1237663544779276481	21.810938	1.153343	0.59	0.074
(79)	1237651709428367652	201.811089	−1.152914	0.82	0.079
	1237646588221128874	21.810953	1.153343	0.54	0.071
(80)	1237651709428367652	201.811089	−1.152914	0.82	0.079
	1237657737950789725	21.810925	1.153345	0.64	0.073
(81)	1237651709428367652	201.811089	−1.152914	0.82	0.079
	1237666409525739588	21.810911	1.153346	0.60	0.080
(82)	1237651709428367652	201.811089	−1.152914	0.82	0.079
	1237656513889894587	21.810929	1.153348	0.59	0.072
(83)	1237651709428367652	201.811089	−1.152914	0.82	0.079
	1237656513889894586	21.810936	1.153349	0.64	0.073
(84)	1237651709428367652	201.811089	−1.152914	0.82	0.079
	1237657072230400220	21.810933	1.153349	0.61	0.076
(85)	1237651709428367652	201.811089	−1.152914	0.82	0.079
	1237678617427378399	21.810925	1.153356	0.66	0.079
(86)	1237651709428367652	201.811089	−1.152914	0.82	0.079
	1237678617427378397	21.810932	1.153362	0.59	0.076
(87)	1237651279931506991	201.811075	−1.152912	0.76	0.085
	1237656909048971424	21.810940	1.153316	0.59	0.072
(88)	1237651279931506991	201.811075	−1.152912	0.76	0.085
	1237666662924943502	21.810933	1.153321	0.56	0.070
(89)	1237651279931506991	201.811075	−1.152912	0.76	0.085
	1237657235442630860	21.810947	1.153325	0.57	0.078
(90)	1237651279931506991	201.811075	−1.152912	0.76	0.085
	1237657815262625899	21.810926	1.153330	0.57	0.075
(91)	1237651279931506991	201.811075	−1.152912	0.76	0.085
	1237646588221128876	21.810946	1.153332	0.67	0.074
(92)	1237651279931506991	201.811075	−1.152912	0.76	0.085
	1237666340801871988	21.810938	1.153333	0.59	0.072
(93)	1237651279931506991	201.811075	−1.152912	0.76	0.085
	1237660237652623499	21.810934	1.153333	0.64	0.071
(94)	1237651279931506991	201.811075	−1.152912	0.76	0.085
	1237662969220497579	21.810936	1.153334	0.67	0.073
(95)	1237651279931506991	201.811075	−1.152912	0.76	0.085
	1237663205460607081	21.810925	1.153336	0.61	0.070
(96)	1237651279931506991	201.811075	−1.152912	0.76	0.085
	1237657106606063792	21.810926	1.153337	0.65	0.077
(97)	1237651279931506991	201.811075	−1.152912	0.76	0.085
	1237659915498881211	21.810939	1.153337	0.64	0.076
(98)	1237651279931506991	201.811075	−1.152912	0.76	0.085
	1237660010021060695	21.810935	1.153338	0.58	0.069

Table A6. *Cont.*

	Id SDSS DR8	*Ra*	*Dec*	*Sp*	*Zphot*
(99)	1237651279931506991	201.811075	−1.152912	0.76	0.085
	1237660010021060693	21.810943	1.153338	0.58	0.069
(100)	1237651279931506991	201.811075	−1.152912	0.76	0.085
	1237663544779276481	21.810938	1.153343	0.59	0.074
(101)	1237651279931506991	201.811075	−1.152912	0.76	0.085
	1237646588221128874	21.810953	1.153343	0.54	0.071
(102)	1237651279931506991	201.811075	−1.152912	0.76	0.085
	1237657737950789725	21.810925	1.153345	0.64	0.073
(103)	1237651279931506991	201.811075	−1.152912	0.76	0.085
	1237666409525739588	21.810911	1.153346	0.60	0.080
(104)	1237651279931506991	201.811075	−1.152912	0.76	0.085
	1237656513889894587	21.810929	1.153348	0.59	0.072
(105)	1237651279931506991	201.811075	−1.152912	0.76	0.085
	1237656513889894586	21.810936	1.153349	0.64	0.073
(106)	1237651279931506991	201.811075	−1.152912	0.76	0.085
	1237657072230400220	21.810933	1.153349	0.61	0.076
(107)	1237651279931506991	201.811075	−1.152912	0.76	0.085
	1237678617427378399	21.810925	1.153356	0.66	0.079
(108)	1237651279931506991	201.811075	−1.152912	0.76	0.085
	1237678617427378397	21.810932	1.153362	0.59	0.076
(109)	1237648702974525748	201.811090	−1.152907	0.82	0.071
	1237656909048971424	21.810940	1.153316	0.59	0.072
(110)	1237648702974525748	201.811090	−1.152907	0.82	0.071
	1237666662924943502	21.810933	1.153321	0.56	0.070
(111)	1237648702974525748	201.811090	−1.152907	0.82	0.071
	1237657235442630860	21.810947	1.153325	0.57	0.078
(112)	1237648702974525748	201.811090	−1.152907	0.82	0.071
	1237657815262625899	21.810926	1.153330	0.57	0.075
(113)	1237648702974525748	201.811090	−1.152907	0.82	0.071
	1237646588221128876	21.810946	1.153332	0.67	0.074
(114)	1237648702974525748	201.811090	−1.152907	0.82	0.071
	1237666340801871988	21.810938	1.153333	0.59	0.072
(115)	1237648702974525748	201.811090	−1.152907	0.82	0.071
	1237660237652623499	21.810934	1.153333	0.64	0.071
(116)	1237648702974525748	201.811090	−1.152907	0.82	0.071
	1237662969220497579	21.810936	1.153334	0.67	0.073
(117)	1237648702974525748	201.811090	−1.152907	0.82	0.071
	1237663205460607081	21.810925	1.153336	0.61	0.070
(118)	1237648702974525748	201.811090	−1.152907	0.82	0.071
	1237657106606063792	21.810926	1.153337	0.65	0.077
(119)	1237648702974525748	201.811090	−1.152907	0.82	0.071
	1237659915498881211	21.810939	1.153337	0.64	0.076
(120)	1237648702974525748	201.811090	−1.152907	0.82	0.071
	1237660010021060695	21.810935	1.153338	0.58	0.069
(121)	1237648702974525748	201.811090	−1.152907	0.82	0.071
	1237660010021060693	21.810943	1.153338	0.58	0.069
(122)	1237648702974525748	201.811090	−1.152907	0.82	0.071
	1237663544779276481	21.810938	1.153343	0.59	0.074
(123)	1237648702974525748	201.811090	−1.152907	0.82	0.071
	1237646588221128874	21.810953	1.153343	0.54	0.071
(124)	1237648702974525748	201.811090	−1.152907	0.82	0.071
	1237657737950789725	21.810925	1.153345	0.64	0.073
(125)	1237648702974525748	201.811090	−1.152907	0.82	0.071
	1237666409525739588	21.810911	1.153346	0.60	0.080
(126)	1237648702974525748	201.811090	−1.152907	0.82	0.071
	1237656513889894587	21.810929	1.153348	0.59	0.072

Table A6. *Cont.*

	Id SDSS DR8	*Ra*	*Dec*	*Sp*	*Zphot*
(127)	1237648702974525748	201.811090	−1.152907	0.82	0.071
	1237656513889894586	21.810936	1.153349	0.64	0.073
(128)	1237648702974525748	201.811090	−1.152907	0.82	0.071
	1237657072230400220	21.810933	1.153349	0.61	0.076
(129)	1237648702974525748	201.811090	−1.152907	0.82	0.071
	1237678617427378399	21.810925	1.153356	0.66	0.079
(130)	1237648702974525748	201.811090	−1.152907	0.82	0.071
	1237678617427378397	21.810932	1.153362	0.59	0.076
(131)	1237666406859014666	62.174674	−1.016796	0.90	0.081
	1237655551815123559	242.174946	1.016715	0.92	0.088
(132)	1237666406859014666	62.174674	−1.016796	0.90	0.081
	1237648705676575427	242.174888	1.016716	0.91	0.084
(133)	1237666406859014666	62.174674	−1.016796	0.90	0.081
	1237648705676575428	242.174884	1.016720	0.92	0.076
(134)	1237646748740026642	62.174702	−1.016792	0.90	0.099
	1237655551815123559	242.174946	1.016715	0.92	0.088
(135)	1237646748740026642	62.174702	−1.016792	0.90	0.099
	1237648705676575427	242.174888	1.016716	0.91	0.084
(136)	1237646748740026642	62.174702	−1.016792	0.90	0.099
	1237648705676575428	242.174884	1.016720	0.92	0.076
(137)	1237652997934416225	62.174709	−1.016787	0.89	0.074
	1237655551815123559	242.174946	1.016715	0.92	0.088
(138)	1237652997934416225	62.174709	−1.016787	0.89	0.074
	1237648705676575427	242.174888	1.016716	0.91	0.084
(139)	1237652997934416225	62.174709	−1.016787	0.89	0.074
	1237648705676575428	242.174884	1.016720	0.92	0.076
(140)	1237657761048166683	62.174720	−1.016787	0.89	0.113
	1237655551815123559	242.174946	1.016715	0.92	0.088
(141)	1237657761048166683	62.174720	−1.016787	0.89	0.113
	1237648705676575427	242.174888	1.016716	0.91	0.084
(142)	1237657761048166683	62.174720	−1.016787	0.89	0.113
	1237648705676575428	242.174884	1.016720	0.92	0.076
(143)	1237646748740026643	62.174751	−1.016781	0.90	0.076
	1237655551815123559	242.174946	1.016715	0.92	0.088
(144)	1237646748740026643	62.174751	−1.016781	0.90	0.076
	1237648705676575427	242.174888	1.016716	0.91	0.084
(145)	1237646748740026643	62.174751	−1.016781	0.90	0.076
	1237648705676575428	242.174884	1.016720	0.92	0.076
(146)	1237649823937986797	62.174705	−1.016778	0.89	0.071
	1237655551815123559	242.174946	1.016715	0.92	0.088
(147)	1237649823937986797	62.174705	−1.016778	0.89	0.071
	1237648705676575427	242.174888	1.016716	0.91	0.084
(148)	1237649823937986797	62.174705	−1.016778	0.89	0.071
	1237648705676575428	242.174884	1.016720	0.92	0.076
(149)	1237646585554469394	62.174713	−1.016760	0.91	0.083
	1237655551815123559	242.174946	1.016715	0.92	0.088
(150)	1237646585554469394	62.174713	−1.016760	0.91	0.083
	1237648705676575427	242.174888	1.016716	0.91	0.084
(151)	1237646585554469394	62.174713	−1.016760	0.91	0.083
	1237648705676575428	242.174884	1.016720	0.92	0.076
(152)	1237666497028096411	62.174701	−1.016724	0.93	0.085
	1237655551815123559	242.174946	1.016715	0.92	0.088
(153)	1237666497028096411	62.174701	−1.016724	0.93	0.085
	1237648705676575427	242.174888	1.016716	0.91	0.084

Table A6. *Cont.*

	Id SDSS DR8	*Ra*	*Dec*	*Sp*	*Zphot*
(154)	1237666497028096411	62.174701	−1.016724	0.93	0.085
	1237648705676575428	242.174884	1.016720	0.92	0.076
(155)	1237660007354335814	62.174679	−1.016717	0.89	0.068
	1237655551815123559	242.174946	1.016715	0.92	0.088
(156)	1237660007354335814	62.174679	−1.016717	0.89	0.068
	1237648705676575427	242.174888	1.016716	0.91	0.084
(157)	1237660007354335814	62.174679	−1.016717	0.89	0.068
	1237648705676575428	242.174884	1.016720	0.92	0.076
(158)	1237666497028096412	62.174717	−1.016711	0.92	0.089
	1237655551815123559	242.174946	1.016715	0.92	0.088
(159)	1237666497028096412	62.174717	−1.016711	0.92	0.089
	1237648705676575427	242.174888	1.016716	0.91	0.084
(160)	1237666497028096412	62.174717	−1.016711	0.92	0.089
	1237648705676575428	242.174884	1.016720	0.92	0.076
(161)	1237666497538883899	2.523832	−0.444620	0.66	0.260
	1237648705113555092	182.524814	0.444527	0.57	0.110
(162)	1237666497538883899	2.523832	−0.444620	0.66	0.260
	1237674651003519212	182.524830	0.444553	0.68	0.088
(163)	1237666299997782594	2.523821	−0.444607	0.72	0.310
	1237648705113555092	182.524814	0.444527	0.57	0.110
(164)	1237648673959378974	161.910785	−0.193158	0.79	0.150
	1237653012428554879	341.911767	0.192386	0.59	0.131
(165)	1237648673959378974	161.910785	−0.193158	0.79	0.150
	1237663479262544284	341.911769	0.192406	0.63	0.119
(166)	1237648673959378974	161.910785	−0.193158	0.79	0.150
	1237663479262544283	341.911769	0.192406	0.62	0.116
(167)	1237648673959378974	161.910785	−0.193158	0.79	0.150
	1237663526510395758	341.911752	0.192409	0.74	0.135
(168)	1237648721222828169	161.910801	−0.193142	0.69	0.123
	1237653012428554879	341.911767	0.192386	0.59	0.131
(169)	1237648721222828169	161.910801	−0.193142	0.69	0.123
	1237663479262544284	341.911769	0.192406	0.63	0.119
(170)	1237648721222828169	161.910801	−0.193142	0.69	0.123
	1237663479262544283	341.911769	0.192406	0.62	0.116
(171)	1237648721222828169	161.910801	−0.193142	0.69	0.123
	1237663526510395758	341.911752	0.192409	0.74	0.135

Table A7. Pairs of elliptical galaxies (with parameter elliptical > 0.5) for the effect of cosmic lens [39]. Accuracy is of 0.001° for *ra* and *dec*. SpecObjID is ID of optical spectroscopic object in SDSS.

	SpecObjID	*Ra*	*Dec*	*z*	*Elliptical*
(1)	4839208601778651136	2.66932	1.37162	0.2678	0.935
	4329151476691107840	182.669	−1.3722	0.5809	0.892
(2)	4914588370669666304	2.99248	−3.2495	0.0003	0.861
	5346040858121076736	182.993	3.24996	0.6052	0.958
(3)	734224488962484224	4.30274	−9.4565	0.1170	0.663
	6075454403388112896	184.303	9.45639	2.4796	0.730
(4)	734242081148528640	4.62338	−8.8278	0.1047	0.686
	1384895138274240512	184.623	8.82687	0.4819	0.997
(5)	1680006812310464512	5.91966	0.54668	0.0596	0.709
	4331440114590285824	185.92	−0.546	0.5116	0.995
(6)	735378151655368704	6.86606	−8.8217	0.1888	0.550
	1830869162549864448	186.866	8.822	0.0855	0.911

Table A7. *Cont.*

	SpecObjID	*Ra*	*Dec*	*z*	*Elliptical*
(6)	735378151655368704	6.86606	−8.8217	0.1888	0.550
	1830869162549864448	186.866	8.822	0.0855	0.911
(7)	4844864764419506176	8.16193	2.99506	0.4595	0.708
	376056649636407296	188.161	−2.9954	0.0991	0.792
(8)	4919173338989330432	9.19367	−2.8909	0.4721	0.999
	5351416371190693888	189.193	2.89151	0.5333	0.999
(9)	4753611070676402176	10.3652	−0.5698	0.4595	0.994
	4333736164478943232	190.365	0.5689	0.0006	0.661
(10)	4039789700742381568	10.3652	−0.5698	0.4594	0.995
	4333736164478943232	190.365	0.5689	0.0006	0.661
(11)	4920278343259521024	11.2634	−2.7318	0.3479	0.998
	5353712700990423040	191.263	2.73184	0.4950	0.636
(12)	1683253395470706688	11.3174	−0.1229	0.4762	0.913
	4333669644025462784	191.318	0.12199	0.0004	0.788
(13)	778123041480665088	11.5428	1.11225	0.2160	0.885
	4270781151322832896	191.542	−1.1128	0.5737	0.877
(14)	4920246732300222464	11.7652	−2.4001	0.5587	0.995
	5354974390096756736	191.766	2.40077	0.4318	0.966
(15)	779218704851298304	12.1667	0.06339	0.3315	0.827
	4333606696984772608	192.167	−0.0629	0.6460	0.988
(16)	4848371932909273088	12.7862	2.31558	0.3916	0.995
	4254850052604297216	192.786	−2.3157	0.3638	0.927
(17)	4755887885000376320	13.4472	−0.2816	0.6521	0.988
	4334910722825256960	193.448	0.28142	0.6379	0.998
(18)	4921514474173104128	13.5581	−1.4265	0.6410	0.891
	4334919244040372224	193.559	1.42684	2.7379	0.512
(19)	1219440076220557312	13.8081	1.19783	0.1501	0.630
	4334772459238064128	193.809	−1.1978	0.0008	0.784
(20)	445869587716663296	16.9041	−1.2101	0.1278	0.744
	4511605535782993920	196.904	1.21051	0.6376	0.920
(21)	4858431363432841216	17.7868	2.55229	0.1187	0.975
	4563366149601361920	197.787	−2.5522	0.4748	0.999
(22)	781377596066654208	18.153	−0.8043	0.4344	0.825
	4511537915817885696	198.152	0.8038	0.4538	0.743
(23)	447132651329972224	18.6371	0.23377	0.0449	0.812
	3294404095737096192	198.638	−0.233	0.0003	0.524
(24)	743193205964564480	19.0036	−8.5384	0.1251	0.834
	2023364803757631488	199.003	8.53769	0.0524	0.910
(25)	783713783397771264	19.6607	−0.1202	0.0774	0.815
	4508350431508299776	199.66	0.12022	0.4957	0.989
(26)	4900146835093979136	21.7069	−1.6754	0.3576	0.814
	4554394684994617344	201.707	1.67542	0.5282	0.995
(27)	4898954139939635200	22.8196	−1.7604	0.6082	0.997
	4554317994058579968	202.82	1.76101	−0.0006	0.797
(28)	3240357324111505408	22.9715	−9.9891	1.7556	0.784
	2028969828722698240	202.972	9.98944	0.0708	0.740
(29)	2156103604883187712	25.3766	−10.301	0.0001	0.616
	6125025335974559744	205.376	10.3015	0.0976	0.768
(30)	4808852734936088576	28.5418	1.69838	0.0835	0.889
	1029209999458461696	208.541	−1.6974	0.9782	0.728
(31)	4950684244306821120	30.6002	−9.3223	0.2858	0.994
	2036853600411478016	210.6	9.32152	0.1129	0.612
(32)	4767095206971965440	31.0675	−1.1378	0.5428	0.819
	599056024569145344	211.067	1.13788	0.2413	0.941
(33)	4950627894335897600	31.3118	−9.568	0.5654	0.996
	6136202696354955264	211.312	9.56828	0.5225	0.994
(34)	4946296918419963904	32.0863	−3.3337	0.5013	0.994
	599121995266811904	212.086	3.33396	0.1804	0.941

Table A7. *Cont.*

	SpecObjID	*Ra*	*Dec*	*z*	*Elliptical*
(35)	1753144407835568128	33.0844	0.47945	0.1208	0.788
	4541919901161881600	213.085	−0.4803	0.3592	0.973
(36)	4942780405423538176	33.8174	−4.757	0.2931	0.973
	5384229646118682624	213.817	4.75723	0.5377	0.731
(37)	4948567407985164288	34.7932	−7.0072	0.3011	0.990
	5473179862867378176	214.793	7.00645	0.3060	0.977
(38)	4770627388076195840	35.1163	0.11026	4.2378	0.744
	4538720871560773632	215.117	−0.1095	0.3080	0.869
(39)	4802194917118443520	36.5091	2.8207	0.5139	0.999
	1033647348191881216	216.509	−2.8206	0.1083	0.759
(40)	793836711925803008	36.9665	−1.1694	0.0705	0.937
	4533999294172626944	216.967	1.16883	0.5898	0.998
(41)	4941630309399003136	38.565	−9.3922	3.1585	0.552
	6155479883750834176	218.565	9.39272	1.7961	0.540
(42)	1700186150221670400	39.1133	−1.1598	0.1325	0.765
	4530637812533821440	219.113	1.15965	−0.0001	0.768
(43)	4938232268730138624	39.5952	−5.0323	0.3833	0.999
	5470806016826802176	219.596	5.033	0.3147	0.747
(44)	1204870173954172928	40.3719	0.94366	0.3124	0.984
	4533100713194553344	220.371	−0.9445	0.9001	0.959
(45)	1701291433513740288	41.581	−1.0697	0.1536	0.707
	604667932487739392	221.582	1.0688	2.7213	0.593
(46)	1757550146414995456	42.5052	−1.2479	0.1107	0.895
	4523926393155223552	222.505	1.24716	0.5312	0.998
(47)	4776111202286174208	44.2673	−0.0568	0.4766	0.923
	4525024526048165888	224.268	0.05648	0.6359	0.870
(48)	913192280402192384	46.5123	−0.1553	0.1095	0.768
	4521668546195357696	226.512	0.15569	0.3529	0.986
(49)	909757953937008640	46.6698	−0.1322	0.3371	0.977
	4521657276201172992	226.669	0.13306	0.5010	0.994
(50)	517948624043272192	50.282	−8.0389	0.0723	0.852
	6181271678262706176	230.281	8.03859	0.4335	0.896
(51)	1835370579998304256	53.5805	−6.229	0.2550	0.979
	2049174459813750784	233.581	6.2284	0.1394	0.787
(52)	2970257888494249984	55.4657	0.6257	0.5709	0.991
	354686810980378624	235.466	−0.6265	0.0809	0.870
(53)	521458539768604672	58.4107	−4.9795	0.1134	0.770
	5491059571152125952	238.41	4.97862	0.9057	0.767
(54)	522580316506843136	60.0968	−5.0671	0.1395	0.861
	2051397380066011136	240.096	5.06799	0.1615	0.712
(55)	2727025575481862144	124.032	13.3341	0.2018	0.588
	3532033024394895360	304.032	−13.334	−0.0004	0.551
(56)	5482152155748499456	136.731	6.56935	0.5701	0.995
	718431927618529280	316.73	−6.5703	0.1258	0.880
(57)	5482200534260121600	137.823	7.38189	0.5085	0.882
	718370629845280768	317.822	−7.3824	0.1306	0.874
(58)	531483062945474560	138.414	−0.6326	0.2941	0.824
	1155301165563406336	318.414	0.63161	0.1408	0.831
(59)	4303412737826357248	139.318	2.8441	0.4084	0.997
	4934949682486444032	319.319	−2.8444	1.2665	0.589
(60)	4302094698111565824	139.494	−0.1787	0.4557	0.997
	1155338274080843776	319.493	0.17935	0.1378	0.978
(61)	532577351456811008	140.024	1.07582	0.0880	0.845
	4719817306338230272	320.024	−1.0758	0.5385	0.970
(62)	533708750112974848	142.116	−0.1828	1.1383	0.770
	1112513395053062144	322.115	0.18204	0.1382	0.581
(63)	4306817925153030144	143.7	1.11628	0.0002	0.732
	4722047115600592896	323.699	−1.116	0.5033	0.986

Table A7. *Cont.*

	SpecObjID	*Ra*	*Dec*	*z*	*Elliptical*
(64)	4241523696663527424	144.728	−0.9367	0.0001	0.637
	1114734407618422784	324.727	0.93737	0.0914	0.707
(65)	4258301419972984832	144.786	−1.7252	0.4087	0.560
	5792911249252024320	324.785	1.72534	0.1804	0.908
(66)	1468184248975386624	145.258	8.63748	0.1826	0.954
	1325221896005904384	325.259	−8.6378	0.0862	0.751
(67)	5332337919582011392	145.395	1.96721	0.2884	0.985
	4937343042257944576	325.394	−1.9665	0.5580	0.992
(68)	4258354471409025024	146.058	−1.6501	0.5357	0.992
	5792991238722945024	326.059	1.64999	0.5321	0.980
(69)	5340192281129910272	147.855	1.6496	0.4277	0.612
	4926010103331028992	327.856	−1.6498	0.3152	0.806
(70)	5333521268954628096	148.617	2.03358	0.4854	0.875
	4926055458185674752	328.617	−2.0334	0.4969	0.998
(71)	300635368191977472	149.071	−0.1031	0.0844	0.660
	1162049428530423808	329.071	0.10394	0.1914	0.936
(72)	6000020484002414592	150.64	7.2737	0.5548	0.996
	807373628705368064	330.639	−7.2731	0.0585	0.558
(73)	6000135382967517184	151.226	9.18359	0.5679	0.998
	808475060082862080	331.225	−9.1836	0.1162	0.960
(74)	564246864883378176	152.036	2.60955	0.2255	0.550
	4928117316342251520	332.035	−2.6104	−0.0011	0.525
(75)	4312372383706513408	152.52	0.79	0.4913	0.962
	421174006381570048	332.519	−0.7906	0.0954	0.729
(76)	4312233570363506688	153.639	−0.8249	0.0003	0.716
	1243118065701382144	333.639	0.82408	0.2721	0.978
(77)	567537979422173184	155.631	1.86663	0.2492	0.983
	4930524972818366464	335.632	−1.8675	1.2607	0.995
(78)	4314694547482869760	157.533	0.24703	0.4817	0.995
	4731051565992378368	337.533	−0.2472	0.4740	0.999
(79)	4315711870633246720	157.653	0.02593	1.4246	0.742
	4732332497072291840	337.652	−0.026	0.5039	0.669
(80)	307417161767348224	158.238	−0.4138	0.1182	0.769
	757890377641388032	338.239	0.41328	−0.0003	0.744
(81)	4315788836447191040	159.178	0.27608	0.6207	0.772
	4733403696661528576	339.177	−0.2753	0.2538	0.973
(82)	570967906565777408	162.893	2.27202	0.1158	0.731
	4913639497436495872	342.893	−2.2713	−0.0006	0.566
(83)	4318991988898136064	165.716	−0.3594	0.5770	0.981
	4737931210767466496	345.715	0.35921	0.4103	0.999
(84)	4318962576962093056	166.315	−0.0114	0.4667	0.999
	762409377880631296	346.316	0.01125	0.2943	0.908
(85)	4318962576962093056	166.315	−0.0114	0.4667	0.999
	4736665947745026048	346.316	0.01125	0.2940	0.894
(86)	313068375699908608	166.741	−1.0969	0.0896	0.716
	763483055649220608	346.741	1.09744	0.2620	0.826
(87)	574323066767697920	168.514	3.22425	0.0752	0.585
	4909015221106376704	348.514	−3.2248	0.2472	0.992
(88)	5326812049438146560	168.772	2.64553	0.5162	0.895
	4908998453554053120	348.773	−2.6464	0.3090	0.975
(89)	4321409544887992320	169.357	0.84778	0.6557	0.958
	4740153048352423936	349.358	−0.8468	0.3819	0.682
(90)	5325629249368358912	170.61	1.43599	0.2828	0.962
	4907992950069788672	350.61	−1.4356	0.4622	0.977

Table A7. *Cont.*

	SpecObjID	*Ra*	*Dec*	*z*	*Elliptical*
(91)	315397411373606912	170.823	1.21037	0.0736	0.711
	1232915690747357184	350.822	−1.2105	0.1875	0.953
(92)	4322558259443007488	171.391	0.9829	0.5939	0.998
	4741256958060265472	351.39	−0.9824	0.3199	0.850
(93)	5325578671833481216	171.703	1.74119	0.7231	0.965
	4906813179126349824	351.704	−1.7413	0.0639	0.502
(94)	4266153857560084480	171.74	−2.1658	0.4919	0.997
	4823580149407023104	351.74	2.16561	0.0877	0.694
(95)	576595475898066944	171.814	2.39126	0.1273	0.864
	4906808781079838720	351.814	−2.3912	0.4541	0.996
(96)	316509842296563712	171.978	0.46955	0.1836	0.982
	4741226446612594688	351.979	−0.4687	0.5093	0.989
(97)	5325776034170667008	172.454	3.30746	3.9018	0.821
	4906774146463563776	352.455	−3.3076	2.2473	0.963
(98)	4323644302036566016	173.063	0.77839	0.2855	0.966
	4742391654076907520	353.062	−0.7788	0.3492	0.979
(99)	4266283325054255104	173.131	−0.3697	0.4066	0.946
	1673219253177706496	353.131	0.36908	0.1208	0.963
(100)	5336938551446077440	173.505	3.17503	0.5416	0.962
	4906696356015898624	353.504	−3.1742	0.6170	0.892
(101)	368204767274493952	173.585	−3.5904	0.0001	0.668
	4822247541330935808	353.584	3.59006	0.3967	0.978
(102)	577726048678995968	174.184	2.67686	0.4598	0.998
	4905651545024495616	354.183	−2.6774	0.5341	0.999
(103)	368325163797735424	174.441	−1.3075	0.0774	0.630
	4821148298591600640	354.441	1.30798	0.5238	0.994
(104)	6057568923170635776	176.508	10.675	0.5038	0.601
	729620840840194048	356.507	−10.676	0.1151	0.626
(105)	578737599460435968	176.726	1.68594	0.1707	0.866
	4904637795303686144	356.727	−1.6865	0.0800	0.745
(106)	4326846349808500736	179.997	−0.6119	0.1915	0.757
	1676605474079795200	359.998	0.61259	0.1477	0.591

Table A8. Pairs of spiral galaxies (with parameter spiral > 0.5) for the effect of cosmic lens [39]. Accuracy is of 0.005° for *ra* and *dec*. SpecObjID is ID of optical spectroscopic object in SDSS.

	SpecObjID	*Ra*	*Dec*	*z*	*Spiral*
(1)	734165115334584320	3.13101	−11.1988	0.1065	0.667
	1383909057404620 80	183.132	11.1974	0.0782	0.733
(2)	734165115334584320	3.13101	−11.1988	0.1065	0.667
	6073191609364119552	183.129	11.2007	0.4462	0.671
(3)	743129709168060416	19.6432	−10.9021	0.1409	0.832
	1911855335291774976	199.642	10.8989	0.1491	0.844
(4)	731860813924558848	0.62585	−10.9018	0.0288	0.743
	1382729651062859776	180.622	10.8979	0.0616	0.572
(5)	731920737308272640	358.864	−10.4171	0.2912	0.588
	1381612822210832384	178.866	10.415	0.1168	0.544
(6)	735277821219334144	5.62372	−10.3846	0.0877	0.634
	1385018008698644480	185.628	10.3872	0.0216	0.707
(7)	743125036243642368	19.8544	−10.0195	0.1420	0.655
	2024520104594663424	199.85	10.0161	0.0486	0.772
(8)	748746839045466112	28.8179	−9.94469	0.1934	0.714
	2033534720653944832	208.821	9.94239	0.1512	0.721

Table A8. *Cont.*

	SpecObjID	*Ra*	*Dec*	*z*	*Spiral*
99)	749919467877722112	29.7612	−9.64619	0.3374	0.511
	2034618849453697024	209.757	9.64868	0.0704	0.902
(10)	738753377525065728	12.1847	−9.44537	0.0958	0.633
	6092283803341422592	192.18	9.44541	0.4549	0.600
(11)	735331972167002112	5.53528	−9.40561	0.0530	0.717
	1386048526860969984	185.532	9.4091	0.1333	0.786
(12)	735345166306535424	6.11665	−9.38702	0.1427	0.630
	1386035332721436672	186.119	9.38824	0.0708	0.749
(13)	752127287444400128	34.9428	−9.36809	0.0684	0.760
	2039106770269399040	214.939	9.36446	0.0042	0.623
(14)	737601914207758336	10.3014	−9.34322	0.0559	0.512
	2014319942068889600	190.302	9.34553	0.0952	0.786
(15)	4949578408943681536	31.7084	−9.32514	0.2485	0.564
	2036888509905659904	211.713	9.3212	0.0240	0.602
(16)	730872079066359808	358.978	−9.22965	0.0756	0.764
	1381502596170147840	178.983	9.2295	0.1318	0.695
(17)	737567279591483392	9.46966	−8.87285	2.7401	0.690
	1388259919773329408	189.471	8.87691	0.1868	0.607
(18)	809694968183547904	335.363	−8.64717	0.0373	0.754
	1393917732184942592	155.36	8.6444	0.0450	0.871
(19)	809695792817268736	335.426	−8.40569	0.0705	0.685
	1393918556818663424	155.43	8.40975	0.0865	0.599
(20)	749954102493997056	29.4351	−8.39294	0.0792	0.737
	2033379689514428416	209.439	8.39684	0.0629	0.851
(21)	811867328701556736	336.686	−8.18604	0.1324	0.738
	1395060674505238528	156.685	8.18211	0.0321	0.696
(22)	519107509064067072	52.3919	−7.93974	0.1274	0.780
	1939981130342098944	232.395	7.93993	0.0749	0.853
(23)	811897015515506688	337.822	−7.80632	0.1330	0.828
	1395012845749430272	157.821	7.80735	0.0667	0.557
(24)	811928351596898304	338.431	−7.72959	0.1669	0.638
	1124917262550067200	158.428	7.73371	0.0673	0.678
(25)	808545978582853632	332.595	−7.52507	0.0563	0.742
	1392816571306502144	152.598	7.52229	0.0707	0.647
(26)	4949674616211111936	32.8596	−7.47662	0.2186	0.677
	2037965481578620928	212.857	7.47175	0.1091	0.501
(27)	519084419319883776	52.782	−6.98112	0.2000	0.591
	2048172260535068672	232.778	6.98277	0.0348	0.750
(28)	719544634476357632	318.955	−6.6414	−0.0001	0.822
	1343369057658759168	138.954	6.63737	0.0453	0.668
(29)	4951848077784252416	30.0436	−6.05043	0.2459	0.537
	2035663110638954496	210.045	6.04801	0.0804	0.700
(30)	717316199754524672	315.639	−5.41605	0.0911	0.781
	1342204125038798848	135.644	5.4139	0.1766	0.553
(31)	717315649998710784	315.543	−5.41414	0.0631	0.741
	1341003733638604800	135.54	5.41015	0.1514	0.932
(32)	4937148978455642112	324.03	−3.01385	0.5287	0.563
	640660174721280000	144.029	3.01168	0.0186	0.644
(33)	4557716584164491264	202.738	−2.64609	0.3604	0.507
	4814542157820461056	22.7336	2.64401	0.0437	0.727
(34)	4908072664662802432	352.216	−2.11621	0.0609	0.730
	576509713991100416	172.212	2.11888	0.0743	0.757
(35)	4891051125555855360	36.2809	−2.02219	0.3070	0.670
	601262744473200640	216.278	2.01777	0.0261	0.716
(36)	4892303194623311872	36.2808	−2.02121	0.8932	0.607
	601262744473200640	216.278	2.01777	0.0261	0.716

Table A8. *Cont.*

	SpecObjID	*Ra*	*Dec*	*z*	*Spiral*
(37)	1106828368889800704	312.725	−1.24782	0.1293	0.630
	525966537325045760	132.72	1.25011	0.0347	0.708
(38)	304075195369416704	151.728	−1.23313	0.0335	0.700
	1244241217248585728	331.733	1.23424	0.0495	0.703
(39)	1680994448646891520	7.38777	−1.10037	0.0591	0.694
	325539587847907328	187.385	1.1025	0.0782	0.504
(40)	1659576786771535872	330.756	−1.0931	0.4383	0.697
	564131141284554752	150.752	1.08967	0.1729	0.898
(41)	336658118953953280	206.035	−1.07384	0.0886	0.630
	1212741028830799872	26.0389	1.07793	0.0592	0.584
(42)	774688716978415616	5.28659	−1.03586	0.1077	0.711
	324403517626279936	185.29	1.03245	0.0993	0.710
(43)	422226519742507008	336.167	−0.89711	0.0990	0.505
	306369326917642240	156.167	0.893717	0.0937	0.583
(44)	315310824832919552	170.316	−0.89299	0.0403	0.681
	1234154023318218752	350.319	0.892361	0.1263	0.802
(45)	427900268781266944	344.85	−0.78249	0.1220	0.874
	311974911520303104	164.846	0.777527	0.0403	0.748
(46)	1658520430555719680	327.446	−0.75649	0.3044	0.681
	300719755709409280	147.45	0.758068	0.0732	0.850
(47)	794950517187962880	39.1814	−0.71337	0.0879	0.724
	345754653394233344	219.186	0.710053	0.0562	0.720
(48)	803929404051843072	55.401	−0.67076	0.0367	0.836
	354808032137340928	235.399	0.674322	0.0865	0.760
(49)	1659619117969205248	329.993	−0.63486	0.1275	0.595
	562961531747198976	149.997	0.638209	0.0329	0.757
(50)	1679888065054664704	5.2273	−0.60555	0.1595	0.919
	324402692992559104	185.224	0.608647	0.1025	0.566
(51)	306262399411841024	157.048	−0.54237	0.2214	0.805
	423454949158971392	337.053	0.543207	0.0584	0.632
(52)	309696723461105664	161.174	−0.50356	0.1161	0.866
	425721592429963264	341.171	0.498878	0.1068	0.780
(53)	533738162049017856	140.545	−0.46001	0.3197	0.664
	1111393817388410880	320.544	0.464496	0.1344	0.613
(54)	325434309609547776	186.904	−0.38401	0.1155	0.691
	1681098352495716352	6.90859	0.387528	0.1697	0.874
(55)	1239663120406833152	339.376	−0.1986	0.1883	0.616
	307543330726635520	159.371	0.194265	0.0965	0.508
(56)	773536159199422464	4.18587	−0.10027	0.1272	0.732
	324366134230935552	184.19	0.099486	0.0721	0.599
(57)	305206317520283648	153.857	−0.07052	0.1443	0.836
	421228432207144960	333.859	0.073314	0.0452	0.701
(58)	385078137475590144	237.596	−0.00662	0.0830	0.536
	1399629972804495360	57.6003	0.011409	0.0839	0.629

Table A9. Pairs of opposite stars in [39] with accuracy of 0.001° for *ra* and *dec*. SpecObjID is ID of optical spectroscopic object in SDSS.

	SpecObjID	*Ra*	*Dec*	*z*	*Star*
(1)	2954423276568340480	0.694712	−5.24687	−0.0002	0.974
	948114688929982464	180.694	5.24762	0.1423	0.791
(2)	1676640383573977088	0.9439	0.28991	−0.0002	0.968
	322071453446989824	180.944	−0.289746	1.0926	0.765

Table A9. *Cont.*

	SpecObjID	*Ra*	*Dec*	*z*	*Star*
(3)	1227362888558077952	1.52502	0.610184	0.0000	0.980
	322044240534202368	181.525	−0.610271	0.1814	0.546
(4)	1224979697541081088	5.97699	−1.04043	−0.0001	0.997
	2891434450627880960	185.977	1.04139	0.0001	0.592
(5)	4841613233993809920	6.05869	2.55233	1.6621	0.928
	4269537328760356864	186.058	−2.5523	0.0006	0.758
(6)	1265610500226443264	7.42917	0.131164	0.0001	0.773
	2880060552376248320	187.429	−0.131837	0.0001	1.000
(7)	1276880489881298944	8.18923	0.647915	−0.0001	0.875
	3259547102262355968	188.189	−0.648561	0.0006	0.992
(8)	1275677080259946496	9.27467	−0.0541519	0.0000	0.988
	3259523737640265728	189.275	0.05479	−0.0004	0.990
9)	739725621168465920	14.4364	−10.0952	1.9325	0.609
	3336213574535112704	194.437	10.0945	0.0001	0.998
(10)	1217134125643753472	18.1146	−0.700653	−0.0003	0.961
	3294508274463827968	198.115	0.700001	0.0005	0.814
(11)	3224609293978331136	19.2516	−9.86777	0.0004	0.997
	6109206662252855296	199.252	9.86821	2.1820	0.866
(12)	4760371418590871552	20.3504	−0.882473	2.5398	0.621
	3723477244270714880	200.351	0.882389	0.0000	0.599
(13)	4940696823976689664	38.2399	−5.23203	3.4576	0.582
	658818330399893504	218.239	5.2316	0.2002	0.976
(14)	1703605094194374656	45.1314	0.64229	2.6116	0.852
	3731245568798859264	225.132	−0.642758	−0.0002	0.995
(15)	2328467167030306816	46.0127	0.329006	−0.0004	0.904
	4521696583741865984	226.013	−0.32927	0.0001	0.996
(16)	531439632236177408	139.112	−0.747577	0.6402	0.627
	1252158529679157248	319.113	0.74727	−0.0002	1.000
(17)	2681979409950337024	140.333	6.52503	0.0005	1.000
	719600434691467264	320.333	−6.52547	0.0000	0.995
(18)	4306676088153047040	142.445	0.0328297	3.0603	0.627
	1112430931680978944	322.444	−0.0324278	−0.0002	0.805
(19)	533850312235051008	142.445	0.0328401	3.0611	0.635
	1112430931680978944	322.444	−0.0324278	−0.0002	0.805
(20)	305140071944710144	155.122	−0.10081	0.8089	0.683
	1241932791512328192	335.123	0.101456	−0.0001	0.827
(21)	567512965532641280	156.507	0.887376	0.0000	0.791
	1240819811034884096	336.506	−0.887341	−0.0001	0.995
(22)	4320303161044107264	167.537	0.858582	0.6269	0.566
	4739039243643912192	347.537	−0.857903	−0.0003	0.997
(23)	315371023094540288	170.337	0.306388	0.0000	0.913
	1672033429870372864	350.336	−0.306994	0.0002	0.775
(24)	3640122716687802368	171.106	−0.155472	0.0005	0.999
	1672091978864551936	351.106	0.155463	−0.0005	0.657
(25)	315279763629434880	171.106	−0.155471	0.0006	0.999
	1672091978864551936	351.106	0.155463	−0.0005	0.657
(26)	316494998889588736	171.432	0.43459	0.0000	1.000
	1232900572462475264	351.432	−0.433976	−0.0004	0.972
(27)	4322575576751144960	171.712	0.731312	2.4768	0.950
	1232886553689221120	351.711	−0.730549	0.0931	0.798
(28)	367067598732421120	172.137	−3.61907	0.0004	0.991
	4822344848109993984	352.138	3.61852	1.5191	0.508
(29)	369354306480007168	175.039	−3.43229	0.0004	0.930
	4820051266384691200	355.039	3.43141	0.4810	0.549
(30)	3256182321551796224	179.776	−0.658958	0.0006	0.999
	1228487139180701696	359.777	0.658661	−0.0003	1.000

Table A10. Pairs of spiral galaxies (with parameter spiral > 0.5) for the effect of cosmic mirror [39]—alternative approach. Accuracy is of 0.005° for *ra* and *dec* and *z*/2 for *z*. SpecObjID is ID of optical spectroscopic object in SDSS.

	SpecObjID	*Ra*	*Dec*	*z*	*Spiral*
(1)	734165115334584320	3.13101	−11.1988	0.1065	0.667
	1383900905740462080	183.132	11.1974	0.0782	0.733
(2)	743129709168060416	19.6432	−10.9021	0.1409	0.832
	1911855335291774976	199.642	10.8989	0.1491	0.844
(3)	731860813924558848	0.625854	−10.9018	0.0288	0.743
	1382729651062859776	180.622	10.8979	0.0616	0.572
(4)	731920737308272640	358.864	−10.4171	0.2912	0.588
	1381612822210832384	178.866	10.415	0.1168	0.544
(5)	743125036243642368	19.8544	−10.0195	0.1420	0.655
	2024520104594663424	199.85	10.0161	0.0486	0.772
(6)	748746839045466112	28.8179	−9.94469	0.1934	0.714
	2033534720653944832	208.821	9.94239	0.1512	0.721
(7)	735331972167002112	5.53528	−9.40561	0.0530	0.717
	1386048526860969984	185.532	9.4091	0.1333	0.786
(8)	735345166306535424	6.11665	−9.38702	0.1427	0.630
	1386035332721436672	186.119	9.38824	0.0708	0.749
(9)	737601914207758336	10.3014	−9.34322	0.0559	0.512
	2014319942068889600	190.302	9.34553	0.0952	0.786
(10)	730872079066359808	358.978	−9.22965	0.0756	0.764
	1381502596170147840	178.983	9.2295	0.1318	0.695
(11)	809694968183547904	335.363	−8.64717	0.0373	0.754
	1393917732184942592	155.36	8.6444	0.0450	0.871
(12)	809695792817268736	335.426	−8.40569	0.0705	0.685
	1393918556818663424	155.43	8.40975	0.0865	0.599
(13)	749954102493997056	29.4351	−8.39294	0.0792	0.737
	2033379689514428416	209.439	8.39684	0.0629	0.851
(14)	519107509064067072	52.3919	−7.93974	0.1274	0.780
	1939981130342098944	232.395	7.93993	0.0749	0.853
(15)	811897015515506688	337.822	−7.80632	0.1330	0.828
	1395012845749430272	157.821	7.80735	0.0667	0.557
(16)	811928351596898304	338.431	−7.72959	0.1669	0.638
	1124917262550067200	158.428	7.73371	0.0673	0.678
(17)	808545978582853632	332.595	−7.52507	0.0563	0.742
	1392816571306502144	152.598	7.52229	0.0707	0.647
(18)	4949674616211111936	32.8596	−7.47662	0.2186	0.677
	2037965481578620928	212.857	7.47175	0.1091	0.501
(19)	717316199754524672	315.639	−5.41605	0.0911	0.781
	1342204125038798848	135.644	5.4139	0.1766	0.553
(20)	717315649998710784	315.543	−5.41414	0.0631	0.741
	1341003733638604800	135.54	5.41015	0.1514	0.932
(21)	4908072664662802432	352.216	−2.11621	0.0609	0.730
	576509713991100416	172.212	2.11888	0.0743	0.757
(22)	304075195369416704	151.728	−1.23313	0.0335	0.700
	1244241217248585728	331.733	1.23424	0.0495	0.703
(23)	1680994448646891520	7.38777	−1.10037	0.0591	0.694
	325539587847907328	187.385	1.1025	0.0782	0.504
(24)	1659576786771535872	330.756	−1.0931	0.4383	0.697
	564131141284554752	150.752	1.08967	0.1729	0.898
(25)	336658118953953280	206.035	−1.07384	0.0886	0.630
	1212741028830799872	26.0389	1.07793	0.0592	0.584
(26)	774688716978415616	5.28659	−1.03586	0.1077	0.711
	324403517626279936	185.29	1.03245	0.0993	0.710
(27)	422226519742507008	336.167	−0.897112	0.0990	0.505
	306369326917642240	156.167	0.893717	0.0937	0.583
(28)	794950517187962880	39.1814	−0.713369	0.0879	0.724
	345754653394233344	219.186	0.710053	0.0562	0.720

Table A10. *Cont.*

	SpecObjID	*Ra*	*Dec*	*z*	*Spiral*
(29)	803929404051843072	55.401	−0.670755	0.0367	0.836
	354808032137340928	235.399	0.674322	0.0865	0.760
(30)	1679888065054664704	5.2273	−0.605546	0.1595	0.919
	324402692992559104	185.224	0.608647	0.1025	0.566
(31)	309696723461105664	161.174	−0.503556	0.1161	0.866
	425721592429963264	341.171	0.498878	0.1068	0.780
(32)	533738162049017856	140.545	−0.460014	0.3197	0.664
	1111393817388410880	320.544	0.464496	0.1344	0.613
(33)	325434309609547776	186.904	−0.38401	0.1155	0.691
	1681098352495716352	6.90859	0.387528	0.1697	0.874
(34)	1239663120406833152	339.376	−0.1986	0.1883	0.616
	307543330726635520	159.371	0.194265	0.0965	0.508
(35)	773536159199422464	4.18587	−0.100271	0.1272	0.732
	324366134230935552	184.19	0.0994864	0.0721	0.599
(36)	385078137475590144	237.596	−0.00662	0.0830	0.536
	1399629972804495360	57.6003	0.0114088	0.0839	0.629

Appendix C

Table A11. Pairs of opposite quasars from GAIADR2Q catalog for mirror and lens effects. Source_id—the unique identification number in GAIA DR2 database. Accuracy is of 0.001° for *ra* and *dec*. Redshift *z* is unknown.

	Allwise_Name	*Source_Id*	*Ra*	*Dec*
(1)	J210304.14-762224.9	6368528062846000640	315.7673682	−76.37360527
	J090304.41+762224.0	1125452302531483520	135.7684166	76.37343393
(2)	J000923.83-752826.7	4685204141864675840	2.349349915	−75.47408959
	J120924.56+752830.2	1692570332734552320	182.3515394	75.47502083
(3)	J005511.81-723727.8	4688988630882739328	13.79922983	−72.6245651
	J125511.51+723731.8	1689619312245569024	193.7978223	72.62551077
(4)	J054056.36-604959.0	4759331807060038272	85.23483284	−60.83306433
	J174056.57+605000.8	1435781247493233280	265.2357231	60.83356526
(5)	J042637.98-602917.9	4678309551123478016	66.65829152	−60.4883202
	J162638.53+602917.1	1624874054648019712	246.6600443	60.48800541
(6)	J003634.96-450211.3	4979663732423902336	9.145683022	−45.03652837
	J123635.26+450208.0	1541170364728499840	189.1469143	45.03558095
(7)	J023912.05-424657.5	4947107506659554304	39.80039767	−42.78281482
	J143911.83+424655.0	1492995984312364928	219.7994728	42.78193739
(8)	J010933.66-415122.0	4984721382832208000	17.39027938	−41.85614291
	J130933.48+415122.3	1525961816813896576	197.3894785	41.8561489
(9)	J030635.12-342620.5	5048328852053654272	46.6464308	−34.43910643
	J150634.97+342621.0	1290665847434238336	226.6455941	34.43914596
(10)	J144620.40-322022.3	6215805347992022144	221.5850719	−32.33959386
	J024620.21+322020.8	133564171416873728	41.58418524	32.33907625
(11)	J020549.77-245224.7	5121462661817011712	31.45738864	−24.87356749
	J140549.73+245227.4	1257473141874860032	211.457199	24.87428879
(12)	J120429.60-215735.5	3493448195802870400	181.1233688	−21.95989953
	J000429.68+215736.0	2847161965440082176	1.123715043	21.9600063
(13)	J043710.51-215420.2	4898466860297217536	69.29392704	−21.90553489
	J163710.55+215416.4	1297817517737857024	249.2939377	21.90458255
(14)	J040147.38-180917.4	5096949256234108800	60.4473916	−18.15484375
	J160147.61+180917.7	1199646075865168128	240.4484116	18.155046

Table A11. *Cont.*

	Allwise_Name	*Source_Id*	*Ra*	*Dec*
(15)	J124510.71-180851.9	3522237773904469248	191.294554	−18.1478664
	J004510.62+180851.9	2782801120299995520	11.29451879	18.14802663
(16)	J150108.76-134935.8	6311851640047858048	225.2865151	−13.82676674
	J030108.57+134935.1	29187876189414144	45.28574655	13.8264156
(17)	J035733.19-083041.3	3194958963846806144	59.38814002	−8.511587953
	J155733.13+083042.9	4454299557503538688	239.3880677	8.511930041

Appendix D

Table A12. Pairs of opposite quasars from the Milliquas 6.3 catalog for the lens effect. Accuracy is of 0.001° for *ra* and *dec*. Descrip column is the classification of object, see [47]. Redshift *z* is given when available, although is not essential here.

	Ra	*Dec*	*Name*	*Descrip*	*Z*
(1)	255.5777892	−77.0249529	WISEA J170218.69-770129.2	q	2.3
	75.5809969	77.0255634	WISEA J050219.24+770131.4	q	2.3
(2)	315.7673595	−76.3736026	WISEA J210304.14-762224.9	q	1
	135.7683983	76.3734303	WISEA J090304.41+762224.0	q	2.4
(3)	2.3493535	−75.4740875	WISEA J000923.83-752826.7	q	0.8
	182.3515932	75.4750181	WISEA J120924.56+752830.2	q	0.7
(4)	85.679027	−68.1421484	WISEA J054242.99-680831.9	q	1.4
	265.6773749	68.1413691	SDSS J174242.55+680829.1	q	1.5
(5)	352.8305884	−66.7005686	WISEA J233119.35-664201.9	q	
	172.8287239	66.7011287	SDSS J113118.89+664204.0	q	1.5
(6)	350.1300997	−64.0960807	WISEA J232031.22-640545.8	q	0.8
	170.1297219	64.0966844	SDSS J112031.12+640548.1	q	1.4
(7)	77.2847276	−61.1581631	WISEA J050908.30-610929.5	q	0.6
	257.2851687	61.1587398	SDSS J170908.44+610931.4	q	0.9
(8)	85.2348298	−60.8330635	WISEA J054056.36-604959.0	q	0.6
	265.2357267	60.8335658	WISEA J174056.57+605000.8	q	1.9
(9)	66.6582972	−60.4883083	WISEA J042637.98-602917.9	q	2.8
	246.6600372	60.4879967	WISEA J162638.53+602917.1	q	
(10)	55.6305834	−55.3800834	J034231.34-552248.3	X	
	235.6289338	55.3794316	SDSS J154230.94+552245.9	Q	2.268
(11)	12.2865176	−55.3358661	WISEA J004908.81-552009.3	q	1.3
	192.2854767	55.3366013	SDSS J124908.51+552011.7	q	1.9
(12)	18.9229286	−55.1625237	WISEA J011541.50-550945.0	qR	0.7
	198.9241743	55.16331	SDSS J131541.80+550947.9	Q	2.518
(13)	350.4801742	−55.0232756	XXLS J232155.23-550123.3	QX	1.788
	170.4785659	55.0239884	SDSS J112154.85+550126.3	Q	1.73
(14)	13.9470844	−54.2692763	WISEA J005547.29-541609.5	q	2
	193.9459076	54.2689056	SDSS J125547.01+541608.0	q	0.3
(15)	2.4579845	−53.9814555	WISEA J000949.91-535853.2	q	0.2
	182.4575348	53.980648	SDSS J120949.80+535850.3	q	0.3
(16)	323.9286029	−53.3487347	WISEA J213542.85-532055.4	q	0.9
	143.9271545	53.3484154	SDSS J093542.51+532054.2	q	0.5
(17)	348.3491422	−53.3478756	XXLS J231323.75-532051.9	QX	0.496
	168.3507385	53.3479691	SDSS J111324.17+532052.6	q	0.3
(18)	80.7328764	−52.4533568	WISEA J052255.89-522712.0	q	
	260.732699	52.4532957	SDSS J172255.84+522712.0	q	2.1
(19)	38.535212	−50.9830297	WISEA J023408.44-505858.7	q	
	218.5348844	50.9840003	SDSS J143408.35+505902.3	Q	3.175
(20)	315.5807126	−50.5996161	WISEA J210219.36-503558.6	q	2.2
	135.5799944	50.6005463	SDSS J090219.19+503601.9	Q	2.619

Table A12. *Cont.*

	Ra	*Dec*	*Name*	*Descrip*	*Z*
(21)	68.3167757	−50.5098938	WISEA J043316.02-503035.6	q	1.1
	248.3167223	50.5106667	PGC 2375138	GR2	
(22)	27.2491308	−50.0692574	WISEA J014859.79-500409.4	q	1.8
	207.2486497	50.0702154	SDSS J134859.67+500412.8	Q	1.559
(23)	70.1774106	−49.1605048	WISEA J044042.58-490937.9	q	0.9
	250.1779433	49.1604959	SDSS J164042.70+490937.7	q	3.2
(24)	352.4638668	−46.4933229	WISEA J232951.30-462936.0	q	
	172.4629902	46.4929967	SDSS J112951.12+462934.8	Q	1.874
(25)	51.7544779	−45.8163472	WISEA J032701.07-454859.0	q	2.1
	231.753214	45.816666	SDSS J152700.77+454859.9	q	0.9
(26)	13.7156676	−45.5401862	WISEA J005451.73-453224.7	q	1
	193.7148005	45.5407984	SDSS J125451.55+453226.8	Q	0.599
(27)	9.1456769	−45.036539	WISEA J003634.96-450211.3	q	1.6
	189.1469172	45.0355819	SDSS J123635.25+450208.0	Q	0.401
(28)	312.4572617	−43.5311298	WISEA J204949.73-433151.7	q	1.7
	132.4578712	43.5314134	SDSS J084949.88+433153.1	q	2.6
(29)	39.8003988	−42.7828145	WISEA J023912.05-424657.5	q	1.8
	219.7994764	42.7819417	SDSS J143911.87+424655.0	Q	2.376
(30)	58.8593889	−42.1836389	J035526.25-421101.1	X	
	238.859031	42.1833947	SDSS J155526.16+421100.1	Q	1.222
(31)	75.7744245	−40.7936211	WISEA J050305.91-404736.8	q	2.3
	255.7743683	40.7937126	SDSS J170305.84+404737.3	q	0.3
(32)	327.4360427	−38.6604478	WISEA J214944.65-383937.5	q	0.6
	147.4361286	38.659581	SDSS J094944.67+383934.5	Q	1.326
(33)	17.7159333	−38.4864674	WISEA J011051.83-382911.3	q	2.2
	197.7147558	38.4865089	SDSS J131051.54+382911.4	Q	0.817
(34)	35.9159531	−37.2880557	WISEA J022339.81-371716.8	q	0.7
	215.9154018	37.2873321	SDSS J142339.69+371714.3	q	1.4
(35)	5.4863222	−36.9636832	WISEA J002156.72-365749.2	q	1.6
	185.4861944	36.9634266	SDSS J122156.67+365748.3	Q	2.097
(36)	288.7726299	−36.2604918	WISEA J191505.43-361537.9	q	1
	108.771553	36.2600021	SDSS J071505.17+361536.0	q	0.4
(37)	48.2374301	−35.2506342	WISEA J031256.97-351502.2	qX	1.9
	228.2368457	35.250557	SDSS J151256.83+351502.0	q	1.3
(38)	71.9969184	−34.9231867	WISEA J044759.25-345523.3	q	2.5
	251.99809	34.922451	DEEP J164759.54+345520.8	A	0.743
(39)	51.0522347	−34.8159832	WISEA J032412.53-344857.3	q	0.7
	231.051651	34.815155	SDSS J152412.39+344854.5	q	0
(40)	64.4053066	−34.4443255	WISEA J041737.25-342639.2	q	2.3
	244.4049248	34.4447566	SDSS J161737.18+342641.1	q	1.9
(41)	46.6464316	−34.4391069	WISEA J030635.12-342620.5	q	1.5
	226.6455899	34.4391456	SDSS J150634.94+342620.9	Q	2.275
(42)	13.9539794	−33.5205216	Q 0053-3347	Q	2.08
	193.9543304	33.519737	SDSS J125549.03+333111.0	q	0.9
(43)	61.3792872	−33.3589696	WISEA J040531.02-332132.4	q	1.3
	241.3804819	33.3584594	SDSS J160531.31+332130.4	q	0.6
(44)	52.3380705	−33.1624587	WISEA J032921.13-330944.7	q	1
	232.3374622	33.1619242	SDSS J152921.00+330942.9	q	0.9
(45)	35.6523275	−32.9501625	WISEA J022236.55-325700.5	q	2
	215.6517237	32.9500411	SDSS J142236.40+325700.2	q	1.8
(46)	24.818008	−32.6980218	WISEA J013916.33-324152.7	q	1.6
	204.8176575	32.6980515	SDSS J133916.23+324152.9	q	0
(47)	331.3013548	−31.5723459	2QZ J220512.3-313421	Q	1.934
	151.3004456	31.5727386	SDSS J100512.10+313421.8	q	0.9
(48)	178.0274651	−31.4001968	WISEA J115206.58-312400.4	q	2.4
	358.026947	31.4004002	SDSS J235206.46+312401.4	q	1
(49)	341.9315476	−31.0519246	6QZ J224743.5-310306	Q	2.614
	161.9314813	31.0522394	SDSS J104743.55+310308.0	q	0

Table A12. *Cont.*

	Ra	*Dec*	*Name*	*Descrip*	*Z*
(50)	309.9034723	−30.9013056	J203936.83-305404.7	X	
	129.9024969	30.9010042	SDSS J083936.60+305403.6	Q	1.1
(51)	15.5519167	−30.6883056	2QZ J010212.4-304118	N	0.201
	195.5513019	30.6890974	SDSS J130212.30+304120.7	QX	0.897
(52)	188.680682	−30.5578933	WISEA J123443.36-303328.3	q	1
	8.6803036	30.558761	SDSS J003443.27+303331.6	Q	1.254
(53)	300.1895832	−30.1375161	WISEA J200045.51-300814.8	q	0.6
	120.1898279	30.1370937	SDSS J080045.55+300813.5	Q	1.343
(54)	332.1756094	−29.9838041	2QZ J220842.1-295902	Q	1.023
	152.1766832	29.9847166	SDSS J100842.39+295905.0	Q	2.56
(55)	12.3530442	−29.9213175	Q 0046-3011	Q	1.081
	192.3529914	29.9214458	SDSS J124924.71+295517.2	q	2.2
(56)	183.3282018	−29.1793456	WISEA J121318.77-291045.5	q	0.3
	3.327841	29.1787777	SDSS J001318.68+291043.5	q	0.9
(57)	338.8539592	−28.7111297	2QZ J223525.0-284240	Q	2.567
	158.8546667	28.71175	J103525.12+284242.3	R	
(58)	333.8811688	−28.3336528	2QZ J221531.4-282001	Q	1.909
	153.8815524	28.3342401	SDSS J101531.57+282003.3	Q	2.395
(59)	80.438152	−28.1840351	WISEA J052145.16-281102.6	q	0.6
	260.437853	28.1849529	SDSS J172145.08+281105.8	q	1.3
(60)	65.5058337	−27.9944556	WISEA J042201.40-275940.0	q	0.2
	245.5051373	27.993782	SDSS J162201.23+275937.6	Q	2.29
(61)	189.5249477	−27.4782258	WISEA J123805.97-272841.7	q	2.3
	9.5243507	27.4772773	SDSS J003805.84+272838.2	Q	1.937
(62)	44.5344194	−26.5790235	WISEA J025808.26-263444.5	q	1.5
	224.5352818	26.5780647	SDSS J145808.46+263441.0	q	2.1
(63)	42.3864196	−26.4011219	WISEA J024932.73-262404.3	q	3
	222.3872658	26.401885	SDSS J144932.94+262406.7	qR	0.3
(64)	197.0438404	−25.791086	WISEA J130810.53-254728.0	q	1.1
	17.0442989	25.7919436	SDSS J010810.62+254730.9	Q	1.843
(65)	47.3495546	−25.1085428	WISEA J030923.89-250630.5	q	1
	227.3495813	25.1081434	SDSS J150923.90+250629.2	q	1.8
(66)	31.4573892	−24.8735666	WISEA J020549.77-245224.7	q	0.3
	211.4572001	24.8742878	SDSS J140549.72+245227.4	QX	0.93
(67)	48.9227	−24.5943481	WISEA J031541.43-243539.7	qR	1
	228.9221526	24.5946659	SDSS J151541.31+243540.7	Q	3.21
(68)	314.8735964	−23.9469948	WISEA J205929.66-235649.1	q	0.4
	134.8731466	23.946707	SDSS J085929.56+235648.1	Q	1.085
(69)	211.3857165	−23.9417462	WISEA J140532.57-235630.1	q	2.3
	31.3864591	23.9416464	SDSS J020532.75+235629.9	Q	2.005
(70)	9.3024771	−23.7730802	SDSS J003712.58-234622.9	q	1.7
	189.3025669	23.7724481	SDSS J123712.61+234620.8	Q	2.644
(71)	55.1065124	−23.5058167	WISEA J034025.56-233020.9	q	2.5
	235.1074677	23.5059795	SDSS J154025.79+233021.5	q	0.1
(72)	325.6254779	−23.1632401	WISEA J214230.10-230947.5	q	0.9
	145.6252854	23.1622808	SDSS J094230.07+230944.1	q	1.4
(73)	40.1013553	−23.0486453	J024024.32-230255.1	X	
	220.1017934	23.0486683	SDSS J144024.43+230255.2	q	1.6
(74)	330.2260385	−23.0089209	WISEA J220054.23-230032.0	q	0.6
	150.2259947	23.0087942	SDSS J100054.23+230031.6	Q	3.027
(75)	15.629173	−22.6311972	WISEA J010230.99-223752.2	qR	1.9
	195.6286965	22.6311474	SDSS J130230.88+223752.2	Q	3.405
(76)	152.8034904	−22.2785203	WISEA J101112.84-221642.2	qR	0.4
	332.802887	22.2781582	SDSS J221112.69+221641.3	q	0
(77)	181.1233682	−21.9598988	WISEA J120429.60-215735.5	q	0.8
	1.1237153	21.9600067	WISEA J000429.68+215736.0	q	1.4
(78)	69.293922	−21.9055291	WISEA J043710.51-215420.2	q	0.7
	249.293937	21.9045811	SDSS J163710.55+215416.4	Q	1.411

Table A12. *Cont.*

	Ra	*Dec*	*Name*	*Descrip*	*Z*
(79)	199.0397778	−21.5273612	J131609.54-213138.5	R	
	19.0390736	21.5264408	SDSS J011609.37+213135.1	Q	2.088
(80)	22.013869	−20.8937502	SDSS J012803.33-205337.4	q	1.6
	202.0134583	20.8942223	SDSS J132803.22+205339.2	q	0.3
(81)	341.8649478	−20.6885193	WISEA J224727.58-204119.2	q	1.2
	161.8640315	20.6894371	SDSS J104727.36+204121.9	Q	2.262
(82)	347.9339167	−20.5751112	J231144.14-203430.4	R	
	167.9335297	20.5758125	SDSS J111144.05+203432.9	q	0
(83)	191.7714081	−20.2647247	SDSS J124705.13-201553.0	q	0.3
	11.7713099	20.2641487	SDSS J004705.11+201550.9	q	4.5
(84)	29.9053228	−19.4208582	WISEA J015937.24-192514.6	q	0.3
	209.9044189	19.4200344	SDSS J135937.06+192512.1	q	0
(85)	315.432881	−19.3894197	WISEA J210143.86-192321.5	q	1.8
	135.4334805	19.3888631	SDSS J090144.03+192319.9	q	1.4
(86)	315.2686772	−19.0978465	WISEA J210104.48-190552.1	q	1.1
	135.2689056	19.0972805	SDSS J090104.53+190550.2	q	0.4
(87)	331.1935682	−18.7863235	QSM3:36	QX	0.873
	151.1930394	18.7867023	SDSS J100446.32+184712.1	q	1.5
(88)	190.1060207	−18.3141455	WISEA J124025.44-181851.0	q	0.3
	10.105106	18.314339	SDSS J004025.23+181851.6	Q	1.156
(89)	60.4473986	−18.154863	WISEA J040147.38-180917.4	q	0.4
	240.4484093	18.1550387	WISEA J160147.61+180917.7	q	0.8
(90)	191.2945552	−18.1478667	WISEA J124510.71-180851.9	q	1.5
	11.2945118	18.1480237	SDSS J004510.68+180852.8	Q	2.955
(91)	173.7006562	−18.0690647	WISEA J113448.15-180408.7	q	2.3
	353.7006507	18.0682592	SDSS J233448.15+180405.7	Q	2.881
(92)	24.9069328	−17.90944	SDSS J013937.65-175434.1	qX	2
	204.9072341	17.910056	SDSS J133937.73+175436.2	q	1.3
(93)	352.4344723	−17.8641457	WISEA J232944.27-175150.9	q	1.3
	172.4351845	17.8639806	SDSS J112944.45+175150.4	q	3.3
(94)	16.7804723	−17.6221112	J010707.31-173719.6	X	
	196.7801056	17.6227665	SDSS J130707.22+173721.9	q	0
(95)	29.9174996	−17.2967528	SDSS J015940.19-171747.7	q	0.9
	209.9180908	17.2973289	SDSS J135940.34+171750.3	q	1.8
(96)	166.796621	−17.1482174	SDSS J110711.18-170853.6	q	1.1
	346.7956543	17.1488914	SDSS J230710.95+170856.0	q	1.1
(97)	43.6995104	−17.1177057	WISEA J025447.88-170703.8	q	1.9
	223.699538	17.1176163	SDSS J145447.88+170703.4	q	1.1
(98)	354.8260594	−16.8908891	WISEA J233918.25-165327.1	q	1.5
	174.8269911	16.8898926	SDSS J113918.48+165323.6	N	0.062
(99)	165.3264823	−16.8833416	SDSS J110118.35-165300.0	q	2
	345.3268127	16.8840275	SDSS J230118.43+165302.4	q	0.9
(100)	43.6272916	−16.2718962	SDSS J025430.54-161618.8	q	0.3
	223.6267804	16.2723981	SDSS J145430.42+161620.6	N	0.158
(101)	310.9503012	−16.1176807	SDSS J204348.07-160703.6	q	2.1
	130.9494101	16.1168221	SDSS J084347.85+160700.5	q	0.5
(102)	352.1153529	−16.006742	WISEA J232827.67-160024.4	q	0.8
	172.1161957	16.0070877	SDSS J112827.88+160025.5	q	3.1
(103)	149.4813563	−15.5088164	WISEA J095755.52-153031.8	q	2.2
	329.4811707	15.5078583	SDSS J215755.48+153028.2	q	0.8
(104)	5.3051921	−14.5195128	SDSS J002113.24-143110.2	q	2
	185.3048056	14.5204167	J122113.15+143113.5	X	
(105)	310.7940674	−14.2887297	SDSS J204310.57-141719.4	q	4.1
	130.7950205	14.2880621	SDSS J084310.80+141717.0	Q	0.887
(106)	321.3724784	−14.2055432	WISEA J212529.39-141219.9	q	1
	141.3732103	14.2057221	SDSS J092529.57+141220.5	A	0.473
(107)	335.04035	−13.9567208	J222009.68-135724.1	R	
	155.0393304	13.9561601	WISEA J102009.42+135722.3	q	1.2

Table A12. *Cont.*

	Ra	*Dec*	*Name*	*Descrip*	*Z*
(108)	225.2865096	−13.8267692	WISEA J150108.76-134935.8	q	1.8
	45.2857528	13.8264077	WISEA J030108.57+134935.1	q	0.7
(109)	22.4869537	−13.2917978	WISEA J012956.87-131730.2	q	1.6
	202.4875051	13.2909737	SDSS J132957.00+131727.5	Q	3.144
(110)	190.3695441	−13.095317	SDSS J124128.69-130543.1	q	0.6
	10.3688927	13.0956669	SDSS J004128.53+130544.4	q	0.4
(111)	178.5013735	−12.8384611	WISEA J115400.32-125018.4	q	0.9
	358.501349	12.8377738	SDSS J235400.32+125015.9	q	1.7
(112)	56.1097236	−12.7916261	WISEA J034426.33-124729.7	q	0.3
	236.109024	12.7923546	SDSS J154426.16+124732.4	q	0.5
(113)	39.5398838	−11.856346	WISEA J023809.57-115122.9	q	1.1
	219.5404339	11.8565365	SDSS J143809.70+115123.5	q	1.1
(114)	304.7146082	−11.8357393	SDSS J201851.51-115008.7	q	3
	124.7154201	11.8347625	SDSS J081851.70+115005.1	Q	3.092
(115)	18.0162381	−10.9062962	SDSS J011203.89-105422.6	q	1.9
	198.0161728	10.9057355	SDSS J131203.88+105420.7	q	0.8
(116)	9.0308609	−10.8671694	SDSS J003607.40-105201.8	q	0
	189.0314246	10.867996	SDSS J123607.54+105204.8	q	1.4
(117)	33.4777451	−10.6369173	SDSS J021354.65-103812.8	q	1.7
	213.4776649	10.6378738	SDSS J141354.63+103816.3	q	2.1
(118)	24.1238435	−10.5259013	SDSS J013629.72-103133.2	q	2.3
	204.1232718	10.5261989	SDSS J133629.58+103134.3	QX	2.83
(119)	4.7525	−10.4661945	J001900.60-102758.3	X	
	184.7530212	10.4664478	SDSS J121900.72+102759.2	q	0.3
(120)	3.1000975	−10.3740423	FIRST J0012-1022	QRX	0.228
	183.0995052	10.3736727	SDSS J121223.88+102225.2	q	1.8
(121)	334.8985316	−9.69364	SDSS J221935.64-094137.1	q	2
	154.8980454	9.6929715	SDSS J101935.52+094134.7	Q	2.313
(122)	38.5649712	−9.3922666	SDSS J023415.59-092332.0	Q	3.159
	218.5647491	9.3927159	SDSS J143415.53+092333.7	Q	1.796
(123)	140.4377101	−9.3709292	WISEA J092145.05-092215.4	q	0.8
	320.4374695	9.3712921	SDSS J212144.99+092216.6	q	1.2
(124)	158.5661086	−9.1451916	WISEA J103415.86-090842.6	q	
	338.56533	9.1442883	SDSS J223415.68+090839.5	q	1.6
(125)	37.7328056	−9.0068612	J023055.87-090024.7	X	
	217.7330967	9.0059802	SDSS J143055.94+090021.5	Q	2.383
(126)	30.7570701	−8.6899451	SDSS J020301.69-084123.8	q	2.2
	210.757843	8.6908655	SDSS J140301.88+084127.1	q	0
(127)	59.3881301	−8.5115865	WISEA J035733.19-083041.3	q	0.3
	239.388068	8.511933	SDSS J155733.13+083042.9	A	0.047
(128)	358.0582864	−8.2121914	SDSS J235213.99-081244.0	q	2
	178.0589787	8.211923	SDSS J115214.15+081242.8	q	1.1
(129)	338.7737732	−8.142704	SDSS J223505.70-080833.7	q	0.4
	158.773734	8.1430363	SDSS J103505.69+080834.9	q	0.9
(130)	332.3883082	−7.9754252	SDSS J220933.20-075831.4	q	2
	152.3875951	7.9759758	SDSS J100933.02+075833.4	Q	2.532
(131)	9.7862066	−7.7658426	SDSS J003908.70-074557.1	q	1.7
	189.7870789	7.765204	SDSS J123908.89+074554.7	q	0.3
(132)	47.6100042	−7.6891097	SDSS J031026.40-074120.8	q	1.6
	227.6091204	7.6900591	AX J1510+0742	AX	0.459
(133)	16.9498272	−7.6777906	SDSS J010747.95-074040.0	q	1
	196.9504416	7.6768407	WISEA J130748.10+074036.6	q	0.1
(134)	25.2191067	−7.6683216	SDSS J014052.58-074005.9	q	0
	205.2184797	7.668935	SDSS J134052.43+074008.1	Q	1.077
(135)	46.2892799	−7.2429566	SDSS J030509.42-071434.6	q	0.5
	226.2901611	7.2421827	SDSS J150509.63+071431.8	q	1
(136)	42.2919481	−7.135162	SDSS J024910.06-070806.6	Q	2.561
	222.2917609	7.1344065	SDSS J144910.02+070803.8	q	1.5

Table A12. *Cont.*

	Ra	*Dec*	*Name*	*Descrip*	*Z*
(137)	5.8514071	−7.0936418	SDSS J002324.33-070537.1	q	0.6
	185.8513794	7.093749	SDSS J122324.33+070537.4	qX	0.6
(138)	328.3192139	−6.7707705	SDSS J215316.61-064614.7	q	1.7
	148.3194775	6.7699293	SDSS J095316.66+064611.7	Q	1.092
(139)	209.4759723	−6.7408847	SDSS J135754.23-064427.1	q	1.7
	29.4751402	6.7413482	LAMOSTJ015754.04+064428.9	Q	1.565
(140)	28.0452862	−6.7327127	SDSS J015210.86-064357.7	q	0.4
	208.0451896	6.732888	SDSS J135210.84+064358.3	q	1.6
(141)	310.9553801	−6.521875	SDSS J204349.29-063118.7	q	2.2
	130.9551195	6.521617	SDSS J084349.22+063117.8	q	1.1
(142)	10.7848358	−6.4319367	SDSS J004308.36-062554.9	q	0.7
	190.7848032	6.4326671	SDSS J124308.35+062557.6	q	2.2
(143)	17.3667355	−6.3337412	SDSS J010928.01-062001.4	q	0.3
	197.3658023	6.3341348	WISEA J130927.78+062002.7	q	1.4
(144)	42.0314865	−6.0404835	SDSS J024807.55-060225.7	q	1.1
	222.031267	6.0407225	SDSS J144807.50+060226.5	Q	2.324
(145)	155.888588	−5.987767	WISEA J102333.26-055915.9	q	1
	335.8882692	5.9887381	WISEA J222333.18+055919.4	q	0.8
(146)	30.4249489	−5.8591802	VIPERS 101146840	Q	2.126
	210.4239741	5.858464	SDSS J140141.75+055130.4	q	1.1
(147)	345.5845337	−5.7119699	SDSS J230220.28-054243.0	q	5.5
	165.5838875	5.7116443	SDSS J110220.13+054242.0	q	1.2
(148)	38.2399412	−5.2320188	SDSS J023257.58-051355.2	Q	3.458
	218.2393005	5.2315766	MS 14304+0527	QX	0.2
(149)	318.9673157	−5.08287	SDSS J211552.15-050458.3	q	0.4
	138.967392	5.0823555	SDSS J091552.17+050456.4	q	0.6
(150)	2.9218395	−4.9358745	SDSS J001141.24-045609.1	q	3.1
	182.9209776	4.9351431	SDSS J121141.03+045606.5	q	2
(151)	339.1091419	−4.9108333	SDSS J223626.19-045438.9	q	1.6
	159.1097246	4.9101383	Q 1033+051	Q	1.048
(152)	44.1149634	−4.8954605	SDSS J025627.59-045343.6	Q	1.645
	224.1147795	4.8951414	SDSS J145627.54+045342.5	q	0.4
(153)	318.953949	−4.8887081	SDSS J211548.94-045319.3	q	0.5
	138.9544497	4.8892847	LAMOSTJ091549.07+045321.5	Q	1.974
(154)	11.8971845	−4.6937364	SDSS J004735.33-044137.5	Q	1.931
	191.8971312	4.6943342	SDSS J124735.31+044139.5	Q	0.868
(155)	215.4113925	−4.6316734	WISEA J142138.70-043753.9	q	1.5
	35.4120872	4.6310081	SDSS J022138.89+043751.6	Q	2.018
(156)	44.1504799	−4.5690993	SDSS J025636.11-043408.8	Q	3.094
	224.1496194	4.5693052	WISEA J145635.91+043409.4	q	1.9
(157)	356.0054037	−4.4881222	SDSS J234401.30-042917.1	q	2.1
	176.0057901	4.4880115	SDSS J114401.38+042916.8	q	2.2
(158)	313.1420516	−4.4458056	WISEA J205234.08-042644.8	q	2.3
	133.1429183	4.4466583	SDSS J085234.29+042648.0	Q	2.745
(159)	28.6933545	−3.9445188	SDSS J015446.40-035640.2	Q	2.322
	208.6934509	3.9447002	SDSS J135446.42+035640.9	q	0.8
(160)	190.871543	−3.9282525	SDSS J124329.17-035541.7	qR	2.2
	10.8722192	3.9287007	SDSS J004329.33+035543.2	q	0.1
(161)	36.0865531	−3.5906219	SDSS J022420.77-033526.2	QX	0.552
	216.0868377	3.5907531	SDSS J142420.83+033526.7	q	1.8
(162)	23.3642954	−3.508162	SDSS J013327.43-033029.3	Q	1.724
	203.3644091	3.5075679	SDSS J133327.45+033027.2	q	1
(163)	342.6967773	−3.4136071	SDSS J225047.22-032448.9	q	1.3
	162.6963654	3.4144416	SDSS J105047.12+032451.9	q	0.3
(164)	29.2919507	−3.3900862	SDSS J015710.06-032324.3	Q	1.504
	209.2925571	3.3891148	WISEA J135710.20+032320.9	q	0.7
(165)	351.8889506	−3.1861348	SDSS J232733.34-031109.9	q	2.6
	171.889383	3.186412	SDSS J112733.45+031111.0	q	

Table A12. *Cont.*

	Ra	*Dec*	*Name*	*Descrip*	*Z*
(166)	215.9122427	−3.1485981	SDSS J142338.93-030854.9	q	2
	35.911743	3.1485686	SDSS J022338.81+030854.7	Q	2.173
(167)	59.7010545	−3.0252538	WISEA J035848.22-030131.3	q	0.9
	239.7015228	3.0244355	SDSS J155848.36+030127.9	q	1
(168)	357.4388055	−2.8983433	SDSS J234945.32-025354.0	Q	0.938
	177.4378903	2.899283	SDSS J114945.07+025357.3	q	1.5
(169)	316.7376204	−2.8595332	WISEA J210657.03-025134.3	q	1.5
	136.7379203	2.8594311	SDSS J090657.10+025133.9	A	0.194
(170)	11.9639927	−2.8499138	SDSS J004751.36-025059.6	Q	1.262
	191.9631892	2.849156	SDSS J124751.16+025056.9	Q	1.568
(171)	323.6482118	−2.7731332	SDSS J213435.57-024623.2	Q	3.228
	143.6486958	2.7735964	SDSS J093435.68+024624.9	Q	0.763
(172)	31.1501826	−2.6833719	SDSS J020436.04-024100.0	Q	2.149
	211.1496969	2.6833621	SDSS J140435.92+024100.1	q	0.4
(173)	11.428722	−2.6318303	SDSS J004542.89-023754.5	q	1
	191.4280252	2.6316203	WISEA J124542.71+023753.8	qX	0.7
(174)	9.1659024	−2.4347542	SDSS J003639.81-022604.9	Q	1.055
	189.165748	2.4344829	SDSS J123639.77+022604.1	q	2
(175)	17.5345544	−2.4323457	SDSS J011008.29-022556.4	Q	1.068
	197.5339023	2.4329717	SDSS J131008.13+022558.6	q	1.6
(176)	145.7966766	−2.4094768	SDSS J094311.20-022434.1	q	0.9
	325.7966554	2.410309	SDSS J214311.19+022437.1	q	1.2
(177)	73.1702424	−2.260853	WISEA J045240.88-021539.0	q	2.4
	253.170835	2.2612845	J165241.00+021540.6	X	
(178)	181.200555	−2.225128	2QZ J120448.1-021331	Q	0.888
	1.2006668	2.2249101	SDSS J000448.16+021329.6	q	1.2
(179)	21.4036505	−2.1947235	SDSS J012536.87-021141.0	Q	2.542
	201.4034175	2.1940664	SDSS J132536.82+021138.6	q	1.2
(180)	172.9620056	−2.1642234	SDSS J113150.88-020951.2	q	0.9
	352.9627548	2.1647976	SDSS J233151.04+020953.2	q	1.4
(181)	221.5816508	−2.0546804	2QZ J144619.5-020317	Q	1.021
	41.5820598	2.0548802	SDSS J024619.69+020317.5	Q	1.611
(182)	42.9641686	−1.8095775	SDSS J025151.40-014834.4	Q	1.943
	222.9651434	1.8088515	SDSS J145151.63+014831.8	q	0.6
(183)	325.6085362	−1.7636978	SDSS J214226.05-014549.2	q	1.4
	145.6089432	1.7631901	SDSS J094226.14+014547.5	Q	2.335
(184)	133.334329	−1.6598129	SDSS J085320.23-013935.3	qX	1.4
	313.3345032	1.6590253	SDSS J205320.28+013932.4	q	0.1
(185)	14.2851195	−1.5772589	SDSS J005708.42-013438.1	Q	1.329
	194.2848358	1.5782201	SDSS J125708.36+013441.5	qX	0.8
(186)	316.4041208	−1.4412537	SDSS J210536.98-012628.4	q	2
	136.4042816	1.4411682	SDSS J090537.02+012628.2	q	0
(187)	36.4121461	−1.4221784	SDSS J022538.91-012519.8	Q	0.727
	216.412656	1.4224802	2QZ J142539.0+012521	Q	1.136
(188)	179.9376714	−1.3721402	2QZ J115945.0-012220	Q	1.275
	359.9384294	1.3712088	SDSS J235945.22+012216.3	Q	1.222
(189)	309.459063	−1.3256484	J203750.17-011932.3	X	
	129.4598151	1.3266144	SDSS J083750.35+011935.7	q	2.5
(190)	169.1804623	−1.2787242	SDSS J111643.31-011643.4	Q	0.878
	349.1801163	1.2778387	SDSS J231643.23+011640.2	qX	2.1
(191)	40.8886891	−1.1553956	SDSS J024333.28-010919.3	Q	2.265
	220.889267	1.1561131	SDSS J144333.42+010922.0	q	1.5
(192)	181.0820052	−1.1238078	J120419.68-010725.7	X	
	1.0822232	1.1242868	SDSS J000419.73+010727.4	Q	2.086
(193)	322.0407105	−1.1103891	2SLAQ J212809.77-010637.4	Q	2.016
	142.0406886	1.109918	SDSS J092809.76+010635.6	Q	0.691
(194)	323.8986908	−1.1047641	SDSS J213535.68-010617.1	q	0.1
	143.898949	1.1039692	SDSS J093535.74+010614.2	q	1.4

Table A12. *Cont.*

	Ra	*Dec*	*Name*	*Descrip*	*Z*
(195)	359.5996406	−1.1012612	SDSS J235823.91-010604.5	A	0.172
	179.5999641	1.1017779	SDSS J115823.98+010606.4	q	1.1
(196)	333.6993254	−1.0151735	SDSS J221447.83-010054.6	q	2.1
	153.700119	1.0157703	SDSS J101448.02+010056.7	q	0.4
(197)	191.5187354	−0.947775	2QZ J124604.4-005652	Q	1.74
	11.5188728	0.9486683	SDSS J004604.52+005655.1	Q	2.394
(198)	136.812282	−0.9465473	WISEA J090714.94-005647.5	q	0.4
	316.8128149	0.9471022	SDSS J210715.08+005649.5	q	0.6
(199)	335.2752368	−0.9282428	SDSS J222106.05-005541.6	Q	2.32
	155.27575	0.92775	2QZ J102106.1+005539	K	0.246
(200)	322.1036971	−0.8306041	SDSS J212824.88-004950.1	q	3.8
	142.1045748	0.8311082	SDSS J092825.09+004951.9	Q	0.85
(201)	318.5432739	−0.6772609	SDSS J211410.38-004038.1	q	1
	138.5425553	0.6770332	SDSS J091410.21+004037.3	q	2.2
(202)	149.5630798	−0.6754175	LAMOSTJ095815.14-004031.4	Q	0.954
	329.5624984	0.6744513	SDSS J215814.99+004028.0	q	3.6
(203)	176.6971288	−0.6466236	SDSS J114647.31-003847.8	q	1.6
	356.6970072	0.6459298	SDSS J234647.28+003845.3	q	3.2
(204)	10.1452528	−0.6391804	SDSS J004034.86-003821.0	Q	1.836
	190.1442813	0.638343	2QZ J124034.6+003816	Q	1.856
(205)	322.7183019	−0.5829681	SDSS J213052.39-003458.6	Q	2.654
	142.7177224	0.5830358	PKS 0928+008	QRX	1.769
(206)	321.3839569	−0.535798	SDSS J212532.14-003208.8	q	3.6
	141.3843083	0.5359621	2SLAQ J092532.23+003209.5	Q	1.451
(207)	359.9532206	−0.5350152	SDSS J235948.77-003206.0	Q	1.443
	179.9524587	0.5345278	2QZ J115948.5+003203	Q	2.27
(208)	328.4185019	−0.4744671	SDSS J215340.44-002828.0	q	4.7
	148.4176331	0.4748041	SDSS J095340.23+002829.2	q	2
(209)	158.5922393	−0.4348561	2SLAQ J103422.14-002605.5	Q	1.161
	338.5917053	0.434891	SDSS J223422.00+002605.6	qR	0.1
(210)	348.1098247	−0.4195352	2SLAQ J231226.35-002510.3	Q	1.105
	168.1100567	0.4190823	2QZ J111226.3+002508	Q	1.309
(211)	44.7576857	−0.2819373	SDSS J025901.84-001654.9	Q	1.406
	224.7571	0.2811774	2SLAQ J145901.70+001652.2	Q	1.58
(212)	358.9575115	−0.2437697	SDSS J235549.80-001437.5	q	1.3
	178.9582363	0.243	SDSS J115549.97+001434.7	q	1.2
(213)	148.4235067	−0.1395639	2QZ J095341.5-000822	Q	0.284
	328.4236129	0.1398213	SDSS J215341.66+000823.3	q	0.1
(214)	182.3428955	−0.097823	SDSS J120922.29-000552.1	q	0.3
	2.3425216	0.098785	SDSS J000922.19+000555.6	Q	1.99
(215)	321.2974555	−0.0852931	2SLAQ J212511.38-000507.0	Q	2.308
	141.2979338	0.08586	2SLAQ J092511.51+000509.0	Q	2.698
(216)	314.6144714	−0.0745742	SDSS J205827.47-000428.4	q	1.2
	134.6143136	0.073984	SDSS J085827.43+000426.3	q	2
(217)	309.3637298	−0.0379301	SDSS J203727.29-000216.5	q	2.1
	129.3627777	0.037032	SDSS J083727.06+000213.3	q	0.6
(218)	9.8680615	−0.0269525	2SLAQ J003928.32-000137.0	Q	2.478
	189.8671854	0.0272719	SDSS J123928.12+000138.1	q	0.6
(219)	129.7712982	−0.0251763	SDSS J083905.11-000130.6	Q	2.511
	309.7715133	0.0243675	SDSS J203905.16+000127.7	q	2.5

Table A13. Pairs of opposite quasars from the Milliquas 6.3 catalog for the lens effect. Accuracy is of 0.0005° for *ra* and *dec*. Descrip column is the classification of object, see [47]. Redshift *z* is given when available, although is not essential here.

	Ra	*Dec*	*Name*	*Descrip*	*Z*
(1)	315.7673595	−76.3736026	WISEA J210304.14-762224.9	q	1
	135.7683983	76.3734303	WISEA J090304.41+762224.0	q	2.4
(2)	80.7328764	−52.4533568	WISEA J052255.89-522712.0	q	
	260.732699	52.4532957	SDSS J172255.84+522712.0	q	2.1
(3)	70.1774106	−49.1605048	WISEA J044042.58-490937.9	q	0.9
	250.1779433	49.1604959	SDSS J164042.70+490937.7	q	3.2
(4)	312.4572617	−43.5311298	WISEA J204949.73-433151.7	q	1.7
	132.4578712	43.5314134	SDSS J084949.88+433153.1	q	2.6
(5)	58.8593889	−42.1836389	J035526.25-421101.1	X	
	238.859031	42.1833947	SDSS J155526.16+421100.1	Q	1.222
(6)	75.7744245	−40.7936211	WISEA J050305.91-404736.8	q	2.3
	255.7743683	40.7937126	SDSS J170305.84+404737.3	q	0.3
(7)	5.4863222	−36.9636832	WISEA J002156.72-365749.2	q	1.6
	185.4861944	36.9634266	SDSS J122156.67+365748.3	Q	2.097
(8)	48.2374301	−35.2506342	WISEA J031256.97-351502.2	qX	1.9
	228.2368457	35.250557	SDSS J151256.83+351502.0	q	1.3
(9)	64.4053066	−34.4443255	WISEA J041737.25-342639.2	q	2.3
	244.4049248	34.4447566	SDSS J161737.18+342641.1	q	1.9
(10)	24.818008	−32.6980218	WISEA J013916.33-324152.7	q	1.6
	204.8176575	32.6980515	SDSS J133916.23+324152.9	q	0
(11)	178.0274651	−31.4001968	WISEA J115206.58-312400.4	q	2.4
	358.026947	31.4004002	SDSS J235206.46+312401.4	q	1
(12)	341.9315476	−31.0519246	6QZ J224743.5-310306	Q	2.614
	161.9314813	31.0522394	SDSS J104743.55+310308.0	q	0
(13)	300.1895832	−30.1375161	WISEA J200045.51-300814.8	q	0.6
	120.1898279	30.1370937	SDSS J080045.55+300813.5	Q	1.343
(14)	12.3530442	−29.9213175	Q 0046-3011	Q	1.081
	192.3529914	29.9214458	SDSS J124924.71+295517.2	q	2.2
(15)	47.3495546	−25.1085428	WISEA J030923.89-250630.5	q	1
	227.3495813	25.1081434	SDSS J150923.90+250629.2	q	1.8
(16)	48.9227	−24.5943481	WISEA J031541.43-243539.7	qR	1
	228.9221526	24.5946659	SDSS J151541.31+243540.7	Q	3.21
(17)	314.8735964	−23.9469948	WISEA J205929.66-235649.1	q	0.4
	134.8731466	23.946707	SDSS J085929.56+235648.1	Q	1.085
(18)	40.1013553	−23.0486453	J024024.32-230255.1	X	
	220.1017934	23.0486683	SDSS J144024.43+230255.2	q	1.6
(19)	330.2260385	−23.0089209	WISEA J220054.23-230032.0	q	0.6
	150.2259947	23.0087942	SDSS J100054.23+230031.6	Q	3.027
(20)	15.629173	−22.6311972	WISEA J010230.99-223752.2	qR	1.9
	195.6286965	22.6311474	SDSS J130230.88+223752.2	Q	3.405
(21)	181.1233682	−21.9598988	WISEA J120429.60-215735.5	q	0.8
	1.1237153	21.9600067	WISEA J000429.68+215736.0	q	1.4
(22)	22.013869	−20.8937502	SDSS J012803.33-205337.4	q	1.6
	202.0134583	20.8942223	SDSS J132803.22+205339.2	q	0.3
(23)	191.2945552	−18.1478667	WISEA J124510.71-180851.9	q	1.5
	11.2945118	18.1480237	SDSS J004510.68+180852.8	Q	2.955
(24)	43.6995104	−17.1177057	WISEA J025447.88-170703.8	q	1.9
	223.699538	17.1176163	SDSS J145447.88+170703.4	q	1.1
(25)	38.5649712	−9.3922666	SDSS J023415.59-092332.0	Q	3.159
	218.5647491	9.3927159	SDSS J143415.53+092333.7	Q	1.796
(26)	140.4377101	−9.3709292	WISEA J092145.05-092215.4	q	0.8
	320.4374695	9.3712921	SDSS J212144.99+092216.6	q	1.2
(27)	59.3881301	−8.5115865	WISEA J035733.19-083041.3	q	0.3
	239.388068	8.511933	SDSS J155733.13+083042.9	A	0.047

Table A13. *Cont.*

	Ra	*Dec*	*Name*	*Descrip*	*Z*
(28)	338.7737732	−8.142704	SDSS J223505.70-080833.7	q	0.4
	158.773734	8.1430363	SDSS J103505.69+080834.9	q	0.9
(29)	5.8514071	−7.0936418	SDSS J002324.33-070537.1	q	0.6
	185.8513794	7.093749	SDSS J122324.33+070537.4	qX	0.6
(30)	28.0452862	−6.7327127	SDSS J015210.86-064357.7	q	0.4
	208.0451896	6.732888	SDSS J135210.84+064358.3	q	1.6
(31)	310.9553801	−6.521875	SDSS J204349.29-063118.7	q	2.2
	130.9551195	6.521617	SDSS J084349.22+063117.8	q	1.1
(32)	42.0314865	−6.0404835	SDSS J024807.55-060225.7	q	1.1
	222.031267	6.0407225	SDSS J144807.50+060226.5	Q	2.324
(33)	44.1149634	−4.8954605	SDSS J025627.59-045343.6	Q	1.645
	224.1147795	4.8951414	SDSS J145627.54+045342.5	q	0.4
(34)	356.0054037	−4.4881222	SDSS J234401.30-042917.1	q	2.1
	176.0057901	4.4880115	SDSS J114401.38+042916.8	q	2.2
(35)	28.6933545	−3.9445188	SDSS J015446.40-035640.2	Q	2.322
	208.6934509	3.9447002	SDSS J135446.42+035640.9	q	0.8
(36)	36.0865531	−3.5906219	SDSS J022420.77-033526.2	QX	0.552
	216.0868377	3.5907531	SDSS J142420.83+033526.7	q	1.8
(37)	351.8889506	−3.1861348	SDSS J232733.34-031109.9	q	2.6
	171.889383	3.186412	SDSS J112733.45+031111.0	q	
(38)	215.9122427	−3.1485981	SDSS J142338.93-030854.9	q	2
	35.911743	3.1485686	SDSS J022338.81+030854.7	Q	2.173
(39)	316.7376204	−2.8595332	WISEA J210657.03-025134.3	q	1.5
	136.7379203	2.8594311	SDSS J090657.10+025133.9	A	0.194
(40)	323.6482118	−2.7731332	SDSS J213435.57-024623.2	Q	3.228
	143.6486958	2.7735964	SDSS J093435.68+024624.9	Q	0.763
(41)	31.1501826	−2.6833719	SDSS J020436.04-024100.0	Q	2.149
	211.1496969	2.6833621	SDSS J140435.92+024100.1	q	0.4
(42)	9.1659024	−2.4347542	SDSS J003639.81-022604.9	Q	1.055
	189.165748	2.4344829	SDSS J123639.77+022604.1	q	2
(43)	181.200555	−2.225128	2QZ J120448.1-021331	Q	0.888
	1.2006668	2.2249101	SDSS J000448.16+021329.6	q	1.2
(44)	221.5816508	−2.0546804	2QZ J144619.5-020317	Q	1.021
	41.5820598	2.0548802	SDSS J024619.69+020317.5	Q	1.611
(45)	316.4041208	−1.4412537	SDSS J210536.98-012628.4	q	2
	136.4042816	1.4411682	SDSS J090537.02+012628.2	q	0
(46)	181.0820052	−1.1238078	J120419.68-010725.7	X	
	1.0822232	1.1242868	SDSS J000419.73+010727.4	Q	2.086
(47)	322.0407105	−1.1103891	2SLAQ J212809.77-010637.4	Q	2.016
	142.0406886	1.109918	SDSS J092809.76+010635.6	Q	0.691
(48)	321.3839569	−0.535798	SDSS J212532.14-003208.8	q	3.6
	141.3843083	0.5359621	2SLAQ J092532.23+003209.5	Q	1.451
(49)	348.1098247	−0.4195352	2SLAQ J231226.35-002510.3	Q	1.105
	168.1100567	0.4190823	2QZ J111226.3+002508	Q	1.309
(50)	148.4235067	−0.1395639	2QZ J095341.5-000822	Q	0.284
	328.4236129	0.1398213	SDSS J215341.66+000823.3	q	0.1

Table A14. Pairs of opposite quasars from the Milliquas 6.3 catalog for the cosmic mirror effect. Accuracy is of 0.001° for *ra* and *dec* and 0.2 for redshift *z*. Descrip column is the classification of object, see [47].

	Ra	*Dec*	*Name*	*Descrip*	*Z*
(1)	255.5777892	−77.0249529	WISEA J170218.69-770129.2	q	2.3
	75.5809969	77.0255634	WISEA J050219.24+770131.4	q	2.3
(2)	2.3493535	−75.4740875	WISEA J000923.83-752826.7	q	0.8
	182.3515932	75.4750181	WISEA J120924.56+752830.2	q	0.7
(3)	85.679027	−68.1421484	WISEA J054242.99-680831.9	q	1.4
	265.6773749	68.1413691	SDSS J174242.55+680829.1	q	1.5
(4)	350.4801742	−55.0232756	XXLS J232155.23-550123.3	QX	1.788
	170.4785659	55.0239884	SDSS J112154.85+550126.3	Q	1.73
(5)	2.4579845	−53.9814555	WISEA J000949.91-535853.2	q	0.2
	182.4575348	53.980648	SDSS J120949.80+535850.3	q	0.3
(6)	348.3491422	−53.3478756	XXLS J231323.75-532051.9	QX	0.496
	168.3507385	53.3479691	SDSS J111324.17+532052.6	q	0.3
(7)	52.3380705	−33.1624587	WISEA J032921.13-330944.7	q	1
	232.3374622	33.1619242	SDSS J152921.00+330942.9	q	0.9
(8)	35.6523275	−32.9501625	WISEA J022236.55-325700.5	q	2
	215.6517237	32.9500411	SDSS J142236.40+325700.2	q	1.8
(9)	166.796621	−17.1482174	SDSS J110711.18-170853.6	q	1.1
	346.7956543	17.1488914	SDSS J230710.95+170856.0	q	1.1
(10)	43.6272916	−16.2718962	SDSS J025430.54-161618.8	q	0.3
	223.6267804	16.2723981	SDSS J145430.42+161620.6	N	0.158
(11)	190.3695441	−13.095317	SDSS J124128.69-130543.1	q	0.6
	10.3688927	13.0956669	SDSS J004128.53+130544.4	q	0.4
(12)	39.5398838	−11.856346	WISEA J023809.57-115122.9	q	1.1
	219.5404339	11.8565365	SDSS J143809.70+115123.5	q	1.1
(13)	304.7146082	−11.8357393	SDSS J201851.51-115008.7	q	3
	124.7154201	11.8347625	SDSS J081851.70+115005.1	Q	3.092
(14)	5.8514071	−7.0936418	SDSS J002324.33-070537.1	q	0.6
	185.8513794	7.093749	SDSS J122324.33+070537.4	qX	0.6
(15)	209.4759723	−6.7408847	SDSS J135754.23-064427.1	q	1.7
	29.4751402	6.7413482	LAMOSTJ015754.04+064428.9	Q	1.565
(16)	155.888588	−5.987767	WISEA J102333.26-055915.9	q	1
	335.8882692	5.9887381	WISEA J222333.18+055919.4	q	0.8
(17)	318.9673157	−5.08287	SDSS J211552.15-050458.3	q	0.4
	138.967392	5.0823555	SDSS J091552.17+050456.4	q	0.6
(18)	356.0054037	−4.4881222	SDSS J234401.30-042917.1	q	2.1
	176.0057901	4.4880115	SDSS J114401.38+042916.8	q	2.2
(19)	215.9122427	−3.1485981	SDSS J142338.93-030854.9	q	2
	35.911743	3.1485686	SDSS J022338.81+030854.7	Q	2.173
(20)	59.7010545	−3.0252538	WISEA J035848.22-030131.3	q	0.9
	239.7015228	3.0244355	SDSS J155848.36+030127.9	q	1
(21)	179.9376714	−1.3721402	2QZ J115945.0-012220	Q	1.275
	359.9384294	1.3712088	SDSS J235945.22+012216.3	Q	1.222
(22)	136.812282	−0.9465473	WISEA J090714.94-005647.5	q	0.4
	316.8128149	0.9471022	SDSS J210715.08+005649.5	q	0.6
(23)	10.1452528	−0.6391804	SDSS J004034.86-003821.0	Q	1.836
	190.1442813	0.638343	2QZ J124034.6+003816	Q	1.856
(24)	44.7576857	−0.2819373	SDSS J025901.84-001654.9	Q	1.406
	224.7571	0.2811774	2SLAQ J145901.70+001652.2	Q	1.58
(25)	358.9575115	−0.2437697	SDSS J235549.80-001437.5	q	1.3
	178.9582363	0.243	SDSS J115549.97+001434.7	q	1.2
(26)	148.4235067	−0.1395639	2QZ J095341.5-000822	Q	0.284
	328.4236129	0.1398213	SDSS J215341.66+000823.3	q	0.1
(27)	129.7712982	−0.0251763	SDSS J083905.11-000130.6	Q	2.511
	309.7715133	0.0243675	SDSS J203905.16+000127.7	q	2.5

Table A15. Pairs of opposite quasars from the Milliquas 6.3 catalog for the cosmic mirror effect—alternative approach. Accuracy is of 0.001° for *ra* and *dec* and z/2 for redshift *z*. Descrip column is the classification of object, see [47].

	Ra	*Dec*	*Name*	*Descrip*	*Z*
(1)	255.5777892	−77.0249529	WISEA J170218.69-770129.2	q	2.3
	75.5809969	77.0255634	WISEA J050219.24+770131.4	q	2.3
(2)	315.7673595	−76.3736026	WISEA J210304.14-762224.9	q	1
	135.7683983	76.3734303	WISEA J090304.41+762224.0	q	2.4
(3)	2.3493535	−75.4740875	WISEA J000923.83-752826.7	q	0.8
	182.3515932	75.4750181	WISEA J120924.56+752830.2	q	0.7
(4)	85.679027	−68.1421484	WISEA J054242.99-680831.9	q	1.4
	265.6773749	68.1413691	SDSS J174242.55+680829.1	q	1.5
(5)	350.1300997	−64.0960807	WISEA J232031.22-640545.8	q	0.8
	170.1297219	64.0966844	SDSS J112031.12+640548.1	q	1.4
(6)	77.2847276	−61.1581631	WISEA J050908.30-610929.5	q	0.6
	257.2851687	61.1587398	SDSS J170908.44+610931.4	q	0.9
(7)	12.2865176	−55.3358661	WISEA J004908.81-552009.3	q	1.3
	192.2854767	55.3366013	SDSS J124908.51+552011.7	q	1.9
(8)	350.4801742	−55.0232756	XXLS J232155.23-550123.3	QX	1.788
	170.4785659	55.0239884	SDSS J112154.85+550126.3	Q	1.73
(9)	2.4579845	−53.9814555	WISEA J000949.91-535853.2	q	0.2
	182.4575348	53.980648	SDSS J120949.80+535850.3	q	0.3
(10)	323.9286029	−53.3487347	WISEA J213542.85-532055.4	q	0.9
	143.9271545	53.3484154	SDSS J093542.51+532054.2	q	0.5
(11)	348.3491422	−53.3478756	XXLS J231323.75-532051.9	QX	0.496
	168.3507385	53.3479691	SDSS J111324.17+532052.6	q	0.3
(12)	315.5807126	−50.5996161	WISEA J210219.36-503558.6	q	2.2
	135.5799944	50.6005463	SDSS J090219.19+503601.9	Q	2.619
(13)	27.2491308	−50.0692574	WISEA J014859.79-500409.4	q	1.8
	207.2486497	50.0702154	SDSS J134859.67+500412.8	Q	1.559
(14)	51.7544779	−45.8163472	WISEA J032701.07-454859.0	q	2.1
	231.753214	45.816666	SDSS J152700.77+454859.9	q	0.9
(15)	13.7156676	−45.5401862	WISEA J005451.73-453224.7	q	1
	193.7148005	45.5407984	SDSS J125451.55+453226.8	Q	0.599
(16)	312.4572617	−43.5311298	WISEA J204949.73-433151.7	q	1.7
	132.4578712	43.5314134	SDSS J084949.88+433153.1	q	2.6
(17)	39.8003988	−42.7828145	WISEA J023912.05-424657.5	q	1.8
	219.7994764	42.7819417	SDSS J143911.87+424655.0	Q	2.376
(18)	327.4360427	−38.6604478	WISEA J214944.65-383937.5	q	0.6
	147.4361286	38.659581	SDSS J094944.67+383934.5	Q	1.326
(19)	17.7159333	−38.4864674	WISEA J011051.83-382911.3	q	2.2
	197.7147558	38.4865089	SDSS J131051.54+382911.4	Q	0.817
(20)	35.9159531	−37.2880557	WISEA J022339.81-371716.8	q	0.7
	215.9154018	37.2873321	SDSS J142339.69+371714.3	q	1.4
(21)	5.4863222	−36.9636832	WISEA J002156.72-365749.2	q	1.6
	185.4861944	36.9634266	SDSS J122156.67+365748.3	Q	2.097
(22)	288.7726299	−36.2604918	WISEA J191505.43-361537.9	q	1
	108.771553	36.2600021	SDSS J071505.17+361536.0	q	0.4
(23)	48.2374301	−35.2506342	WISEA J031256.97-351502.2	qX	1.9
	228.2368457	35.250557	SDSS J151256.83+351502.0	q	1.3
(24)	64.4053066	−34.4443255	WISEA J041737.25-342639.2	q	2.3
	244.4049248	34.4447566	SDSS J161737.18+342641.1	q	1.9
(25)	46.6464316	−34.4391069	WISEA J030635.12-342620.5	q	1.5
	226.6455899	34.4391456	SDSS J150634.94+342620.9	Q	2.275
(26)	13.9539794	−33.5205216	Q 0053-3347	Q	2.08
	193.9543304	33.519737	SDSS J125549.03+333111.0	q	0.9
(27)	61.3792872	−33.3589696	WISEA J040531.02-332132.4	q	1.3
	241.3804819	33.3584594	SDSS J160531.31+332130.4	q	0.6

Table A15. *Cont.*

	Ra	*Dec*	*Name*	*Descrip*	*Z*
(28)	52.3380705	−33.1624587	WISEA J032921.13-330944.7	q	1
	232.3374622	33.1619242	SDSS J152921.00+330942.9	q	0.9
(29)	35.6523275	−32.9501625	WISEA J022236.55-325700.5	q	2
	215.6517237	32.9500411	SDSS J142236.40+325700.2	q	1.8
(30)	331.3013548	−31.5723459	2QZ J220512.3-313421	Q	1.934
	151.3004456	31.5727386	SDSS J100512.10+313421.8	q	0.9
(31)	178.0274651	−31.4001968	WISEA J115206.58-312400.4	q	2.4
	358.026947	31.4004002	SDSS J235206.46+312401.4	q	1
(32)	188.680682	−30.5578933	WISEA J123443.36-303328.3	q	1
	8.6803036	30.558761	SDSS J003443.27+303331.6	Q	1.254
(33)	300.1895832	−30.1375161	WISEA J200045.51-300814.8	q	0.6
	120.1898279	30.1370937	SDSS J080045.55+300813.5	Q	1.343
(34)	332.1756094	−29.9838041	2QZ J220842.1-295902	Q	1.023
	152.1766832	29.9847166	SDSS J100842.39+295905.0	Q	2.56
(35)	12.3530442	−29.9213175	Q 0046-3011	Q	1.081
	192.3529914	29.9214458	SDSS J124924.71+295517.2	q	2.2
(36)	333.8811688	−28.3336528	2QZ J221531.4-282001	Q	1.909
	153.8815524	28.3342401	SDSS J101531.57+282003.3	Q	2.395
(37)	80.438152	−28.1840351	WISEA J052145.16-281102.6	q	0.6
	260.437853	28.1849529	SDSS J172145.08+281105.8	q	1.3
(38)	189.5249477	−27.4782258	WISEA J123805.97-272841.7	q	2.3
	9.5243507	27.4772773	SDSS J003805.84+272838.2	Q	1.937
(39)	44.5344194	−26.5790235	WISEA J025808.26-263444.5	q	1.5
	224.5352818	26.5780647	SDSS J145808.46+263441.0	q	2.1
(40)	197.0438404	−25.791086	WISEA J130810.53-254728.0	q	1.1
	17.0442989	25.7919436	SDSS J010810.62+254730.9	Q	1.843
(41)	47.3495546	−25.1085428	WISEA J030923.89-250630.5	q	1
	227.3495813	25.1081434	SDSS J150923.90+250629.2	q	1.8
(42)	314.8735964	−23.9469948	WISEA J205929.66-235649.1	q	0.4
	134.8731466	23.946707	SDSS J085929.56+235648.1	Q	1.085
(43)	211.3857165	−23.9417462	WISEA J140532.57-235630.1	q	2.3
	31.3864591	23.9416464	SDSS J020532.75+235629.9	Q	2.005
(44)	9.3024771	−23.7730802	SDSS J003712.58-234622.9	q	1.7
	189.3025669	23.7724481	SDSS J123712.61+234620.8	Q	2.644
(45)	325.6254779	−23.1632401	WISEA J214230.10-230947.5	q	0.9
	145.6252854	23.1622808	SDSS J094230.07+230944.1	q	1.4
(46)	15.629173	−22.6311972	WISEA J010230.99-223752.2	qR	1.9
	195.6286965	22.6311474	SDSS J130230.88+223752.2	Q	3.405
(47)	181.1233682	−21.9598988	WISEA J120429.60-215735.5	q	0.8
	1.1237153	21.9600067	WISEA J000429.68+215736.0	q	1.4
(48)	69.293922	−21.9055291	WISEA J043710.51-215420.2	q	0.7
	249.293937	21.9045811	SDSS J163710.55+215416.4	Q	1.411
(49)	341.8649478	−20.6885193	WISEA J224727.58-204119.2	q	1.2
	161.8640315	20.6894371	SDSS J104727.36+204121.9	Q	2.262
(50)	315.432881	−19.3894197	WISEA J210143.86-192321.5	q	1.8
	135.4334805	19.3888631	SDSS J090144.03+192319.9	q	1.4
(51)	315.2686772	−19.0978465	WISEA J210104.48-190552.1	q	1.1
	135.2689056	19.0972805	SDSS J090104.53+190550.2	q	0.4
(52)	331.1935682	−18.7863235	QSM3:36	QX	0.873
	151.1930394	18.7867023	SDSS J100446.32+184712.1	q	1.5
(53)	60.4473986	−18.154863	WISEA J040147.38-180917.4	q	0.4
	240.4484093	18.1550387	WISEA J160147.61+180917.7	q	0.8
(54)	191.2945552	−18.1478667	WISEA J124510.71-180851.9	q	1.5
	11.2945118	18.1480237	SDSS J004510.68+180852.8	Q	2.955
(55)	173.7006562	−18.0690647	WISEA J113448.15-180408.7	q	2.3
	353.7006507	18.0682592	SDSS J233448.15+180405.7	Q	2.881
(56)	24.9069328	−17.90944	SDSS J013937.65-175434.1	qX	2
	204.9072341	17.910056	SDSS J133937.73+175436.2	q	1.3

Table A15. *Cont.*

	Ra	*Dec*	*Name*	*Descrip*	*Z*
(57)	352.4344723	−17.8641457	WISEA J232944.27-175150.9	q	1.3
	172.4351845	17.8639806	SDSS J112944.45+175150.4	q	3.3
(58)	29.9174996	−17.2967528	SDSS J015940.19-171747.7	q	0.9
	209.9180908	17.2973289	SDSS J135940.34+171750.3	q	1.8
(59)	166.796621	−17.1482174	SDSS J110711.18-170853.6	q	1.1
	346.7956543	17.1488914	SDSS J230710.95+170856.0	q	1.1
(60)	43.6995104	−17.1177057	WISEA J025447.88-170703.8	q	1.9
	223.699538	17.1176163	SDSS J145447.88+170703.4	q	1.1
(61)	165.3264823	−16.8833416	SDSS J110118.35-165300.0	q	2
	345.3268127	16.8840275	SDSS J230118.43+165302.4	q	0.9
(62)	43.6272916	−16.2718962	SDSS J025430.54-161618.8	q	0.3
	223.6267804	16.2723981	SDSS J145430.42+161620.6	N	0.158
(63)	149.4813563	−15.5088164	WISEA J095755.52-153031.8	q	2.2
	329.4811707	15.5078583	SDSS J215755.48+153028.2	q	0.8
(64)	321.3724784	−14.2055432	WISEA J212529.39-141219.9	q	1
	141.3732103	14.2057221	SDSS J092529.57+141220.5	A	0.473
(65)	225.2865096	−13.8267692	WISEA J150108.76-134935.8	q	1.8
	45.2857528	13.8264077	WISEA J030108.57+134935.1	q	0.7
(66)	22.4869537	−13.2917978	WISEA J012956.87-131730.2	q	1.6
	202.4875051	13.2909737	SDSS J132957.00+131727.5	Q	3.144
(67)	190.3695441	−13.095317	SDSS J124128.69-130543.1	q	0.6
	10.3688927	13.0956669	SDSS J004128.53+130544.4	q	0.4
(68)	178.5013735	−12.8384611	WISEA J115400.32-125018.4	q	0.9
	358.501349	12.8377738	SDSS J235400.32+125015.9	q	1.7
(69)	56.1097236	−12.7916261	WISEA J034426.33-124729.7	q	0.3
	236.109024	12.7923546	SDSS J154426.16+124732.4	q	0.5
(70)	39.5398838	−11.856346	WISEA J023809.57-115122.9	q	1.1
	219.5404339	11.8565365	SDSS J143809.70+115123.5	q	1.1
(71)	304.7146082	−11.8357393	SDSS J201851.51-115008.7	q	3
	124.7154201	11.8347625	SDSS J081851.70+115005.1	Q	3.092
(72)	18.0162381	−10.9062962	SDSS J011203.89-105422.6	q	1.9
	198.0161728	10.9057355	SDSS J131203.88+105420.7	q	0.8
(73)	33.4777451	−10.6369173	SDSS J021354.65-103812.8	q	1.7
	213.4776649	10.6378738	SDSS J141354.63+103816.3	q	2.1
(74)	24.1238435	−10.5259013	SDSS J013629.72-103133.2	q	2.3
	204.1232718	10.5261989	SDSS J133629.58+103134.3	QX	2.83
(75)	334.8985316	−9.69364	SDSS J221935.64-094137.1	q	2
	154.8980454	9.6929715	SDSS J101935.52+094134.7	Q	2.313
(76)	38.5649712	−9.3922666	SDSS J023415.59-092332.0	Q	3.159
	218.5647491	9.3927159	SDSS J143415.53+092333.7	Q	1.796
(77)	140.4377101	−9.3709292	WISEA J092145.05-092215.4	q	0.8
	320.4374695	9.3712921	SDSS J212144.99+092216.6	q	1.2
(78)	358.0582864	−8.2121914	SDSS J235213.99-081244.0	q	2
	178.0589787	8.211923	SDSS J115214.15+081242.8	q	1.1
(79)	338.7737732	−8.142704	SDSS J223505.70-080833.7	q	0.4
	158.773734	8.1430363	SDSS J103505.69+080834.9	q	0.9
(80)	332.3883082	−7.9754252	SDSS J220933.20-075831.4	q	2
	152.3875951	7.9759758	SDSS J100933.02+075833.4	Q	2.532
(81)	46.2892799	−7.2429566	SDSS J030509.42-071434.6	q	0.5
	226.2901611	7.2421827	SDSS J150509.63+071431.8	q	1
(82)	42.2919481	−7.135162	SDSS J024910.06-070806.6	Q	2.561
	222.2917609	7.1344065	SDSS J144910.02+070803.8	q	1.5
(83)	5.8514071	−7.0936418	SDSS J002324.33-070537.1	q	0.6
	185.8513794	7.093749	SDSS J122324.33+070537.4	qX	0.6
(84)	328.3192139	−6.7707705	SDSS J215316.61-064614.7	q	1.7
	148.3194775	6.7699293	SDSS J095316.66+064611.7	Q	1.092
(85)	209.4759723	−6.7408847	SDSS J135754.23-064427.1	q	1.7
	29.4751402	6.7413482	LAMOSTJ015754.04+064428.9	Q	1.565

Table A15. *Cont.*

	Ra	*Dec*	*Name*	*Descrip*	*Z*
(86)	310.9553801	−6.521875	SDSS J204349.29-063118.7	q	2.2
	130.9551195	6.521617	SDSS J084349.22+063117.8	q	1.1
(87)	42.0314865	−6.0404835	SDSS J024807.55-060225.7	q	1.1
	222.031267	6.0407225	SDSS J144807.50+060226.5	Q	2.324
(88)	155.888588	−5.987767	WISEA J102333.26-055915.9	q	1
	335.8882692	5.9887381	WISEA J222333.18+055919.4	q	0.8
(89)	30.4249489	−5.8591802	VIPERS 101146840	Q	2.126
	210.4239741	5.858464	SDSS J140141.75+055130.4	q	1.1
(90)	318.9673157	−5.08287	SDSS J211552.15-050458.3	q	0.4
	138.967392	5.0823555	SDSS J091552.17+050456.4	q	0.6
(91)	2.9218395	−4.9358745	SDSS J001141.24-045609.1	q	3.1
	182.9209776	4.9351431	SDSS J121141.03+045606.5	q	2
(92)	339.1091419	−4.9108333	SDSS J223626.19-045438.9	q	1.6
	159.1097246	4.9101383	Q 1033+051	Q	1.048
(93)	11.8971845	−4.6937364	SDSS J004735.33-044137.5	Q	1.931
	191.8971312	4.6943342	SDSS J124735.31+044139.5	Q	0.868
(94)	215.4113925	−4.6316734	WISEA J142138.70-043753.9	q	1.5
	35.4120872	4.6310081	SDSS J022138.89+043751.6	Q	2.018
(95)	44.1504799	−4.5690993	SDSS J025636.11-043408.8	Q	3.094
	224.1496194	4.5693052	WISEA J145635.91+043409.4	q	1.9
(96)	356.0054037	−4.4881222	SDSS J234401.30-042917.1	q	2.1
	176.0057901	4.4880115	SDSS J114401.38+042916.8	q	2.2
(97)	313.1420516	−4.4458056	WISEA J205234.08-042644.8	q	2.3
	133.1429183	4.4466583	SDSS J085234.29+042648.0	Q	2.745
(98)	28.6933545	−3.9445188	SDSS J015446.40-035640.2	Q	2.322
	208.6934509	3.9447002	SDSS J135446.42+035640.9	q	0.8
(99)	23.3642954	−3.508162	SDSS J013327.43-033029.3	Q	1.724
	203.3644091	3.5075679	SDSS J133327.45+033027.2	q	1
(100)	29.2919507	−3.3900862	SDSS J015710.06-032324.3	Q	1.504
	209.2925571	3.3891148	WISEA J135710.20+032320.9	q	0.7
(101)	215.9122427	−3.1485981	SDSS J142338.93-030854.9	q	2
	35.911743	3.1485686	SDSS J022338.81+030854.7	Q	2.173
(102)	59.7010545	−3.0252538	WISEA J035848.22-030131.3	q	0.9
	239.7015228	3.0244355	SDSS J155848.36+030127.9	q	1
(103)	357.4388055	−2.8983433	SDSS J234945.32-025354.0	Q	0.938
	177.4378903	2.899283	SDSS J114945.07+025357.3	q	1.5
(104)	11.9639927	−2.8499138	SDSS J004751.36-025059.6	Q	1.262
	191.9631892	2.849156	SDSS J124751.16+025056.9	Q	1.568
(105)	11.428722	−2.6318303	SDSS J004542.89-023754.5	q	1
	191.4280252	2.6316203	WISEA J124542.71+023753.8	qX	0.7
(106)	9.1659024	−2.4347542	SDSS J003639.81-022604.9	Q	1.055
	189.165748	2.4344829	SDSS J123639.77+022604.1	q	2
(107)	17.5345544	−2.4323457	SDSS J011008.29-022556.4	Q	1.068
	197.5339023	2.4329717	SDSS J131008.13+022558.6	q	1.6
(108)	145.7966766	−2.4094768	SDSS J094311.20-022434.1	q	0.9
	325.7966554	2.410309	SDSS J214311.19+022437.1	q	1.2
(109)	181.200555	−2.225128	2QZ J120448.1-021331	Q	0.888
	1.2006668	2.2249101	SDSS J000448.16+021329.6	q	1.2
(110)	21.4036505	−2.1947235	SDSS J012536.87-021141.0	Q	2.542
	201.4034175	2.1940664	SDSS J132536.82+021138.6	q	1.2
(111)	172.9620056	−2.1642234	SDSS J113150.88-020951.2	q	0.9
	352.9627548	2.1647976	SDSS J233151.04+020953.2	q	1.4
(112)	221.5816508	−2.0546804	2QZ J144619.5-020317	Q	1.021
	41.5820598	2.0548802	SDSS J024619.69+020317.5	Q	1.611
(113)	325.6085362	−1.7636978	SDSS J214226.05-014549.2	q	1.4
	145.6089432	1.7631901	SDSS J094226.14+014547.5	Q	2.335
(114)	14.2851195	−1.5772589	SDSS J005708.42-013438.1	Q	1.329
	194.2848358	1.5782201	SDSS J125708.36+013441.5	qX	0.8

Table A15. *Cont.*

	Ra	*Dec*	*Name*	*Descrip*	*Z*
(115)	36.4121461	−1.4221784	SDSS J022538.91-012519.8	Q	0.727
	216.412656	1.4224802	2QZ J142539.0+012521	Q	1.136
(116)	179.9376714	−1.3721402	2QZ J115945.0-012220	Q	1.275
	359.9384294	1.3712088	SDSS J235945.22+012216.3	Q	1.222
(117)	169.1804623	−1.2787242	SDSS J111643.31-011643.4	Q	0.878
	349.1801163	1.2778387	SDSS J231643.23+011640.2	qX	2.1
(118)	40.8886891	−1.1553956	SDSS J024333.28-010919.3	Q	2.265
	220.889267	1.1561131	SDSS J144333.42+010922.0	q	1.5
(119)	322.0407105	−1.1103891	2SLAQ J212809.77-010637.4	Q	2.016
	142.0406886	1.109918	SDSS J092809.76+010635.6	Q	0.691
(120)	191.5187354	−0.947775	2QZ J124604.4-005652	Q	1.74
	11.5188728	0.9486683	SDSS J004604.52+005655.1	Q	2.394
(121)	136.812282	−0.9465473	WISEA J090714.94-005647.5	q	0.4
	316.8128149	0.9471022	SDSS J210715.08+005649.5	q	0.6
(122)	318.5432739	−0.6772609	SDSS J211410.38-004038.1	q	1
	138.5425553	0.6770332	SDSS J091410.21+004037.3	q	2.2
(123)	176.6971288	−0.6466236	SDSS J114647.31-003847.8	q	1.6
	356.6970072	0.6459298	SDSS J234647.28+003845.3	q	3.2
(124)	10.1452528	−0.6391804	SDSS J004034.86-003821.0	Q	1.836
	190.1442813	0.638343	2QZ J124034.6+003816	Q	1.856
(125)	322.7183019	−0.5829681	SDSS J213052.39-003458.6	Q	2.654
	142.7177224	0.5830358	PKS 0928+008	QRX	1.769
(126)	321.3839569	−0.535798	SDSS J212532.14-003208.8	q	3.6
	141.3843083	0.5359621	2SLAQ J092532.23+003209.5	Q	1.451
(127)	359.9532206	−0.5350152	SDSS J235948.77-003206.0	Q	1.443
	179.9524587	0.5345278	2QZ J115948.5+003203	Q	2.27
(128)	328.4185019	−0.4744671	SDSS J215340.44-002828.0	q	4.7
	148.4176331	0.4748041	SDSS J095340.23+002829.2	q	2
(129)	348.1098247	−0.4195352	2SLAQ J231226.35-002510.3	Q	1.105
	168.1100567	0.4190823	2QZ J111226.3+002508	Q	1.309
(130)	44.7576857	−0.2819373	SDSS J025901.84-001654.9	Q	1.406
	224.7571	0.2811774	2SLAQ J145901.70+001652.2	Q	1.58
(131)	358.9575115	−0.2437697	SDSS J235549.80-001437.5	q	1.3
	178.9582363	0.243	SDSS J115549.97+001434.7	q	1.2
(132)	148.4235067	−0.1395639	2QZ J095341.5-000822	Q	0.284
	328.4236129	0.1398213	SDSS J215341.66+000823.3	q	0.1
(133)	321.2974555	−0.0852931	2SLAQ J212511.38-000507.0	Q	2.308
	141.2979338	0.08586	2SLAQ J092511.51+000509.0	Q	2.698
(134)	314.6144714	−0.0745742	SDSS J205827.47-000428.4	q	1.2
	134.6143136	0.073984	SDSS J085827.43+000426.3	q	2
(135)	129.7712982	−0.0251763	SDSS J083905.11-000130.6	Q	2.511
	309.7715133	0.0243675	SDSS J203905.16+000127.7	q	2.5

Table A16. Pairs of opposite quasars from the Milliquas 6.3 catalog for the cosmic mirror effect—alternative approach. Accuracy is of 0.0005° for *ra* and *dec* and *z*/2 for redshift *z*. Descrip column is the classification of object, see [47].

	Ra	*Dec*	*Name*	*Descrip*	*Z*
(1)	315.7673595	−76.3736026	WISEA J210304.14-762224.9	q	1
	135.7683983	76.3734303	WISEA J090304.41+762224.0	q	2.4
(2)	312.4572617	−43.5311298	WISEA J204949.73-433151.7	q	1.7
	132.4578712	43.5314134	SDSS J084949.88+433153.1	q	2.6
(3)	5.4863222	−36.9636832	WISEA J002156.72-365749.2	q	1.6
	185.4861944	36.9634266	SDSS J122156.67+365748.3	Q	2.097

Table A16. *Cont.*

	Ra	*Dec*	*Name*	*Descrip*	*Z*
(4)	48.2374301	−35.2506342	WISEA J031256.97-351502.2	qX	1.9
	228.2368457	35.250557	SDSS J151256.83+351502.0	q	1.3
(5)	64.4053066	−34.4443255	WISEA J041737.25-342639.2	q	2.3
	244.4049248	34.4447566	SDSS J161737.18+342641.1	q	1.9
(6)	178.0274651	−31.4001968	WISEA J115206.58-312400.4	q	2.4
	358.026947	31.4004002	SDSS J235206.46+312401.4	q	1
(7)	300.1895832	−30.1375161	WISEA J200045.51-300814.8	q	0.6
	120.1898279	30.1370937	SDSS J080045.55+300813.5	Q	1.343
(8)	12.3530442	−29.9213175	Q 0046-3011	Q	1.081
	192.3529914	29.9214458	SDSS J124924.71+295517.2	q	2.2
(9)	47.3495546	−25.1085428	WISEA J030923.89-250630.5	q	1
	227.3495813	25.1081434	SDSS J150923.90+250629.2	q	1.8
(10)	314.8735964	−23.9469948	WISEA J205929.66-235649.1	q	0.4
	134.8731466	23.946707	SDSS J085929.56+235648.1	Q	1.085
(11)	15.629173	−22.6311972	WISEA J010230.99-223752.2	qR	1.9
	195.6286965	22.6311474	SDSS J130230.88+223752.2	Q	3.405
(12)	181.1233682	−21.9598988	WISEA J120429.60-215735.5	q	0.8
	1.1237153	21.9600067	WISEA J000429.68+215736.0	q	1.4
(13)	191.2945552	−18.1478667	WISEA J124510.71-180851.9	q	1.5
	11.2945118	18.1480237	SDSS J004510.68+180852.8	Q	2.955
(14)	43.6995104	−17.1177057	WISEA J025447.88-170703.8	q	1.9
	223.699538	17.1176163	SDSS J145447.88+170703.4	q	1.1
(15)	38.5649712	−9.3922666	SDSS J023415.59-092332.0	Q	3.159
	218.5647491	9.3927159	SDSS J143415.53+092333.7	Q	1.796
(16)	140.4377101	−9.3709292	WISEA J092145.05-092215.4	q	0.8
	320.4374695	9.3712921	SDSS J212144.99+092216.6	q	1.2
(17)	338.7737732	−8.142704	SDSS J223505.70-080833.7	q	0.4
	158.773734	8.1430363	SDSS J103505.69+080834.9	q	0.9
(18)	5.8514071	−7.0936418	SDSS J002324.33-070537.1	q	0.6
	185.8513794	7.093749	SDSS J122324.33+070537.4	qX	0.6
(19)	310.9553801	−6.521875	SDSS J204349.29-063118.7	q	2.2
	130.9551195	6.521617	SDSS J084349.22+063117.8	q	1.1
(20)	42.0314865	−6.0404835	SDSS J024807.55-060225.7	q	1.1
	222.031267	6.0407225	SDSS J144807.50+060226.5	Q	2.324
(21)	356.0054037	−4.4881222	SDSS J234401.30-042917.1	q	2.1
	176.0057901	4.4880115	SDSS J114401.38+042916.8	q	2.2
(22)	28.6933545	−3.9445188	SDSS J015446.40-035640.2	Q	2.322
	208.6934509	3.9447002	SDSS J135446.42+035640.9	q	0.8
(23)	215.9122427	−3.1485981	SDSS J142338.93-030854.9	q	2
	35.911743	3.1485686	SDSS J022338.81+030854.7	Q	2.173
(24)	9.1659024	−2.4347542	SDSS J003639.81-022604.9	Q	1.055
	189.165748	2.4344829	SDSS J123639.77+022604.1	q	2
(25)	181.200555	−2.225128	2QZ J120448.1-021331	Q	0.888
	1.2006668	2.2249101	SDSS J000448.16+021329.6	q	1.2
(26)	221.5816508	−2.0546804	2QZ J144619.5-020317	Q	1.021
	41.5820598	2.0548802	SDSS J024619.69+020317.5	Q	1.611
(27)	322.0407105	−1.1103891	2SLAQ J212809.77-010637.4	Q	2.016
	142.0406886	1.109918	SDSS J092809.76+010635.6	Q	0.691
(28)	321.3839569	−0.535798	SDSS J212532.14-003208.8	q	3.6
	141.3843083	0.5359621	2SLAQ J092532.23+003209.5	Q	1.451
(29)	348.1098247	−0.4195352	2SLAQ J231226.35-002510.3	Q	1.105
	168.1100567	0.4190823	2QZ J111226.3+002508	Q	1.309
(30)	148.4235067	−0.1395639	2QZ J095341.5-000822	Q	0.284
	328.4236129	0.1398213	SDSS J215341.66+000823.3	q	0.1

Appendix E

Table A17. Pairs of opposite quasars from the KQCG catalog for the lens effect (abbr. in name: L_ = LAMOST_). Accuracy is of 0.001° for *ra* and *dec*. Redshift *z* is given when available, although is not essential here.

	Name	*Ra*	*Dec*	*Z*
(1)	J065013.57-814217.6	102.5565628	−81.7049143	
	J185012.45+814220.5	282.5519004	81.7056967	
(2)	J104815.79-775517.6	162.0658158	−77.9215763	
	J224816.91+775517.5	342.0704902	77.9215426	
(3)	J015410.35-770145.4	28.5431453	−77.0292865	
	J135410.15+770146.8	208.5423058	77.0296683	
(4)	J170218.69-770129.2	255.5779108	−77.0247821	
	J050219.24+770131.4	75.5802066	77.0253936	
(5)	LQAC_048-076_004	48.2412	−76.8556	2.251
	J151258.42+765116.6	228.2434304	76.8546334	
(6)	J031257.86-765119.5	48.2411239	−76.855429	
	J151258.42+765116.6	228.2434304	76.8546334	
(7)	J201452.82-764705.1	303.7201147	−76.7847541	
	J081453.75+764706.8	123.7239922	76.7852418	
(8)	J210304.14-762224.9	315.7672779	−76.3735957	
	J090304.41+762224.0	135.7684133	76.3733506	
(9)	J000923.83-752826.7	2.3493314	−75.4740891	
	J120924.56+752830.2	182.3523545	75.4750639	
(10)	J082102.98-732201.4	125.2624384	−73.3670587	
	J202103.69+732201.4	305.2653831	73.3670564	
(11)	J152625.82-732045.8	231.6076131	−73.346071	
	J032626.02+732043.5	51.6084447	73.3454428	
(12)	J075055.11-665252.9	117.7296651	−66.8813702	
	J195054.52+665252.8	297.7271938	66.8813334	
(13)	J003923.34-661033.4	9.8472514	−66.1759482	
	J123923.49+661035.8	189.8478948	66.176629	
(14)	J170820.10-623913.0	257.0837815	−62.6536341	
	J050820.40+623912.3	77.0850212	62.6534285	
(15)	J224505.82-621922.8	341.2742892	−62.3230084	
	104505.93+621922.8	161.2747324	62.32302149	1.342
(16)	J054056.36-604959.0	85.2348533	−60.8330709	
	J174056.57+605000.8	265.2357489	60.8335817	
(17)	J093154.04-604552.0	142.9751737	−60.7644677	
	J213154.02+604550.2	322.975094	60.7639456	
(18)	J073745.76-601648.0	114.4407021	−60.2800092	
	J193745.89+601650.5	294.441231	60.2807195	
(19)	J043547.94-593444.6	68.9497681	−59.5790668	
	J163548.00+593441.4	248.9500066	59.5781862	
(20)	J044902.05-585105.9	72.2585651	−58.8516409	
	J164902.23+585109.5	252.2593095	58.8526408	
(21)	J023030.16-584734.1	37.6256709	−58.7928136	
	143030.20+584736.9	217.6258429	58.79360186	2.603
(22)	J021037.60-574807.6	32.656701	−57.8021278	
	J141037.99+574804.5	212.6583135	57.8012742	
(23)	J234926.29-564624.9	357.3595443	−56.7735858	
	114926.22+564624.9	177.359266	56.77360707	1.459
(24)	J014942.21-561417.0	27.4258981	−56.2380595	
	134942.26+561415.1	207.4260912	56.23755146	1.513
(25)	J232326.69-560831.7	350.861225	−56.1421439	
	J112326.28+560829.4	170.8595139	56.1415184	
(26)	J033029.28-553249.4	52.6220047	−55.5470669	
	LQAC_232+055_010	232.6210224	55.5466683	1.732

Table A17. *Cont.*

	Name	*Ra*	*Dec*	*Z*
(27)	J014520.31-551733.1	26.3346552	−55.2925322	
	J134520.13+551734.6	206.3338867	55.2929689	
(28)	J035335.57-551116.1	58.398228	−55.1878328	
	155335.97+551115.7	238.3998764	55.18770389	2.801
(29)	J011541.50-550945.0	18.9229286	−55.1625237	
	131541.80+550947.9	198.924174	55.1633099	2.518
(30)	J004443.92-544532.5	11.183014	−54.7590464	
	J124443.89+544531.9	191.1828838	54.7588612	
(31)	J020849.23-534047.4	32.2051551	−53.6798564	
	140849.42+534050.9	212.2059195	53.68083276	2.594
(32)	J032510.30-532527.4	51.2929271	−53.4242888	
	LQAC_231+053_004	231.2946008	53.42329979	3.62
(33)	J013702.04-513252.3	24.2585004	−51.5478865	
	133702.07+513252.1	204.2586596	51.54780646	3.123
(34)	J005717.66-505253.0	14.3236008	−50.8814119	
	125717.65+505255.6	194.3235824	50.88212363	1.642
(35)	J210219.36-503558.6	315.580702	−50.5996365	
	090219.19+503601.9	135.579984	50.60054742	2.619
(36)	J014423.74-502934.8	26.0989274	−50.4930215	
	134424.09+502935.3	206.1004142	50.49316354	1.542
(37)	J025356.53-502734.2	43.4855594	−50.4595093	
	J145356.47+502732.3	223.4853141	50.4589903	
(38)	J045351.32-500446.4	73.4638512	−50.0795633	
	J165351.61+500448.1	253.4650669	50.0800473	
(39)	J014859.79-500409.4	27.249139	−50.0693006	
	134859.67+500412.8	207.2486344	50.07024035	1.559
(40)	J115039.86-483126.9	177.6660978	−48.5241579	
	J235039.73+483125.6	357.665564	48.5237961	
(41)	J121222.32-470945.7	183.0930407	−47.1627214	
	L_3.092+47.16228	3.0919976	47.162279	0.435
(42)	J121222.32-470945.7	183.0930407	−47.1627214	
	J001222.08+470944.3	3.0920057	47.1623169	
(43)	J234921.38-463939.4	357.3391246	−46.6609453	
	114921.37+463937.4	177.3390734	46.66041384	2.209
(44)	J000333.34-463348.8	0.8889306	−46.5635617	
	J120333.26+463349.2	180.888613	46.5636756	
(45)	J232951.30-462936.0	352.4637617	−46.4933383	
	112951.12+462934.8	172.4630068	46.49300281	1.874
(46)	J001522.25-462711.2	3.8427405	−46.4531156	
	121521.94+462708.3	183.841433	46.45232349	0.706
(47)	J235842.78-462119.9	359.6782761	−46.3555539	
	115842.73+462119.3	179.6780673	46.35538626	1.441
(48)	J102546.91-460551.1	156.4454829	−46.0975459	
	J222546.61+460552.2	336.444224	46.0978546	
(49)	J022714.20-455207.2	36.8091778	−45.8686727	
	142713.98+455209.2	216.808284	45.86923886	0.89
(50)	J005451.73-453224.7	13.7155508	−45.5401987	
	125451.55+453226.8	193.7148002	45.54079833	0.599
(51)	J002525.65-451116.2	6.3569101	−45.1878378	
	122525.90+451119.4	186.3579518	45.18873483	2.012
(52)	J003634.96-450211.3	9.1456971	−45.0364828	
	LQAC_189+045_001	189.1468986	45.03557266	0.401
(53)	J032340.76-445219.8	50.9198579	−44.8721899	
	J152340.96+445222.6	230.9206887	44.8729639	
(54)	J142118.81-444959.4	215.3284148	−44.8331713	
	J022118.56+444959.6	35.3273534	44.8332385	
(55)	J040922.63-434237.6	62.3443021	−43.7104529	
	J160922.90+434238.0	242.3454381	43.710576	

Table A17. *Cont.*

	Name	*Ra*	*Dec*	*Z*
(56)	J023912.05-424657.5	39.80023	−42.78266	
	LQAC_219+042_028	219.7994832	42.78195298	2.376
(57)	J011902.18-423527.9	19.7591123	−42.5911066	
	131901.96+423525.1	199.7581772	42.59031464	2.418
(58)	J194357.17-423230.3	295.9882428	−42.5417658	
	LQAC_115+042_034	115.9881497	42.54250971	0.785
(59)	J010933.66-415122.0	17.3902687	−41.856116	
	LQAC_197+041_004	197.3894588	41.85616598	1.128
(60)	J065832.76-413600.0	104.6365048	−41.6000057	
	J185832.85+413601.2	284.6368963	41.6003466	
(61)	J225003.90-404750.0	342.5162501	−40.7972425	
	J105003.82+404752.3	162.5159468	40.7978721	
(62)	J054106.29-393853.6	85.2762311	−39.6482362	
	J174106.48+393851.1	265.2770063	39.6475475	
(63)	J214944.65-383937.5	327.4360536	−38.6604439	
	094944.67+383934.5	147.4361304	38.6595897	1.326
(64)	J011051.83-382911.3	17.7159682	−38.4864762	
	LQAC_197+038_041	197.7147781	38.48651802	0.816
(65)	J121926.97-381141.0	184.8623806	−38.1947475	
	J001926.76+381141.9	4.8615332	38.1949744	
(66)	J140113.73-375749.9	210.3072125	−37.9638751	
	J020113.48+375746.6	30.3062011	37.9629542	
(67)	J034937.91-374902.4	57.4079661	−37.8173499	
	J154937.76+374904.2	237.407344	37.8178398	
(68)	J032742.65-372227.2	51.9277313	−37.3742363	
	LQAC_231+037_033	231.9276563	37.37406082	2.635
(69)	J002156.72-365749.2	5.4863348	−36.9636685	
	LQAC_185+036_009	185.4861573	36.96344034	2.097
(70)	J015857.83-364051.5	29.74099	−36.6809782	
	LQAC_209+036_041	209.7415028	36.68102127	1.325
(71)	J020724.39-363533.9	31.8516579	−36.5927588	
	J140724.46+363534.6	211.8519458	36.5929712	
(72)	J221949.29-361508.3	334.9553981	−36.2523091	
	101949.33+361511.6	154.9555568	36.25323484	2.072
(73)	J201205.95-353252.6	303.0248152	−35.5479606	
	J081206.08+353250.7	123.0253608	35.5474366	
(74)	J041151.56-351610.1	62.9648363	−35.2694838	
	J161151.26+351608.7	242.9636226	35.2690879	
(75)	J135450.16-351503.3	208.7090077	−35.2509374	
	J015450.31+351503.4	28.7096451	35.2509711	
(76)	J032412.53-344857.3	51.0522435	−34.8159276	
	J152412.33+344855.8	231.0513838	34.8155136	
(77)	J030635.12-342620.5	46.6463591	−34.4390464	
	LQAC_226+034_022	226.6456048	34.43915382	2.267
(78)	J022031.39-335746.0	35.1308163	−33.9627784	
	J142031.67+335745.7	215.1319667	33.9626953	
(79)	J201529.89-334536.3	303.8745553	−33.7601054	
	LQAC_123+033_045	123.8749216	33.76069163	2.263
(80)	J023025.90-331514.2	37.6079221	−33.2539609	
	J143026.02+331515.8	217.6084382	33.2543894	
(81)	J144620.40-322022.3	221.5850027	−32.3395303	
	J024620.21+322020.8	41.5842294	32.3391357	
(82)	LQAC_031-030_002	31.13416667	−30.7485	1.665
	J140432.01+304451.1	211.1334154	30.7475457	
(83)	J123443.36-303328.3	188.6806682	−30.5578886	
	003443.27+303331.6	8.680297194	30.55878763	1.254
(84)	J200045.51-300814.8	300.1896576	−30.1374469	
	LQAC_120+030_023	120.1897932	30.13710584	1.344

Table A17. *Cont.*

	Name	*Ra*	*Dec*	*Z*
(85)	LQAC_332-029_006	332.17575	−29.98391667	1.023
	100842.39+295905.0	152.176654	29.98472533	2.56
(86)	J091949.60-295507.2	139.956669	−29.9186772	
	J211949.69+295510.1	319.9570695	29.9194956	
(87)	J223635.72-294646.1	339.1488693	−29.7794728	
	LQAC_159+029_002	159.1497968	29.77935241	0.969
(88)	J031933.05-293711.2	49.8877165	−29.6197972	
	J151933.28+293714.8	229.888686	29.6207837	
(89)	J001806.16-292855.6	4.5256732	−29.4821238	
	J121806.13+292853.5	184.5255438	29.4815289	
(90)	J192614.75-292450.8	291.56146	−29.4141247	
	J072614.78+292453.4	111.5615925	29.4148538	
(91)	LQAC_333-028_039	333.8812083	−28.33372222	1.909
	101531.57+282003.3	153.8815418	28.33425215	2.395
(92)	J042201.40-275940.0	65.5058587	−27.9944693	
	LQAC_245+027_035	245.5051328	27.99378112	2.283
(93)	J105219.42-275107.3	163.0809198	−27.8520433	
	225219.63+275104.7	343.0817958	27.85131359	2.107
(94)	J123805.97-272841.7	189.524903	−27.4782619	
	003805.84+272838.2	9.524363473	27.4772968	1.937
(95)	J130810.53-254728.0	197.0439145	−25.7911368	
	010810.62+254730.9	17.04428773	25.79192277	1.843
(96)	J024444.36-252255.5	41.1848409	−25.3821032	
	J144444.41+252254.9	221.1850503	25.3819393	
(97)	J223704.99-251338.9	339.2708283	−25.2274835	
	103704.76+251336.6	159.2698378	25.22684044	0.531
(98)	J014622.54-251130.4	26.5939276	−25.1917856	
	LQAC_206+025_027	206.5933002	25.19165212	2.456
(99)	J020549.77-245224.7	31.4574	−24.87353	
	LQAC_211+024_008	211.4571845	24.87429322	0.928
(100)	J031541.43-243539.7	48.9226614	−24.5943802	
	LQAC_228+024_039	228.9221594	24.59465727	3.209
(101)	J205929.66-235649.1	314.8735964	−23.9469948	
	LQAC_134+023_015	134.873161	23.9466925	1.078
(102)	J140532.57-235630.1	211.3857207	−23.9417186	
	020532.75+235629.9	31.38646701	23.94164901	2.005
(103)	J150948.30-232343.7	227.4512769	−23.3954723	
	J030948.53+232346.1	47.4522222	23.3961525	
(104)	J220054.23-230032.0	330.2259757	−23.0089119	
	100054.23+230031.6	150.2259966	23.00878724	3.027
(105)	J010230.99-223752.2	15.6291536	−22.6311827	
	LQAC_195+022_028	195.6286998	22.63117677	3.406
(106)	J120429.60-215735.5	181.1233627	−21.9598782	
	J000429.68+215736.0	1.1236965	21.9600236	
(107)	J065001.37-212358.7	102.5057101	−21.399642	
	J185001.25+212355.6	282.5052397	21.398792	
(108)	J005650.87-212138.7	14.2119971	−21.3607693	
	LQAC_194+021_035	194.2109514	21.36031333	3.127
(109)	J013938.67-212010.0	24.9111441	−21.3361154	
	LQAC_204+021_041	204.9120593	21.33514981	2.552
(110)	J035233.36-211221.7	58.1390267	−21.2060385	
	J155233.38+211221.7	238.1391178	21.2060426	
(111)	J224727.58-204119.2	341.8649405	−20.6886935	
	LQAC_161+020_031	161.8640312	20.68943703	2.263
(112)	J031653.77-202303.1	49.2240677	−20.3842205	
	LQAC_229+020_017	229.2243051	20.38391551	2.662
(113)	J193418.18-193048.3	293.575751	−19.5134425	
	J073418.08+193051.5	113.5753484	19.5143209	

Table A17. *Cont.*

	Name	*Ra*	*Dec*	*Z*
(114)	J100124.33-192443.5	150.3514045	−19.4120913	
	220124.59+192440.4	330.3524601	19.41123813	2.248
(115)	J220218.01-182459.7	330.5750658	−18.4166105	
	LQAC_150+018_009	150.5756637	18.41574009	3.27
(116)	J025347.91-182055.5	43.4496403	−18.3487653	
	J145347.66+182057.6	223.4485908	18.3493384	
(117)	J124025.44-181851.0	190.1060315	−18.3141709	
	004025.23+181851.6	10.10516218	18.31436067	1.156
(118)	J040147.38-180917.4	60.4474285	−18.1548374	
	J160147.61+180917.7	240.448394	18.1549427	
(119)	J124510.71-180851.9	191.2946306	−18.147767	
	J004510.62+180851.9	11.294273	18.147755	
(120)	J113448.15-180408.7	173.7006493	−18.0690897	
	233448.15+180405.7	353.7006501	18.06825912	2.881
(121)	J101559.49-174442.2	153.9979125	−17.7450573	
	LQAC_333+017_020	333.9971774	17.74470031	2.384
(122)	J150108.76-134935.8	225.2865111	−13.8266261	
	J030108.57+134935.1	45.2857099	13.8264198	
(123)	J012956.87-131730.2	22.4869978	−13.2917386	
	LQAC_202+013_037	202.4875015	13.2909928	3.144
(124)	J055239.68-125839.6	88.1653641	−12.9776924	
	J175239.90+125836.8	268.1662789	12.9768908	
(125)	J143527.45-115442.8	218.8644074	−11.9119024	
	J023527.48+115445.4	38.8645354	11.9126238	
(126)	J000055.44-113218.8	0.2310389	−11.5385816	
	J120055.36+113219.3	180.2306821	11.5387135	
(127)	J123939.37-104706.9	189.9140688	−10.7852747	
	LQAC_009+010_017	9.913255077	10.78543594	2.425
(128)	J000622.70-095633.6	1.5946224	−9.9426718	
	LQAC_181+009_011	181.5946887	9.941953343	1.534
(129)	J202753.35-094134.4	306.9723332	−9.6928923	
	LQAC_126+009_048	126.9724849	9.693554141	0.83
(130)	J145149.26-093928.7	222.9552738	−9.6579802	
	J025149.19+093931.4	42.9549795	9.6587312	
(131)	LQAC_038-009_025	38.5649606	−9.392240877	3.159
	LQAC_218+009_031	218.5647428	9.392719278	1.796
(132)	J000505.01-090230.9	1.2708766	−9.041933	
	J120505.01+090230.4	181.2708763	9.0417792	
(133)	J035733.19-083041.3	59.388302	−8.5114804	
	J155733.13+083042.9	239.3880664	8.5119305	0.047
(134)	J204510.69-081616.2	311.2945797	−8.2711881	
	LQAC_131+008_030	131.2935706	8.271914842	2.247
(135)	J110555.82-080323.2	166.4826173	−8.0564548	
	J230555.63+080319.9	346.4818073	8.0555318	
(136)	J110555.82-080323.2	166.4826173	−8.0564548	
	L_346.482+8.05556	346.4818408	8.0555638	1.52
(137)	J224014.32-072909.9	340.059673	−7.4861023	
	LQAC_160+007_019	160.0601378	7.487028237	3.14
(138)	J144108.90-070313.6	220.2870849	−7.053796	
	J024108.85+070311.3	40.2869077	7.053151	
(139)	J102333.26-055915.9	155.888588	−5.987767	
	J222333.18+055919.4	335.8882806	5.988737	
(140)	LQAC_038-005_001	38.2399343	−5.232025068	3.458
	LQAC_218+005_005	218.2393199	5.231581596	0.2
(141)	J213604.22-050152.0	324.0175956	−5.0311184	
	LQAC_144+005_022	144.0166292	5.031056212	2.409
(142)	025627.59-045343.6	44.11496329	−4.895460489	1.645
	J145627.50+045340.4	224.1146139	4.8945605	

Table A17. *Cont.*

	Name	*Ra*	*Dec*	*Z*
(143)	004735.33-044137.5	11.89721807	−4.693753563	1.931
	LQAC_191+004_014	191.8971418	4.694341169	0.868
(144)	J142138.70-043753.9	215.4112822	−4.6316548	
	022138.89+043751.6	35.41205565	4.631021039	2.018
(145)	025636.11-043408.8	44.15049337	−4.569125414	3.094
	J145635.91+043409.4	224.1496303	4.5692848	
(146)	J205234.08-042644.8	313.1420064	−4.4457967	
	LQAC_133+004_022	133.1429082	4.446671684	2.745
(147)	J014824.02-033047.7	27.100084	−3.5132583	
	J134823.84+033045.8	207.0993466	3.5127227	
(148)	015710.06-032324.3	29.29195061	−3.390086166	1.504
	J135710.20+032320.9	209.2925121	3.3891406	
(149)	J210657.03-025134.3	316.7376479	−2.8595533	
	LQAC_136+002_017	136.7379	2.8592	0.194
(150)	004751.36-025059.6	11.96401317	−2.84989781	1.262
	LQAC_191+002_029	191.9631831	2.849151807	1.569
(151)	LQAC_323-002_008	323.6482112	−2.773133154	3.227
	LQAC_143+002_018	143.648699	2.773614173	0.763
(152)	LQAC_197-002_026	197.6704167	−2.227027778	1.765
	J011040.87+021336.5	17.6703106	2.2268189	
(153)	LQAC_221-002_011	221.5815417	−2.054722222	1.021
	024619.69+020317.5	41.58205972	2.054880133	1.611
(154)	022538.91-012519.8	36.41214596	−1.422178345	0.727
	LQAC_216+001_018	216.4125417	1.4225	1.136
(155)	LQAC_179-001_037	179.9377083	−1.372166667	1.275
	235945.22+012216.3	359.9384346	1.371206026	1.222
(156)	LQAC_322-001_003	322.04071	−1.110389	2.017
	LQAC_142+001_019	142.0406947	1.109906236	0.691
(157)	J134857.45-005815.3	207.2393956	−0.9709267	
	LQAC_027+000_061	27.23865057	0.970120818	2.259
(158)	LQAC_191-000_049	191.5187217	−0.947792721	1.734
	LQAC_011+000_123	11.51886623	0.948653301	2.394
(159)	004034.86-003821.0	10.14525273	−0.63918039	1.836
	LQAC_190+000_011	190.1443333	0.638194444	1.856
(160)	LQAC_322-000_101	322.7183014	−0.582968066	2.654
	LQAC_142+000_040	142.7177231	0.583039252	1.771
(161)	LQAC_158-000_052	158.592239	−0.434856	1.161
	J223422.00+002605.4	338.5917077	0.4348598	
(162)	LQAC_348-000_009	348.109802	−0.419542	1.105
	LQAC_168+000_003	168.1099167	0.419027778	1.309
(163)	025901.84-001654.9	44.75769361	−0.281929479	1.406
	LQAC_224+000_062	224.757095	0.281169	1.58
(164)	01281.493-001442.6	22.00622083	−0.245181678	1.088
	J132801.70+001440.0	202.007088	0.2444674	
(165)	J125103.72-001224.5	192.7655083	−0.2068329	
	005103.89+001227.4	12.766223	0.207611943	2.12
(166)	LQAC_352-000_049	352.8172404	−0.117229211	1.696
	LQAC_172+000_041	172.8182083	0.118	1.784
(167)	LQAC_321-000_023	321.297455	−0.085293	2.308
	LQAC_141+000_022	141.2979311	0.085854987	2.698

Table A18. Pairs of opposite quasars from the KQCG catalog for the lens effect. Accuracy is of 0.0005° for *ra* and *dec*. Redshift *z* is given when available, although is not essential here.

	Name	*Ra*	*Dec*	*Z*
(1)	J015410.35-770145.4	28.5431453	−77.0292865	
	J135410.15+770146.8	208.5423058	77.0296683	
(2)	J210304.14-762224.9	315.7672779	−76.3735957	
	J090304.41+762224.0	135.7684133	76.3733506	
(3)	J224505.82-621922.8	341.2742892	−62.3230084	
	104505.93+621922.8	161.2747324	62.32302149	1.342
(4)	J234926.29-564624.9	357.3595443	−56.7735858	
	114926.22+564624.9	177.359266	56.77360707	1.459
(5)	J014520.31-551733.1	26.3346552	−55.2925322	
	J134520.13+551734.6	206.3338867	55.2929689	
(6)	J004443.92-544532.5	11.183014	−54.7590464	
	J124443.89+544531.9	191.1828838	54.7588612	
(7)	J013702.04-513252.3	24.2585004	−51.5478865	
	133702.07+513252.1	204.2586596	51.54780646	3.123
(8)	J115039.86-483126.9	177.6660978	−48.5241579	
	J235039.73+483125.6	357.665564	48.5237961	
(9)	J000333.34-463348.8	0.8889306	−46.5635617	
	J120333.26+463349.2	180.888613	46.5636756	
(10)	J235842.78-462119.9	359.6782761	−46.3555539	
	115842.73+462119.3	179.6780673	46.35538626	1.441
(11)	J065832.76-413600.0	104.6365048	−41.6000057	
	J185832.85+413601.2	284.6368963	41.6003466	
(12)	J034937.91-374902.4	57.4079661	−37.8173499	
	J154937.76+374904.2	237.407344	37.8178398	
(13)	J032742.65-372227.2	51.9277313	−37.3742363	
	LQAC_231+037_033	231.9276563	37.37406082	2.635
(14)	J002156.72-365749.2	5.4863348	−36.9636685	
	LQAC_185+036_009	185.4861573	36.96344034	2.097
(15)	J015857.83-364051.5	29.74099	−36.6809782	
	LQAC_209+036_041	209.7415028	36.68102127	1.325
(16)	J020724.39-363533.9	31.8516579	−36.5927588	
	J140724.46+363534.6	211.8519458	36.5929712	
(17)	J023025.90-331514.2	37.6079221	−33.2539609	
	J143026.02+331515.8	217.6084382	33.2543894	
(18)	J200045.51-300814.8	300.1896576	−30.1374469	
	LQAC_120+030_023	120.1897932	30.13710584	1.344
(19)	J024444.36-252255.5	41.1848409	−25.3821032	
	J144444.41+252254.9	221.1850503	25.3819393	
(20)	J031541.43-243539.7	48.9226614	−24.5943802	
	LQAC_228+024_039	228.9221594	24.59465727	3.209
(21)	J205929.66-235649.1	314.8735964	−23.9469948	
	LQAC_134+023_015	134.873161	23.9466925	1.078
(22)	J220054.23-230032.0	330.2259757	−23.0089119	
	100054.23+230031.6	150.2259966	23.00878724	3.027
(23)	J010230.99-223752.2	15.6291536	−22.6311827	
	LQAC_195+022_028	195.6286998	22.63117677	3.406
(24)	J120429.60-215735.5	181.1233627	−21.9598782	
	J000429.68+215736.0	1.1236965	21.9600236	
(25)	J035233.36-211221.7	58.1390267	−21.2060385	
	J155233.38+211221.7	238.1391178	21.2060426	
(26)	J031653.77-202303.1	49.2240677	−20.3842205	
	LQAC_229+020_017	229.2243051	20.38391551	2.662
(27)	J124510.71-180851.9	191.2946306	−18.147767	
	J004510.62+180851.9	11.294273	18.147755	
(28)	J000055.44-113218.8	0.2310389	−11.5385816	
	J120055.36+113219.3	180.2306821	11.5387135	
(29)	LQAC_038-009_025	38.5649606	−9.392240877	3.159
	LQAC_218+009_031	218.5647428	9.392719278	1.796

Table A18. *Cont.*

	Name	*Ra*	*Dec*	*Z*
(30)	J000505.01-090230.9	1.2708766	−9.041933	
	J120505.01+090230.4	181.2708763	9.0417792	
(31)	J035733.19-083041.3	59.388302	−8.5114804	
	J155733.13+083042.9	239.3880664	8.5119305	0.047
(32)	J210657.03-025134.3	316.7376479	−2.8595533	
	LQAC_136+002_017	136.7379	2.8592	0.194
(33)	LQAC_323-002_008	323.6482112	−2.773133154	3.227
	LQAC_143+002_018	143.648699	2.773614173	0.763
(34)	LQAC_197-002_026	197.6704167	−2.227027778	1.765
	J011040.87+021336.5	17.6703106	2.2268189	
(35)	022538.91-012519.8	36.41214596	−1.422178345	0.727
	LQAC_216+001_018	216.4125417	1.4225	1.136
(36)	LQAC_322-001_003	322.04071	−1.110389	2.017
	LQAC_142+001_019	142.0406947	1.109906236	0.691

Table A19. Pairs of opposite quasars from the KQCG catalog for the cosmic mirror effect (abbr. in name: L_ = LAMOST_). Accuracy is of 0.01° for *ra* and *dec* and 0.1 for redshift *z*.

	Name	*Ra*	*Dec*	*Z*
(1)	LQAC_323-045_002	323.0704	−45.8867	1.025
	093214.29+455249.2	143.059556	45.8803591	1.094
(2)	LQAC_001-041_001	1.0375	−41.9756	1.72
	120411.17+415814.6	181.0465681	41.97072878	1.691
(3)	LQAC_024-041_004	24.1579	−41.7931	2.2
	133639.64+414711.0	204.1651671	41.78641438	2.166
(4)	LQAC_352-041_001	352.816472	−41.149396	0.252
	113113.06+410907.9	172.8044242	41.15221529	0.27
(5)	LQAC_341-038_001	341.686232	−38.454078	2.16
	LQAC_161+038_026	161.6971609	38.45968469	2.224
(6)	LQAC_338-037_002	338.196898	−37.619514	2.33
	LQAC_158+037_019	158.2064503	37.61361655	2.353
(7)	LQAC_329-036_002	329.2175	−36.8133	1.94
	095651.30+364813.9	149.2137769	36.80387676	1.898
(8)	LQAC_338-036_001	338.1892	−36.5347	2.262
	103246.43+363154.9	158.1934861	36.5319377	2.199
(9)	LQAC_017-032_009	17.217685	−32.875892	2.23
	J130849.50+325201.7	197.2062585	32.8671451	2.239
(10)	LQAC_012-031_011	12.378625	−31.54333333	1.577
	LQAC_192+031_011	192.3716769	31.5394031	1.582
(11)	LQAC_343-031_010	343.14375	−31.32902778	0.805
	105237.20+311957.6	163.1550379	31.33268011	0.801
(12)	LQAC_339-030_005	339.202	−30.62991667	0.856
	J103648.90+303806.7	159.2037895	30.6352135	0.926
(13)	LQAC_326-030_015	326.3645	−30.50294444	1.142
	LQAC_146+030_004	146.3607191	30.49396248	1.165
(14)	LQAC_042-030_018	42.34833333	−30.40694444	2.033
	LQAC_222+030_024	222.3522302	30.4163666	2.029
(15)	LQAC_035-030_020	35.70970833	−30.39716667	1.654
	L_215.718+30.39543	215.7180284	30.3954277	1.657
(16)	LQAC_337-030_014	337.3667083	−30.11483333	0.555
	LQAC_157+030_003	157.3651363	30.11835308	0.561
(17)	LQAC_015-029_022	15.41258333	−29.54566667	1.418
	L_195.403+29.55539	195.403134	29.5553877	1.445
(18)	LQAC_037-029_003	37.03429167	−29.39491667	1.939
	L_217.024+29.40348	217.0237318	29.4034762	1.916

Table A19. *Cont.*

	Name	*Ra*	*Dec*	*Z*
(19)	LQAC_337-029_001	337.0180833	−29.26602778	1.5
	102804.15+291620.6	157.0173061	29.27240187	1.53
(20)	LQAC_341-028_031	341.8202917	−28.21711111	2.062
	104714.52+281330.9	161.8105168	28.2252619	2.019
(21)	LQAC_005-028_016	5.404041667	−28.20741667	1.208
	J122139.32+281151.6	185.4138653	28.1976789	1.128
(22)	LQAC_345-027_028	345.88075	−27.661	1.35
	J110329.85+273905.9	165.8743991	27.6516402	1.428
(23)	LQAC_043-027_005	43.17745833	−27.55630556	1.661
	L_223.187+27.55884	223.1867024	27.5588391	1.666
(24)	LQAC_332-027_003	332.1489167	−27.53458333	0.792
	LQAC_152+027_003	152.1399094	27.54382611	0.886
(25)	LQAC_022-009_008	22.30469877	−9.012753558	1.949
	LQAC_202+009_021	202.312047	9.022032441	2.03
(26)	024703.63-083644.3	41.76514018	−8.612317408	3.168
	LQAC_221+008_036	221.7690357	8.602943548	3.172
(27)	LQAC_046-008_008	46.38831776	−8.530334761	2.258
	LQAC_226+008_021	226.3879189	8.53907539	2.34
(28)	021642.26-051801.7	34.17612153	−5.300498064	1.043
	LQAC_214+005_001	214.1790392	5.303307824	1.09
(29)	024509.67-045526.6	41.29030614	−4.924073165	1.814
	LQAC_221+004_007	221.2829568	4.920292343	1.854
(30)	J021504.48-044619.0	33.7686732	−4.7719598	0.3
	LQAC_213+004_010	213.7746265	4.762817113	0.241
(31)	020427.68-043739.2	31.11533444	−4.62757387	0.212
	LQAC_211+004_004	211.1183809	4.635500685	0.258
(32)	LQAC_031-004_020	31.63195811	−4.613700851	2.301
	LQAC_211+004_022	211.6411524	4.606115539	2.261
(33)	022142.03-042712.6	35.4251408	−4.453523132	2.841
	LQAC_215+004_028	215.4293621	4.460833849	2.832
(34)	005202.36-041315.2	13.00984088	−4.220910489	2.127
	LQAC_193+004_006	193.0041244	4.226636732	2.173
(35)	002316.99-035309.0	5.82080727	−3.885844542	2.179
	LQAC_185+003_036	185.8174826	3.894175851	2.221
(36)	001214.99-034351.5	3.062461902	−3.730985145	1.602
	LQAC_183+003_004	183.0584417	3.738243028	1.505
(37)	023848.33-032632.8	39.7013883	−3.44244926	1.356
	LQAC_219+003_009	219.7041461	3.44386827	1.443
(38)	LQAC_195-003_002	195.2479809	−3.42588229	1.708
	010057.65+032504.1	15.24021079	3.417809261	1.778
(39)	010115.16-031401.5	15.31318916	−3.233765642	2.088
	LQAC_195+003_006	195.3180605	3.240485078	2.102
(40)	020823.25-025701.2	32.09690554	−2.950335837	1.44
	LQAC_212+002_003	212.0902993	2.959248154	1.344
(41)	LQAC_163-002_014	163.3850417	−2.929666667	2.059
	L_343.376+2.93350	343.376148	2.9334976	2.1
(42)	023823.01-025529.0	39.59588451	−2.924741709	2.149
	LQAC_219+002_035	219.5861076	2.924167023	2.171
(43)	LQAC_222-002_009	222.2378325	−2.873268642	1.104
	024854.69+025153.4	42.22789614	2.864856903	1.154
(44)	LQAC_195-002_015	195.4199167	−2.823055556	1.645
	010142.45+024933.5	15.42690572	2.825980823	1.721
(45)	LQAC_179-002_034	179.1020791	−2.777284206	1.896
	235622.51+024641.2	359.0937999	2.778136548	1.841
(46)	LQAC_213-002_014	213.5926667	−2.653888889	1.583
	021424.01+023911.0	33.60007716	2.653061423	1.587
(47)	LQAC_176-002_051	176.783068	−2.542637898	2.769
	LQAC_356+002_027	356.7779822	2.549142614	2.749

Table A19. *Cont.*

	Name	*Ra*	*Dec*	*Z*
(48)	LQAC_206-002_018	206.5271667	−2.509166667	1.916
	014608.18+023051.8	26.53412076	2.514405525	2.008
(49)	LQAC_208-002_045	208.7652311	−2.485529271	2.354
	LQAC_028+002_027	28.77499853	2.480155238	2.358
(50)	LQAC_215-002_027	215.8487083	−2.356361111	0.757
	LQAC_035+002_026	35.84129832	2.362110145	0.84
(51)	LQAC_148-002_037	148.4734564	−2.321739174	2.224
	LQAC_328+002_011	328.4781814	2.316791172	2.299
(52)	LQAC_179-002_002	179.020875	−2.246777778	1.14
	235603.14+021446.8	359.0130905	2.246339818	1.206
(53)	LQAC_174-002_024	174.7015417	−2.005444444	0.992
	L_354.707+1.99734	354.7073047	1.9973398	1.059
(54)	004013.64-013749.5	10.05686326	−1.630422554	1.25
	LQAC_190+001_003	190.0556247	1.635763502	1.341
(55)	LQAC_179-001_037	179.9377083	−1.372166667	1.275
	235945.22+012216.3	359.9384346	1.371206026	1.222
(56)	024059.55-011946.1	40.24816336	−1.329490927	0.829
	LQAC_220+001_009	220.2400454	1.337454418	0.732
(57)	LQAC_207-001_015	207.3852083	−1.317583333	2.123
	014932.65+011923.8	27.38605106	1.323303146	2.114
(58)	LQAC_189-001_016	189.5481398	−1.272113467	1.192
	003811.30+011630.5	9.547112026	1.275139173	1.29
(59)	LQAC_052-001_011	52.90720523	−1.205552203	2.205
	LQAC_232+001_028	232.9102632	1.200941917	2.261
(60)	LQAC_196-001_048	196.9642917	−1.092222222	1.296
	010749.71+010541.9	16.95715341	1.094976798	1.199
(61)	002538.20-010416.9	6.409207232	−1.071365841	1.179
	LQAC_186+001_018	186.4122083	1.067027778	1.199
(62)	LQAC_187-001_015	187.3914685	−1.03950696	2.33
	LQAC_007+001_037	7.389802282	1.037764215	2.276
(63)	LQAC_206-001_014	206.325195	−1.032847	1.891
	014517.74+010212.0	26.32392414	1.036693288	1.88
(64)	023532.16-010157.7	38.88400215	−1.032720469	2.084
	LQAC_218+001_024	218.8835417	1.038777778	2.012
(65)	LQAC_176-001_017	176.4090716	−1.002939638	0.88
	LQAC_356+001_034	356.4154007	1.009270159	0.783
(66)	LQAC_012-001_011	12.6204	−1.0025	0.103
	LQAC_192+001_025	192.6208	1.0053	0.147
(67)	LQAC_034-000_125	34.16339129	−0.98950573	2.214
	LQAC_214+000_030	214.1595018	0.998719425	2.154
(68)	LQAC_034-000_107	34.94479384	−0.97750017	1.155
	LQAC_214+000_027	214.946027	0.984763668	1.125
(69)	LQAC_033-000_121	33.45681868	−0.972846554	2.862
	LQAC_213+000_041	213.4528988	0.967259011	2.842
(70)	L_332.899-0.95608	332.89911	−0.95608	1.064
	LQAC_152+000_068	152.8977796	0.961987871	1.072
(71)	025749.51-005615.4	44.45630123	−0.937630641	1.448
	L_224.466+0.92774	224.4661485	0.9277391	1.465
(72)	LQAC_234-000_006	234.3883287	−0.92714033	0.542
	LQAC_054+000_035	54.38578906	0.92988287	0.625
(73)	LQAC_217-000_018	217.538268	−0.888678729	0.809
	023008.27+005323.1	37.53447644	0.889773333	0.748
(74)	LQAC_220-000_041	220.4374167	−0.874083333	1.474
	024147.26+005202.0	40.44692945	0.867240769	1.491
(75)	LQAC_213-000_072	213.805206	−0.839989	1.013
	021511.24+005017.3	33.79686409	0.838139499	1.091

Table A19. *Cont.*

	Name	*Ra*	*Dec*	*Z*
(76)	LQAC_206-000_070	206.7435	−0.8315	1.758
	014659.79+004932.6	26.74914722	0.825734516	1.706
(77)	LQAC_000-000_043	0.669873496	−0.801015302	1.735
	L_180.661+0.79757	180.6608942	0.7975713	1.786
(78)	J032945.45-004637.9	52.4393772	−0.7772181	0.572
	LQAC_232+000_027	232.4304194	0.77602973	0.647
(79)	LQAC_141-000_050	141.571304	−0.697299	1.358
	LQAC_321+000_037	321.5625466	0.692807157	1.316
(80)	LQAC_165-000_005	165.096619	−0.674177	1.016
	LQAC_345+000_062	345.0945234	0.680428018	1.007
(81)	LQAC_184-000_054	184.0036197	−0.66664066	1.843
	LQAC_004+000_050	4.010976393	0.675646913	1.796
(82)	001902.13-003854.1	4.758914043	−0.648366254	1.149
	LQAC_184+000_035	184.761625	0.651361111	1.206
(83)	004034.86-003821.0	10.14525273	−0.63918039	1.836
	LQAC_190+000_011	190.1443333	0.638194444	1.856
(84)	LQAC_191-000_046	191.4796594	−0.626509606	1.041
	004557.02+003756.0	11.48759265	0.632247161	1.021
(85)	013943.85-003612.0	24.93271241	−0.603355207	1.599
	LQAC_204+000_072	204.927017	0.600137	1.513
(86)	LQAC_200-000_080	200.864944	−0.591986	1.278
	012326.07+003526.9	20.85864192	0.590813358	1.237
(87)	LQAC_190-000_051	190.427048	−0.591902	1.12
	LQAC_010+000_031	10.42275671	0.595793629	1.163
(88)	LQAC_011-000_090	11.99853783	−0.573200853	1.029
	LQAC_192+000_001	192.0050833	0.571	0.947
(89)	LQAC_153-000_082	153.0728207	−0.52940076	2.449
	LQAC_333+000_064	333.0824573	0.526179819	2.382
(90)	025457.39-003121.2	43.73915361	−0.52258078	1.637
	LQAC_223+000_056	223.736237	0.51361	1.724
(91)	014437.46-003109.0	26.15609597	−0.519180884	1.484
	LQAC_206+000_013	206.1542083	0.515277778	1.519
(92)	LQAC_193-000_021	193.4251667	−0.501277778	1.732
	005341.92+002946.8	13.42470551	0.496353312	1.641
(93)	LQAC_329-000_018	329.3428611	−0.492357153	1.92
	LQAC_149+000_015	149.3335	0.4955	1.975
(94)	LQAC_177-000_044	177.2740753	−0.490986415	2.361
	LQAC_357+000_032	357.2708931	0.481955999	2.369
(95)	LQAC_209-000_091	209.930389	−0.487416	2.146
	015941.34+002901.8	29.92227712	0.48385759	2.079
(96)	LQAC_358-000_006	358.0841585	−0.46555538	0.879
	LQAC_178+000_006	178.0850417	0.459777778	0.796
97)	LQAC_137-000_008	137.1205388	−0.411421257	2.629
	LQAC_317+000_030	317.1176049	0.409202564	2.641
(98)	LQAC_207-000_063	207.787033	−0.390158	1.378
	015110.52+002310.9	27.79384904	0.386374118	1.438
(99)	LQAC_200-000_054	200.618759	−0.322608	1.633
	012229.74+001916.2	20.62394575	0.321178062	1.594
(100)	LQAC_039-000_023	39.52240355	−0.281156871	1.237
	LQAC_219+000_042	219.530411	0.271528	1.213
(101)	011435.92-000715.2	18.64967272	−0.120890254	1.643
	LQAC_198+000_052	198.652847	0.122162	1.661
(102)	LQAC_352-000_049	352.8172404	−0.117229211	1.696
	LQAC_172+000_041	172.8182083	0.118	1.784
(103)	025702.92-000634.0	44.26220206	−0.109449378	2.155
	LQAC_224+000_019	224.2601385	0.108301193	2.167

Table A19. *Cont.*

	Name	*Ra*	*Dec*	*Z*
(104)	LQAC_011-000_070	11.75031949	−0.049399404	1.685
	LQAC_191+000_059	191.752487	0.054056	1.622
(105)	012505.61-000246.1	21.27338412	−0.046155587	1.98
	LQAC_201+000_012	201.278641	0.042633	2.075
(106)	LQAC_346-000_064	346.859192	−0.037073	0.704
	LQAC_166+000_061	166.862991	0.0435	0.664
(107)	LQAC_039-000_036	39.74662363	−0.032826977	0.813
	LQAC_219+000_061	219.744125	0.025444444	0.829
(108)	000448.01-000108.7	1.2000593	−0.019109312	2.259
	LQAC_181+000_059	181.2008147	0.026026332	2.257
(109)	LQAC_345-000_001	345.012421	−0.00797	1.703
	LQAC_165+000_003	165.0160833	0.006333333	1.787

Table A20. Pairs of opposite quasars from the KQCG catalog [48] as candidates for the cosmic mirror effect—alternative approach. Accuracy is of 0.001° for *ra* and *dec* and *z*/2 for *z*.

	Name	*Ra*	*Dec*	*Z*
(1)	LQAC_332-029_006	332.17575	−29.98391667	1.0232
	100842.39+295905.0	152.176654	29.98472533	2.56
(2)	LQAC_333-028_039	333.8812083	−28.33372222	1.9087
	101531.57+282003.3	153.8815418	28.33425215	2.395
(3)	LQAC_038-009_025	38.5649606	−9.392240877	3.15853
	LQAC_218+009_031	218.5647428	9.392719278	1.79609
(4)	004735.33-044137.5	11.89721807	−4.693753563	1.93149
	LQAC_191+004_014	191.8971418	4.694341169	0.86833
(5)	004751.36-025059.6	11.96401317	−2.84989781	1.262066
	LQAC_191+002_029	191.9631831	2.849151807	1.56871
(6)	LQAC_221-002_011	221.5815417	−2.054722222	1.0214
	024619.69+020317.5	41.58205972	2.054880133	1.610928
(7)	022538.91-012519.8	36.41214596	−1.422178345	0.72737
	LQAC_216+001_018	216.4125417	1.4225	1.1363
(8)	LQAC_179-001_037	179.9377083	−1.372166667	1.2752
	235945.22+012216.3	359.9384346	1.371206026	1.222477
(9)	LQAC_322-001_003	322.04071	−1.110389	2.0165
	LQAC_142+001_019	142.0406947	1.109906236	0.69137
(10)	LQAC_191-000_049	191.5187217	−0.947792721	1.73388
	LQAC_011+000_123	11.51886623	0.948653301	2.3943
(11)	004034.86-003821.0	10.14525273	−0.63918039	1.835918
	LQAC_190+000_011	190.1443333	0.638194444	1.8557
(12)	LQAC_322-000_101	322.7183014	−0.582968066	2.65398
	LQAC_142+000_040	142.7177231	0.583039252	1.7708
(13)	LQAC_348-000_009	348.109802	−0.419542	1.1047
	LQAC_168+000_003	168.1099167	0.419027778	1.3086
(14)	025901.84-001654.9	44.75769361	−0.281929479	1.405797
	LQAC_224+000_062	224.757095	0.281169	1.5796
(15)	LQAC_352-000_049	352.8172404	−0.117229211	1.69638
	LQAC_172+000_041	172.8182083	0.118	1.7844
(16)	LQAC_321-000_023	321.297455	−0.085293	2.3081
	LQAC_141+000_022	141.2979311	0.085854987	2.69755

References

1. Whittaker, E. Spin in the Universe. In *Yearbook of Roy.Soc.Edinburgh*; The University of Edinburgh: Edinburgh, UK, 1945; pp. 5–13.
2. Lema?tre, G. *L'Hypothèse de L'atome Primitif: Essai de Cosmogonie*; Griffon: Neuchâtel, Switzerland, 1946; p. 201.
3. Weyssenhoff, J.; Raabe, A. Relativistic dynamics of spin fluids and spin particles. *Acta Phys. Polon.* **1947**, *9*, 7–18.
4. Korotkii, V.A.; Obukhov, Y.N. Generalized model of fluid with spin. *Sov. Phys. J.* **1991**, *34*, 165–168. [CrossRef]
5. Balachandran, A.; Маппо, G.; Skagerstram, B.; Stern, A. Gauge fields, extended objects and states of matter. *J. Phys. G* **1981**, *7*, 1001–1017. [CrossRef]
6. Petrova, N.; Sandina, I. On the method of obtaining equations of motion in general relativity theory. In *Fizika*; Kazahskii Gosudarstvennii universitet: Almaty, Kazakhstan, 1970; pp. 220–221. (In Russian)
7. Sandina, I. Motion of extended bodies in general relativity and gravitational radiation. *Sov. Phys. J.* **1985**, *28*, 9–12. [CrossRef]
8. Korotky, V.A.; Obukhov, Y.N. *Microwave Background Radiation in Rotating Cosmology*; Warsaw University: Warsaw, Poland, 1987.
9. Hawking, S. On the rotation of the Universe. *Mon. Not. R. Astron. Soc.* **1969**, *142*, 129–141. [CrossRef]
10. Obukhov, Y.N. Observations in Rotating Cosmologies. In *Gauge Theories of Fundamental Interactions*; Raczka, R., Pawlowski, M., Eds.; World Scientific: Singapore, 1990; pp. 341–366.
11. Hasse, W.; Perlick, V. Geometrical and kinematical characterization of parallax-free world models. *J. Math. Phys.* **1988**, *29*, 2064–2068. [CrossRef]
12. Treder, H.-J. Abberrations-Konstante und Rotation des Kosmos. *Ann. Phys.* **1985**, *42*, 71–72. [CrossRef]
13. Ruben, G. Die Rotation des Kosmos aus der Aberration von Quasaren. *Ann. Phys.* **1987**, *44*, 150–152. [CrossRef]
14. G?del, K. An Example of a New Type of Cosmological Solutions of Einstein's Field Equations of Gravitation. *Rev. Mod. Phys.* **1949**, *21*, 447–450. [CrossRef]
15. Maitra, S. Stationary Dust-Filled Cosmological Solution with $\Lambda = 0$ and without Closed Timelike Lines. *J. Math. Phys.* **1966**, *7*, 1025–1030. [CrossRef]
16. Lee, J.H.; Pak, M.; Lee, H.-R.; Song, H. Galaxy Rotation Coherent with the Motions of Neighbors: Discovery of Observational Evidence. *Astrophys. J.* **2019**, *872*, 78. [CrossRef]
17. Lee, J.H.; Pak, M.; Song, H.; Lee, H.-R.; Kim, S.; Jeong, H. Mysterious coherence in several-megaparsec scales between galaxy rotation and neighbor motion. *Astrophys. J.* **2019**, *884*, 104. [CrossRef]
18. Ray, J.; Smalley, L. Improved perfect fluid energy-momentum tensor with spin in Einstein-Cartan space-time. *Phys. Rev. Lett.* **1982**, *49*, 1059–1061. [CrossRef]
19. Korotkii, V.A.; Obukhov, Y.N. Bianchi-II cosmological models with rotation in general relativity theory. *Russ. Phys. J.* **1994**, *37*, 961–970. [CrossRef]
20. Korotkii, V.A.; Obukhov, Y.N. General-relativistic cosmology with expansion and rotation. *Russ. Phys. J.* **1993**, *36*, 568–573. [CrossRef]
21. Korotkii, V.A.; Obukhov, Y.N. Bianchi-IX cosmological models with rotation in general relativity. *Russ. Phys. J.* **1994**, *37*, 909–914. [CrossRef]
22. Korotky, V.A.; Obukhov, Y.N. Rotating cosmologies in Poincare gauge gravity. In *The Universe Rotation: Pro and Contra*; Myrzakulov, R., Ed.; Nova Science Publishers: Hauppauge, NY, USA, 2017; pp. 157–205.
23. Korotkii, V.A.; Obukhov, Y.N. Rotating and expanding cosmology in ECSK-theory. *Astrophys. Space Sci.* **1992**, *198*, 1–12. [CrossRef]
24. Riess, A.; Filippenko, A.; Challis, P.; Clocchiattia, A.; Diercks, A.; Garnavich, P.M.; Gilliand, R.L.; Hogan, C.J.; Jha, S.; Kirshner, R.P.; et al. Observational Evidence from Supernovae for an Accelerating Universe and a Cosmological Constant. *Astron. J.* **1998**, *116*, 1009–1072. [CrossRef]
25. Perlmutter, S.; Aldering, G.; Goldhaber, G.; Knop, R.; Nugent, P.; Castro, P.G.; Deustua, S.; Fabbro, S.; Goobar, A.; Groom, D.E.; et al. Measurements of Omega and Lambda from 42 High-Redshift Supernovae. *Astrophys. J.* **1999**, *517*, 565–598. [CrossRef]
26. Broadhurst, T.; Ellis, R.; Koo, D.; Szalay, A.S. Large-scale distribution of galaxies at the Galactic poles. *Nature* **1990**, *343*, 726–728. [CrossRef]

27. Hill, C.; Steinhardt, P.; Turner, M. Can oscillating physics explain an apparently periodic universe? *Phys. Lett. B* **1990**, *252*, 343–348. [CrossRef]
28. Korotky, V.A.; Obukhov, Y.N. Can Cosmic Rotation Explain an Apparently Periodic Universe? *Gen. Relativ. Gravit.* **1994**, *26*, 429–435. [CrossRef]
29. Birch, P. Is the Universe rotating? *Nature* **1982**, *298*, 451–454. [CrossRef]
30. Korotkii, V.A.; Obukhov, Y.N. Kinematic analysis of cosmological models with rotation. *Sov. J. Exp. Theor. Phys.* **1991**, *72*, 11–15.
31. Korotkii, V.A.; Obukhov, Y.N. Polarization of radiation in a rotating universe. *Sov. J. Exp. Theor. Phys.* **1995**, *81*, 1031–1035.
32. Panov, V.; Sbytov, Y. Accounting for Birch's observed anisotropy of the universe: Cosmological rotation? *Sov. J. Exp. Theor. Phys.* **1992**, *74*, 411–415.
33. Korotky, V.A.; Obukhov, Y.N. On cosmic rotation. In *Particles and Space-Time*; Pronin, P., Sardanashvily, G., Eds.; World Scientific: Singapore, 1996; pp. 421–439.
34. Korotky, V.A.; Obukhov, Y.N. Bianchi-II rotating world. *Astrophys. Space Sci.* **1999**, *260*, 425–439. [CrossRef]
35. Obukhov, Y.N.; Korotky, V.A. The Weyssenhoff fluid in Einstein-Cartan Theory. *Class. Quantum Gravity* **1987**, *4*, 1633–1657. [CrossRef]
36. Chilingarian, I.V.; Zolotukhin, I.Y.; Katkov, I.Y.; Melchior, A.-L.; Rubtsov, E.V.; Grishin, K.A. RCSED—A value-added reference catalog of spectral energy distributions of 800,299 galaxies in 11 ultraviolet, optical, and near-infrared bands: Morphologies, colors, ionized gas, and stellar population properties. *Astrophys. J. Suppl.* **2017**, *228*, 14. [CrossRef]
37. Kuminski, E.; Shamir, L. Computer-generated visual morphology catalog of ~3,000,000 SDSS galaxies. *Astrophys. J. Suppl.* **2016**, *223*, 20. [CrossRef]
38. Catalog of Broad Morphology of SDSS Galaxies. Available online: http://vfacstaff.ltu.edu/lshamir/data/morph_catalog/wndchrm_w_catalog.csv.gz (accessed on 10 January 2020).
39. Catalog of Broad Morphology of SDSS Galaxies. Available online: http://vfacstaff.ltu.edu/lshamir/data/morph_catalog/wndchrm_spec_catalog.csv.gz (accessed on 10 January 2020).
40. Catalog of Broad Morphology of SDSS Galaxies. Available online: http://vfacstaff.ltu.edu/lshamir/data/morph_catalog/wndchrm_catalog_n.csv.gz (accessed on 10 January 2020).
41. Paul, N.; Virag, N.; Shamir, L. A Catalog of Photometric Redshift and the Distribution of Broad Galaxy Morphologies. *Galaxies* **2018**, *6*, 64. [CrossRef]
42. Lindegren, L.; Hernández, J.; Bombrun, A.; Klioner, S.; Bastian, U.; Ramos-Lerate, M.; de Torres, A.; Steidelmuller, H.; Stephenson, C.; Hobbs, D.; et al. Gaia Data Release 2 The astrometric solution. *Astron. Astrophys.* **2018**, *616*, A2. [CrossRef]
43. Mignard, F.; Klioner, S.A.; Lindegren, L.; Hernandez, J.; Bastian, U.; Bombrun, A.; Hobbs, D.; Lammers, U.; Michalik, D.; Ramos-Lerate, M.; et al. Gaia Data Release 2 The celestial reference frame (Gaia-CRF2). *Astron. Astrophys.* **2018**, *616*, A14.
44. Brown, A.G.A.; Vallenari, A.; Prusti, T.; de Bruijne, J.H.J.; Babusiaux, C.; Barler-Jones, C.A.L.; Biermann, M.; Evans, D.W.; Eyer, L.; Jansen, F.; et al. Gaia Data Release 2 Summary of the contents and survey properties. *Astron. Astrophys.* **2018**, *616*, A1.
45. Flesch, E. The Half Million Quasars (HMQ) Catalogue. *Publ. Astron. Soc. Aust.* **2015**, *32*, E010. [CrossRef]
46. The Million Quasars (Milliquas) Catalog, v6.3. 15 June 2019. Available online: http://quasars.org/milliquas.htm (accessed on 23 July 2019).
47. MILLIQUAS—Million Quasars Catalog, Version 6.3. 16 June 2019. Available online: https://heasarc.gsfc.nasa.gov/W3Browse/all/milliquas.html (accessed on 23 July 2019).
48. Liao, S.-L.; Qi, Z.-X.; Guo, S.-F.; Cao, Z.-H. A compilation of known QSOs for the Gaia mission. *Res. Astron. Astrophys.* **2019**, *19*, 29. [CrossRef]
49. Prokhorov, G.Y.; Teryaev, O.V.; Zakharov, V.I. Axial current in rotating and accelerating medium. *Phys. Rev. D* **2018**, *98*. [CrossRef]
50. Prokhorov, G.Y.; Teryaev, O.V.; Zakharov, V.I. Unruh effect for fermions from the Zubarev density operator. *Phys. Rev. D* **2019**, *99*. [CrossRef]
51. Prokhorov, G.Y.; Teryaev, O.V.; Zakharov, V.I. Effects of rotation and acceleration in the axial current: Density operator vs Wigner function. *J. High Energy Phys.* **2019**, *146*. [CrossRef]

52. Teryaev, O.; Usubov, R. Vorticity and hydrodynamic helicity in heavy-ion collisions in the hadron-string dynamics model. *Phys. Rev. C* **2015**, *92*. [CrossRef]
53. Baznat, M.; Gudima, K.; Sorin, A.; Teryaev, O. Femto-vortex sheets and hyperon polarization in heavy-ion collisions. *Phys. Rev. C* **2016**, *93*. [CrossRef]
54. Rustamov, A.; Rustamov, J.N. On the spiral structures in heavy-ion collisions. *arXiv* **2016**, arXiv:1602.01812.
55. Martynova, A.; Teryaev, O.V. Search for spiral structures in heavy ion physics and astrometry. In Proceedings of the Talk at XVIII Workshop on High Energy Spin Physics (DSPIN19), Dubna, Russia, 2–6 September 2019.